Aus dem Institut für Schlaganfall und Demenzforschung
Institut der Ludwig-Maximilians-Universität München
Vorstand: Prof. Dr. Martin Dichgans

Characterization of Vasogenic Brain Edema Formation after Experimental Traumatic Brain Injury by *in vivo* 2-Photon Microscopy

Dissertation zum Erwerb des Doktorgrades der Humanbiologie
an der Medizinischen Fakultät der
Ludwig-Maximilians-Universität zu München
vorgelegt von

Yue Hu
aus
Yangquan, Shanxi, China

2020

Mit Genehmigung der Medizinischen Fakultät

der Universität München

Berichterstatter:	Univ. Prof. Dr. Nikolaus Plesnila
Mitberichterstatter:	Prof. Dr. Hans-Walter Pfister
	Prof. Ch. Schichor
	PD Dr. Daniela Hauer
Mitbetreuung durch den promovierten Mitarbeiter:	Dr. Susanne Schwarzmaier
Dekan:	Prof. Dr. med. dent. Reinhard Hickel

Tag der mündlichen Prüfung: 15.05.2020

Contents

1 **Introduction** 1

1.1 Epidemiology of Traumatic Brain Injury 4

1.2 Pathophysiology of TBI 5

1.2.1 Primary and Secondary Brain Damage 5

1.2.1.1 Primary Brain Damage 5

1.2.1.1 Secondary Brain Damage 6

1.2.2 Cerebral Edema Formation 9

1.2.2.1 Vasogenic Brain Edema 10

1.2.2.2 Cytotoxic Brain Edema 10

1.2.2.3 Differences and Interactions between two Types of Edema 11

1.3 Technical Limitations for Detecting Edema Formation 12

1.3.1 Conventional Technologies 12

1.3.2 2-photon microscopy 14

1.4 Aim of the Study 14

2 **Materials and Methods** 16

2.1 Materials 16

2.1.1 Equipment 16

2.1.2 Chemicals, Drugs and Solutions 17

2.1.3 Consumables 17

2.1.4 Software 18

2.2 Methods 18

2.2.1 Animals 18

2.2.2 Randomization and Blinding 19

2.2.3 The Controlled Cortical Impact (CCI) Model 19

2.2.4 Acute Cranial Window Preparation 20

2.2.5 2-photon Microscopy 22
2.2.6 Blood gas Measurement 23
2.2.7 Brain Water Content Measurement 24
2.2.8 General Condition Monitoring 24
2.2.9 Quantification of Two-photon Microscopy Images 26
2.2.9.1 Fluorescence Intensity Measurement 26
2.2.9.2 Extravasation Distribution Measurement 27
2.2.10 Experimental Protocols 28
2.2.11 Statistical Analysis 28
3. **Results** 30
3.1 Brain Swelling after TBI 30
3.2 Short-term Development of Vasogenic Brain Edema Formation after TBI 31
3.2.1 Physiological Monitoring 31
3.2.2 Temporal Profile of TMRM Extravasation 33
3.2.3 Spatial Distribution of Vasogenic Brain Edema Formation following Trauma 36
3.3 Long-term Development of Vasogenic Brain Edema Formation after TBI 38
3.3.1 General Conditions after TBI 38
3.3.2 Physiological Parameters during and after Imaging 40
3.3.3 Temporal Profile of TMRM Extravasation 42
3.3.4 Spatial Distribution of Vasogenic Brain Edema Formation following Trauma 47
3.3.4.1 Spatial Distribution of TMRM Extravasation 47
3.3.4.2 Spatial Distribution of TMRM Extravasation in 2-dimensional Heat-map 50
3.4 Characterization of Extravasation Speed after TBI 51
4. **Discussion** 53
4.1. Setup 53
4.2 TBI-induced Cerebral Edema Formation 54

4.2.1 Mechanisms of Vasogenic Edema Formation – BBB Breakdown 54

4.2.2 Other Molecular Candidates Responsible for Vasogenic Edema Formation 55

4.3. Brain edema formation and brain swelling following trauma 57

4.4 Characterization of Vasogenic Brain Edema following Experimental TBI 58

4.4.1 Temporal Profile of Vasogenic Brain Edema formation following TBI 59

4.4.2 Spatial Profile of Vasogenic Brain Edema Formation following TBI 62

4.3.3 Biphasic Pattern of extravasation speed 63

4.5 Clearance Routes of Vasogenic Brain Edema 65

4.6 Limitations and Perspectives 66

5. Summary and conclusion 67

6. References 69

7. List of Abbreviations 87

8. Acknowledgements 89

9. Curriculum Vitae 90

1 Introduction

1.1 Epidemiology of Traumatic Brain Injury

Traumatic brain injury (TBI) is defined as an acute brain injury resulting from mechanical energy to the head caused by direct or indirect external force (Menon et al., 2010). It is often referred to as the “silent epidemic’’ disease and remains a growing public health concern worldwide (Johnson and Griswold, 2017). Recently, data from Lancet Neurology Commission showed that more than 50 million people suffered from TBI annually (Maas et al., 2017). Since the global costs of TBI are approximately $US400 billion per year, TBI is considered as a huge economic burden (Maas et al., 2017). Incidence rates of TBI vary greatly between countries and regions. In 2006, a systematic review of the epidemiology of TBI in Europe included 23 studies published from 1980 to 2003 and the results demonstrated that the incidence rate of TBI was 235 cases per 100,000 people per year (Tagliaferri et al., 2006). Ten years later, according to Brazinova et al., the incidence rates of TBI in Europe (country-level studies) ranged from 47.3 per 100,000, to 694 per 100,000 each year (Brazinova et al., 2016). For the United States, the total number of new TBI patients reached 3.5 million per year in the last decade (Coronado et al., 2012). In China, based on several large population-based studies, the estimate incidence of TBI were 55.4-64.1 per 100 000 people per year (Wang et al., 1986).

TBI varies in severity from mild to severe (Teasdale and Jennett, 1974). The reported mortality rate for severe TBI is estimated to be 39% and 60% of patients having an unfavorable outcome. TBI survivors often suffer from physical, emotional, and cognitive disorders during their lifetime (Jafari et al., 2013; Wilson et al., 2017). Such disorders are not only restricted to severe TBI, but also occur frequently after moderate or mild injury (Fleminger et al., 2003).

According to the World Health Organization (WHO), for young people aged 15-29 years, road traffic accidents are the leading cause of TBI, while in infants (0-1), toddlers (1-4), young children (4-14), and in elder patient (aged over 65 years), most TBI cases were caused by falls (Bruns and Hauser, 2003). In low-income and middle-income countries, the incidence of TBI is rising because of increased transport-related injuries, while in high-income countries traffic-related incidents have decreased due to preventive measures (safety belts, helmets for motor vehicle). However, in these countries falls are now increasingly becoming the leading cause of TBI (Brazinova et al., 2016; Peeters et al., 2015). Other main causes of TBI include sports-related concussion, blast injury, and combat-related injury.

1.2 Pathophysiology of TBI

1.2.1 Primary and Secondary Brain Damage

1.2.1.1 Primary Brain Damage

TBI has a dynamic pathophysiology that evolves over time (Maas et al., 2017; Sahuquillo et al., 2001). Primary brain damage occurs when the insult delivers direct mechanical energy to skull and brain tissue. The injury is usually classified as focal brain damage (due to contact injury) or diffuse brain damage (due to acceleration/deceleration injury) (Dixon, 2017). These damages result primarily in contusion, laceration, intracranial hemorrhage or diffuse axonal injury (DAI) (Baethmann et al., 1998; Jha et al., 2019; Maas et al., 2008; Nortje and Menon, 2004; Sahuquillo et al., 2001). The primary injury damages the cerebral vessels and cells, such as neurons, astrocytes, and oligodendrocytes, leading to a loss of function of the microcirculation, the neurovascular unit, and cellular structures and/or to necrotic cell death. Additionally, both the extravasation of blood and necrotic cell death lead to a release of cytokines and chemokines which are often involved in the development of secondary injury responses.

1.2.1.1 Secondary Brain Damage

Secondary brain injury is an additional brain damage that is caused by a series of pathophysiological changes that are triggered by the primary damage (Dixon, 2017) and develops over hours, days, and potentially weeks, months, or even years after TBI. It mainly includes disturbances of the cerebral microcirculation, cytotoxic and vasogenic brain edema formation, inflammatory responses, cellular and mitochondrial dysfunction, and further cell death (Jassam et al., 2017; Jha et al., 2019; Maas et al., 2008; Sahuquillo et al., 2001; Shlosberg et al., 2010). Since the development of secondary brain damage occurs delayed during the first hours and days following injury, there is time for therapeutic interventions.

A key factor in the pathogenesis of secondary brain damage is brain edema formation with a consecutive increase in intracranial pressure (ICP), which in turn results in microcirculatory alterations and ischemia (Jha and Kochanek, 2018; Maas et al., 2008; Sahuquillo et al., 2001; Unterberg et al., 2004). According to the Monro-Kellie doctrine from 1783, the pressure within the skull is a function of the volume of intracranial compartments, i.e. blood, brain, and CSF (Mokri, 2001). A volume increase of any of the compartments will lead to an increase of ICP. When ICP increase exceeds the natural compliance mechanisms, it will result in perfusion deficits and ischemia (Bouma and Muizelaar, 1992). Consequently, a key mechanism to secondary brain damage is the development of brain edema (Jha and Kochanek, 2018; Unterberg et al., 2004). So far, several mechanisms have been discussed to contribute to brain edema formation.

BBB disruption

The breakdown of BBB results in extracellular accumulation of excitatory amino acids and exposure of the brain tissue to serum-derived molecules (thrombin, albumin, and fibrinogen) (Faden et al., 1989; Teichberg et al., 2009). These factors are discussed to cause microglia activation, proliferation, and production of pro-inflammatory factors, which further leads to edema formation, astrocytic dysfunction, inflammation, alterations in microcirculation, and metabolic disturbances (Blixt et al., 2015b; Corrigan et al., 2016; Lozano et al., 2015; Schwarzmaier et al., 2016; Willis et al., 2004). These processes serve as mediators for brain repair but also facilitate further BBB disruption (Shlosberg et al., 2010). Although BBB breakdown following TBI is recognized a central and critical pathologic process, the underlying molecular changes are still not completely understood (Donkin and Vink, 2010; Jha et al., 2019; Unterberg et al., 2004).

Inflammation

Accumulating evidence suggests that the immune system plays an important role in TBI pathogenesis (Jassam et al., 2017). In patients with TBI, the inflammatory response begins within hours and persists up to several weeks (Corrigan et al., 2016; Morganti-Kossmann et al., 2007). Accordingly, in animal models it was shown that the inflammatory response occurs frequently following TBI and is associated with BBB breakdown (Holmin and Mathiesen, 2000; Tian et al., 2016). The inflammatory cascade after TBI develops within minutes and includes local signaling in neurons, glia and recruited peripheral immune cells (Ziebell and Morganti-Kossmann, 2010). The local microglia is activated by pro-inflammatory cytokines which are released from leukocytes, and contribute to the overall increase in BBB permeability and brain edema (Broux et al., 2015; da Silva Meirelles et al., 2017; Jassam et al., 2017). These processes can be both beneficial and pathogenic, which could be part of the reason why broadly suppressing the immune system has been unsuccessful in altering clinical outcome in TBI patients. In the chronic phase, in some cases, the inflammatory state will persist for weeks, month, or even years after TBI (Acosta et al., 2013; Daneshvar et al., 2015). Interestingly, inflammation has been associated with increased BBB permeability and brain edema formation.

Microcirculatory alterations

Another major consequence of TBI is damage to the cerebral vasculature, which leads to formation of hemorrhage, edema, hypoperfusion, microthrombus formation, ischemia and hypoxia (Salehi et al., 2017). Clinical studies indicate that more than 30% of patients with TBI show global cerebral blood flow (CBF) values below the ischemic thresholds (< 18 ml·100 g^{-1}·min^{-1}) within 12 h of initial trauma (Bouma et al., 1991), which result in neuronal cell death and poor functional outcome (Bouma and Muizelaar, 1992; Bullock et al., 1992). At later times after injury, there is an apparent uncoupling between blood flow and tissue metabolism, which can result in vasospasm and hypo-perfusion (Bouma et al., 1992; Salehi et al., 2017). Alterations of the cerebral microcirculation leading to ischemia of both parenchymal cells and endothelial cells, could contribute to BBB disruption.

Mitochondrial dysfunction

Mitochondria are the energy-producing organelles in cells (van der Bliek et al., 2017). Physiologically, mitochondrial are involved in many key cellular process including acting as an effective storage for calcium, producing ATP production for the supply of energy (Kannurpatti, 2017). After TBI, the brain goes through a state of metabolic crisis and mitochondrial dysfunction becomes apparent (Hill et al., 2017). Mitochondrial dysfunction following TBI mainly leads to oxidative stress and subsequent apoptosis and decreased cellular energy supply (Hiebert et al., 2015). The production of reactive oxygen species (ROS) is increased, which further leads to oxidative damage to neurons, astrocytes and other essential vascular elements (Pierce et al., 2018). ROS also act as a common trigger for many downstream pathways that directly mediate BBB compromise, such as tight junction and matrix metalloproteinases (MMP) (Pun et al., 2009).

The pathophysiologic evolution of TBI is a complex process including primary and secondary injury (Figure 1), in which edema formation plays a central role. Edema formation after TBI may result in a malignant increase in ICP, decrease of CBF, and finally tissue ischemia (Jha and Kochanek, 2018; Klatzo, 1994; Stocchetti and Maas, 2014), which aggravate many secondary processes following TBI (Stokum et al., 2016). Moreover, these alterations may exacerbate edema formation, thus become a vicious circle.

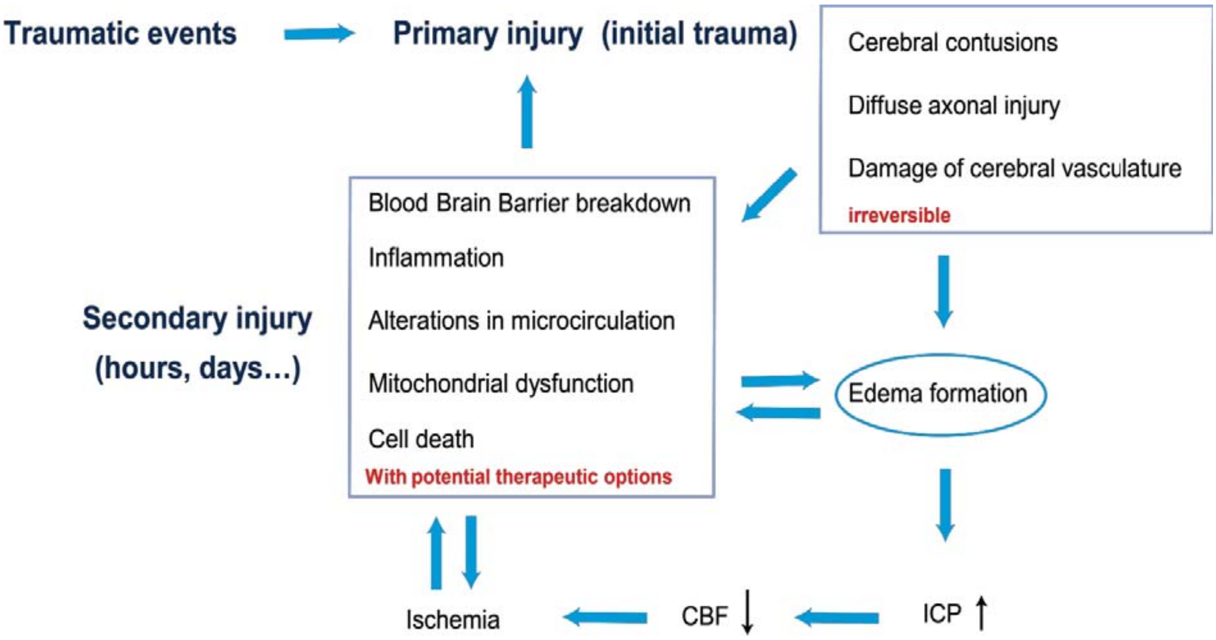

Figure 1: Summary of cascade of brain traumatic events and the central role of edema formation in this pathologic process. CBF=cerebral blood flow; ICP= intracranial pressure.

1.2.2 Cerebral Edema Formation

Since it plays a central role for the development of secondary brain damage, cerebral edema formation after TBI is an important matter. Cerebral edema is defined as an increase in brain tissue water, including water accumulation in the interstitial space and in individual cells (Donkin and Vink, 2010; Unterberg et al., 2004). It is discussed to play an important role for in-hospital mortality following TBI and may influence the long-term outcome as well (Nagata et al., 2018). Evidence from both animal and clinical experiments indicates that edema formation frequently occurs after brain trauma and is associated with unfavorable prognosis (Jha et al., 2019; Shapira et al., 1993; Tanno et al., 1992; Wei et al., 2012). According to Igor Klatzo's definition, there are two major types of brain edema: vasogenic and cytotoxic/cellular edema (Klatzo, 1994).

1.2.2.1 Vasogenic Brain Edema

Vasogenic brain edema occurs when the BBB is disrupted and the permeability of the BBB is increased. This results in the extravasation of water and plasma proteins into the interstitial space (Alluri et al., 2015). Driven by hydrostatic pressure, water together with plasma proteins and electrolytes leaks into the interstitial compartments with ensuing water accumulation (Alves, 2014; Lukaszewicz et al., 2011; Unterberg et al., 2004). The fluid accumulation results in brain swelling, and afterwards, exceeding intracranial compliance in a malignant rise of ICP (Blixt et al., 2015a; Jha and Kochanek, 2018; Katayama and Kawamata, 2003).

It is generally accepted that one factor contributing to vasogenic edema formation is the breakdown of BBB (Stokum et al., 2016). In TBI, shear forces lead to mechanical injury of the microvascular system, including disruption of tight junctions and degradation of endothelial basement membrane proteins (Nag et al., 2011; Sangiorgi et al., 2013). Plasma proteins and water may pass from the vascular compartment to the interstitial space through either trans-endothelial channels or paracellular pathways (Broadwell and Salcman, 1981). The enhanced permeability of BBB further leads to dysregulation of the vascular autoregulatory capacity, inflammatory responses, and reduced neurovascular coupling (Jha et al., 2019; Moretti et al., 2015).

1.2.2.2 Cytotoxic Brain Edema

The second important form of post-traumatic brain edema is called cytotoxic or cellular edema, and it is characterized by an intracellular water accumulation of astrocytes, neurons, and microglia (Jha et al., 2019). Extracellular ions are taken up by astrocytes, which leads to a consecutive water influx. Following brain trauma, this mechanism gets overstrained and finally results in ionic pump failure or activation of selected ion channels and further cell swelling. In contrast to vasogenic edema, in cytotoxic edema water mainly moves from the interstitial to the intracellular space (Hudak et al., 2014; Winkler et al., 2016). Although cytotoxic edema seems more frequent than vasogenic edema in patients after TBI, both entities contribute to increased ICP and secondary ischemic events (Lukaszewicz et al., 2011; Winkler et al., 2016).

1.2.2.3 Differences and Interactions between two Types of Edema

Cytotoxic edema is believed to be caused by a redistribution of water from the interstitial space into the cytoplasm of astrocytes, which does not necessarily result in an increase in brain water content or brain volume. By contrast, vasogenic edema is a redistribution of water from the vasculature into the brain which results in an increase in brain water content, brain swelling and eventually increased ICP. Cellular edema has been confirmed to contribute to vasogenic edema, because oncotic cell death of endothelial cells and astrocytes can cause BBB disruption (Jha et al., 2019). In turn, vasogenic edema can worsen cytotoxic edema by providing more interstitial water for the cells to take up.

	Vasogenic Edema	Cytotoxic Edema
Development	BBB disruption	Uptake of excess ions and metabolites by astrocytes
BBB Permeability	Increased	Unchanged
Edema fluid	Rich in protein	Rich in electrolytes
Morphology	No cell swelling Increased interstitial space	Cell swelling Decreased interstitial space

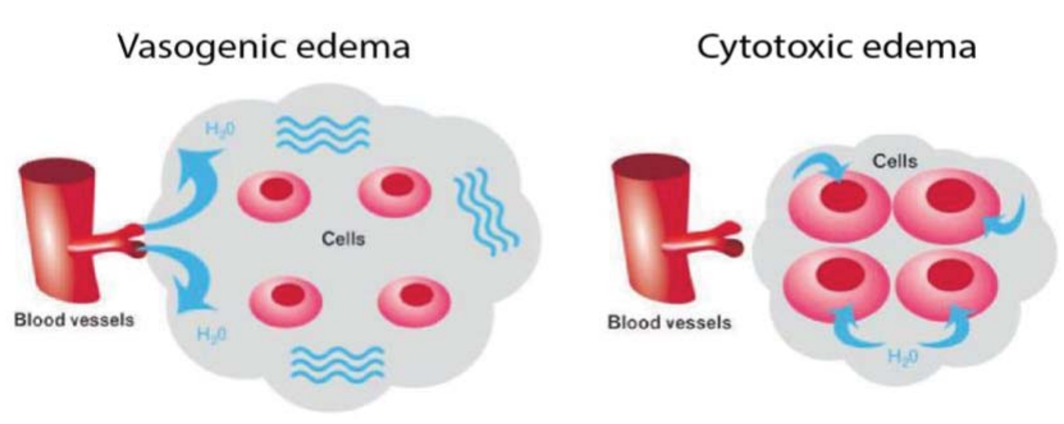

Figure 2: Comparison of vasogenic brain and cytotoxic brain edema. Part of the figure was modified from Donkin, J. J. *et a l (Donkin and Vink, 2010)*.

1.3 Technical Limitations for Detecting Edema Formation

1.3.1 Conventional Technologies

Despite the key role vasogenic brain edema formation has for the generation of secondary brain damage, its underlying mechanisms are still not fully understood. This is mainly due to technical limitations that have restricted the proper detection and quantification in the past. Conventional techniques used to investigate BBB opening include *ex vivo* experiments detecting IgG or Evans blue extravasation from the vessels (Murakami et al., 1999; Rosas-Hernandez et al., 2018), and *in vivo* experiments using MRI (Ren et al., 2019; Shen et al., 2016; Yu et al., 2019), epifluorescence microscopy (Mayhan and Heistad, 1985; Prager et al., 2010; Wahl et al., 1985) or near-infrared (NIR) fluorescence imaging (Klohs et al., 2009).

Evans Blue, a dye which has a high affinity for albumin, was used for measuring vascular permeability as early as 1948 (Allen and Orahovats, 1948). When Evans Blue is injected intravenously, it remains in the intravascular space. However, when vascular permeability is increased and protein leakage occurs , Evans Blue can be observed or measured within the brain parenchyma (Saria and Lundberg, 1983). So far, there are numerous TBI studies which have reported to use Evans Blue for monitoring BBB permeability (Dash et al., 2016; Yang et al., 2019). However, the assessment of Evans Blue extravasation appeared to be not sensitive enough to detect minor vascular leaks (Wick et al., 2018). Additionally, Evans blue extravasation can only be determined *ex vivo* and does not provide *in vivo* information. Consequently, this approach only provides a semi-quantitative assessment for a single time point, and does not allow the dynamic measurement of BBB breakdown.

For *in vivo* investigation of TBI several techniques have been established. One of them is dynamic contrast-enhanced MRI (DCE-MRI) which detects the extravasation of low-molecular weight MRI contrast agents by increased signal intensity in T1-weighted images (Sourbron and Buckley, 2013). This method has proven valuable in the assessment of BBB opening not only in diseases with large abnormalities in BBB dysfunction, such as acute ischemic strokes (Kassner et al., 2009), brain trauma (Ren et al., 2019) or tumors (Singh et al., 2007), but also in diseases with more subtle and chronic BBB disruption like cerebral small vessel disease (Wardlaw et al., 2009; Wardlaw et al., 2008), Alzheimer's disease (Starr et al., 2009) and diabetes (Starr et al., 2003). Theoretically, DCE-MRI seems a valid technique to capture BBB dysfunction *in vivo*, with the advantage to capture information from the whole brain and to provide repeated measurements in one single animal. However, in practice, DCE-MRI has only been used in a limited number of experimental TBI studies due to its technical limitations, like a low signal-to-noise ratio, low spatial and temporal resolution of the dynamic scans, and its relatively poor image quality.

Another widely used technique is intravital fluorescence microscopy (IVM) through an open skull window, which has been used to investigate BBB dysfunction *in vivo* since the 1980ies (Wahl et al., 1985). By injecting fluorescent tracers linked to large molecules such as dextrans intravascularly, BBB disruption was determined by the appearance of the tracer in the parenchyma (Mayhan and Heistad, 1985). Additionally, with this technique regional CBF in small arterioles and venues (Prager et al., 2010) , inflammatory responses such as leukocyte adhesion, the formation of micro thrombi, and alterations of vascular diameters can be investigated (Schwarzmaier and Plesnila, 2014; Schwarzmaier et al., 2015b; Schwarzmaier et al., 2013). Taken together, IVM was successfully used experimentally to assess the functionality of the cerebral microcirculation in real time. However, due to the limited penetration of visible light into brain tissue, studies using epifluorescence microscopy are limited to investigations of the surface of the brain. Variations in fluorescence intensity can only be discriminated superficially, a correlation along the vertical axis is not possible and alterations inside the brain parenchyma cannot be visualized. In order to overcome these limitations, a 3D imaging technique is required.

1.3.2 2-photon microscopy

With 2-photon microscopy, a decent resolution along the vertical axis (z-axis) is possible (Cheng et al., 2019). In a two-photon absorption process, two photons are sent within nanoseconds into the tissue with a relatively long wavelength, thereby achieving a larger penetration depth. These photons arrive in the point of focus virtually simultaneously and excite a fluorescent molecule with their combined energies (Helmchen, 2009). As a result, the fluorescent molecules within the focal point of the objective emit only one photon with the combined energy of the two exciting photons. Therefore, two-photon microscopy provides extremely high spatial resolution both in the horizontal and the vertical axis thereby providing novel options for detecting vascular leakage *in vivo*. So far, there are already several studies that have reported the use of multi-photon microscopy for *in vivo* imaging of cerebrovascular leakage in different experimental models such as micro beam irradiation (Verant et al., 2008), photo chemically induced stroke (Frederix et al., 2007), and ultrasound stimulation (Raymond et al., 2007). The only study performed after TBI has been performed by our laboratory (Schwarzmaier et al., 2015a). In this study, vasogenic edema formation was monitored dynamically with high spatial and temporal resolution after TBI. However, the investigation was reduced to the first few hours following injury, and a chronic characterization of vasogenic brain edema formation is still missing.

1.4 Aim of the Study

The aim of the present study was therefore to characterize the development of vasogenic brain edema formation in a clinically relevant mouse model of experimental TBI *in vivo*, with high spatial and temporal resolution, in both the acute phase following trauma (the first hours) and in the sub-acute phase up to 7 days following injury.

2 Materials and Methods

2.1 Materials

2.1.1 Equipment

Analytical Balances (Mettler Toledo™)	Thermo Fisher Scientific, USA
Axio Imager M2 Microscope	Carl Zeiss, Germany
Blood Gas Analyzer (RAPIDLab 348)	Siemens, Germany
Capnograph (TYPE 340)	HUGO SACHS ELEKTRONIK, Germany
CCI device (Mouse-Katjuscha 2000)	University of Mainz, Germany
Fluorescence Illuminator (X-cite 120)	Lumen Dynamics, USA
Glass Desiccator (DURAN®)	DWK Life Sciences, Germany
Surgical instruments	Fine Scientific Tools, Switzerland
LED light source (KL2500)	Leica, Germany
Microscope (Leica M80)	Leica, Germany
MicroSyringe Pump Controller	World Precision Instrument, USA
Oxygen Sensor, Oxydig	Draegerwerk, Germany
Powerlab 8/35	AD Instruments, Australia
Precision balance (OHAUS®)	Waagendienst Winkler GmbH, Germany
Recovery chamber (CA17 4BG)	MEDIHEATTM, UK
Stereotactic Injection Platform(KOPF®)	Föhr Medical Instruments, Germany
Syringe Pump (SP101IZ)	World Precision Instruments, USA

Temperature controller system	FHC, USA
Two Photon Microscope (LSM 7 MP)	Carl Zeiss, Germany
Volume-controlled ventilator (Minivent 845)	HUGO SACHS ELEKTRONIK, Germany

2.1.2 Chemicals, Drugs and Solutions

Buprenorphine	Bayer, Germany
Dextran, Tetramethylrhodamine, 40,000 MW, Neutral (D1842)	Thermo Fisher Scientific, USA
Heparin-Natrium (25,000 I.E./5ml)	B-Braun, Germany
Isoflurane Isp-Vet (1000 mg/g)	Chanelle, Ireland
Ketamine (50 mg/ml)	Bayer, Germany
Medetomidine	Zoetis, USA
Midazolam	B-Braun, Germany
Tachosil	Takeda, Germany

2.1.3 Consumables

Accelerator INSTA-SET™	Drechseln & Mehr, Germany
Cover glass (2 x 2 mm LOT 2441285)	Thermo Fisher Scientific, USA
Cyano Veneer	Hager & Werken, Germany
Cyano Veneer Powder	Hager & Werken, Germany
Cyanoacrylate Maxi-Cure	Drechseln & Mehr, Germany

Fine Bore Polythene Tubing (0.28mm ID, 0.61 mm OD)	Smiths Medical ASD, Belgium
Gauze (7.5 x 7.5 cm)	Lohmann & Rauscher, Germany

2.1.4 Software

ImageJ2	National Institute of Health, USA
Imaris 9.0	Bitplane AG, Switzerland
LabChart software	AD instrument, USA
Prism7	Graphpad, USA
ZEN 2010	Carl Zeiss, Germany

2.2 Methods

2.2.1 Animals

All protocols and procedures on animals were approved by the Government of Upper Bavaria (protocol number Vet_02-17-23) and are reported in accordance with the ARRIVE (Animal Research: Reporting of in Vivo Experiments) guidelines. The animals that were used were 6-8 -week-old male C57Bl/6 mice with a body weight of 22-26 g (Charles River Laboratories, Germany). All mice were housed in groups of up to five per cage under a 12h light/12h dark cycle with free access to food and water. Prior to surgery, animals were allowed to acclimate to our animal facility for at least five days. After surgery, mice were kept individually in separated cages. Health screens and hygiene management checks were performed daily in accordance with the guidelines and recommendations established by the Federation of European Laboratory Animal Science Associations (FELASA).

2.2.2 Randomization and Blinding

For each series of experiments, mice were randomly assigned to one of the experimental groups after preparation of the craniotomy (see 2.2.3) by drawing lots (n=6 each group). Throughout the experiment, each animal was kept individually and only labeled with a number, i.e. with no information about further treatment. 2-photon microscopy image analysis for each animal was performed off-line by a researcher who was blinded towards the treatment of the respective mouse, i.e. trauma or sham surgery

2.2.3 The Controlled Cortical Impact (CCI) Model

TBI was induced using the controlled cortical impact (CCI) model. It is well established model of contusional TBI and results in a highly reproducible contusion (Krieg et al., 2017; Trabold et al., 2010; Zweckberger et al., 2003). The contusion is produced by a pneumatic driven piston which hits the cortex with a defined velocity and impact depth. The detailed protocol is described below.

For analgesia, the animals received buprenorphine (0.1mg/25g) i.p. 30min before surgery. For short lasting surgical procedures such as inducing CCI, the animals were anesthetized with inhalation of Isoflurane (4% for 60s and 1.5-1.8 % throughout surgery) delivered in a gas mix containing N_2 and 30%-33% O_2. Mice were fixed in a stereotactic frame by a nose clamp. Bepanthen ointment was applied on the eyes to protect them from dryness during surgery. A rectal probe was used to monitor body temperature and a feedback controlled heating pad was used to maintain body temperature during surgery.

Surgery was performed using an upright operation microscope (Carl Zeiss, Germany). Following a longitudinal skin incision along the sagittal suture, a craniotomy of 4 x 4mm was prepared posterolateral to bregma over the right parietal cortex (Fig. 4) by using a dental drill under continuous cooling with saline. The skull was opened carefully and the CCI impactor was placed exactly onto the cortex. The impact was applied perpendicular to the dura with a steel cylinder (diameter: 3.0 mm), a velocity of 6 m/sec, a penetration depth of 0.5 mm and a contact time of 150 ms, as previously described (Schwarzmaier et al., 2015a). Immediately following the impact, the removed bone flap was placed back and fixed with tissue glue. The skin was sutured and the mice were placed in a recovery chamber (33°C and 50% humidity) for 30 min until recovery of motor function. Sham-operated animals were treated as described above (including the craniotomy), except for the induction of CCI.

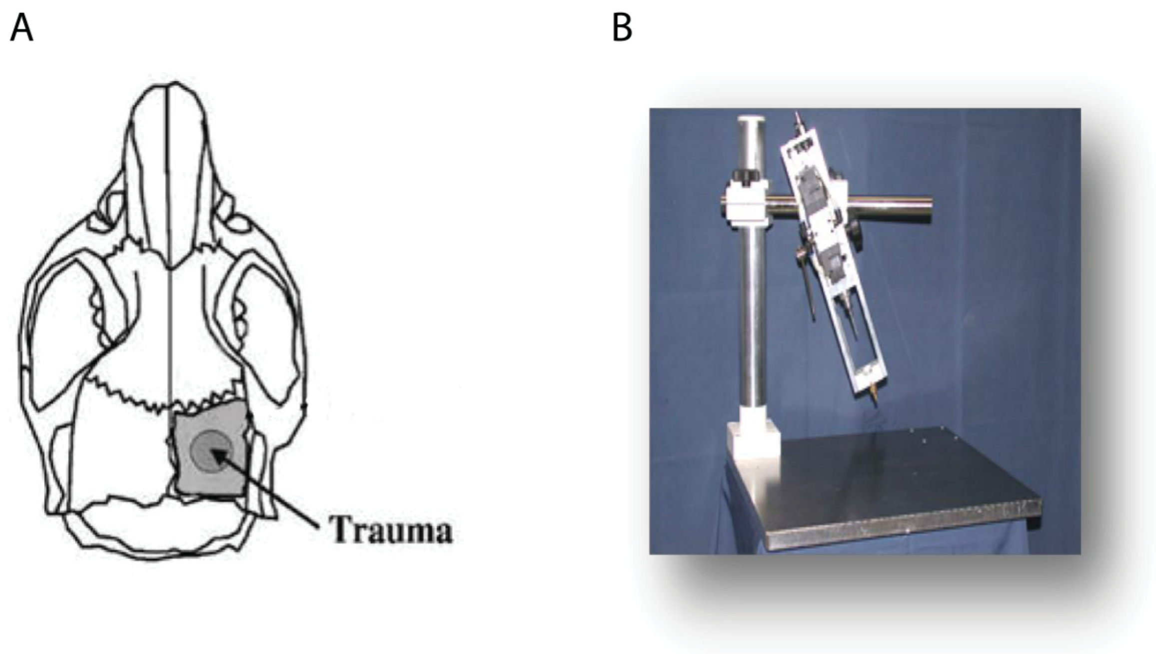

Figure 3: (A) Schematic drawing of the skull of a mouse and of the position of brain trauma; (B): The CCI device.

2.2.4 Acute Cranial Window Preparation

Mice were anesthetized by intraperitoneal injection of a triple combination containing 0.05 mg/kg Fentanyl, 0.5 mg/kg Medetomidine and 5 mg/kg Midazolam (Schwarzmaier et al., 2015a; Thal and Plesnila, 2007). Thereafter the mice were intubated with a custom-made tube connected to a volume-controlled ventilator. Ventilation volume and respiratory frequency was adjusted according to body weight and the end tidal partial pressure of carbon dioxide (pCO_2). Body temperature was maintained by a feedback controlled heating pad. The head was fixated in a nose clamp mounted on a stereotactic frame. For measurement of arterial blood pressure a sterile plastic catheter was inserted into the femoral artery and connected to a pressure transducer. Animals received a continuous infusion of 0.4 ml/h NaCl 0.9% via the arteriolar catheter to compensate for ventilation-induced fluid loss. Body temperature, mean arteriolar blood pressure (MABP) and end-tidal pCO_2 were monitored throughout the experiment and stored for further analysis using Powerlab and LabChart software.

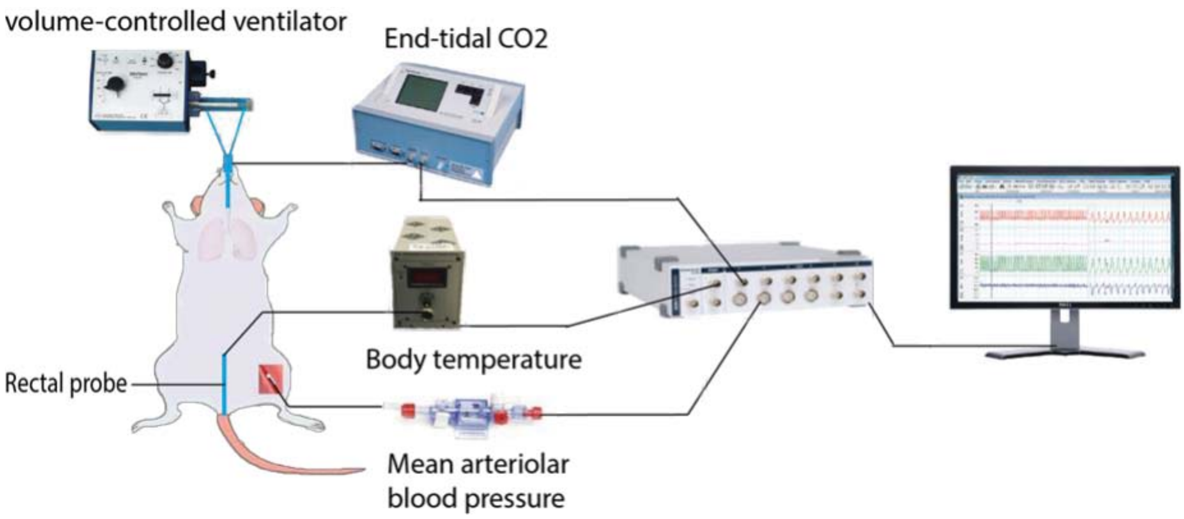

Figure 4: Experimental setup for the measurement of physiological parameters. End-tidal CO_2, core body temperature and mean arterial blood pressure were monitored continuously throughout the experiment.

A square cranial window (2 mm x 2 mm) was prepared as previously described (Schwarzmaier et al., 2015a). Briefly, a cranial window was drilled carefully over the right fronto-parietal cortex under continuous cooling with saline. After removal of the bone flap, the dura mater was gently removed and the surface of the brain was rinsed with saline. Then, a precise-fitting square cover glass with a thickness of 0.175 mm was carefully placed into the window and fixed with dental cement. The window was located 1 mm lateral to the sagittal suture and 1 mm frontal to the coronal suture, thus, a region 1.5–3.5mm frontal to the primary contusion could be imaged.

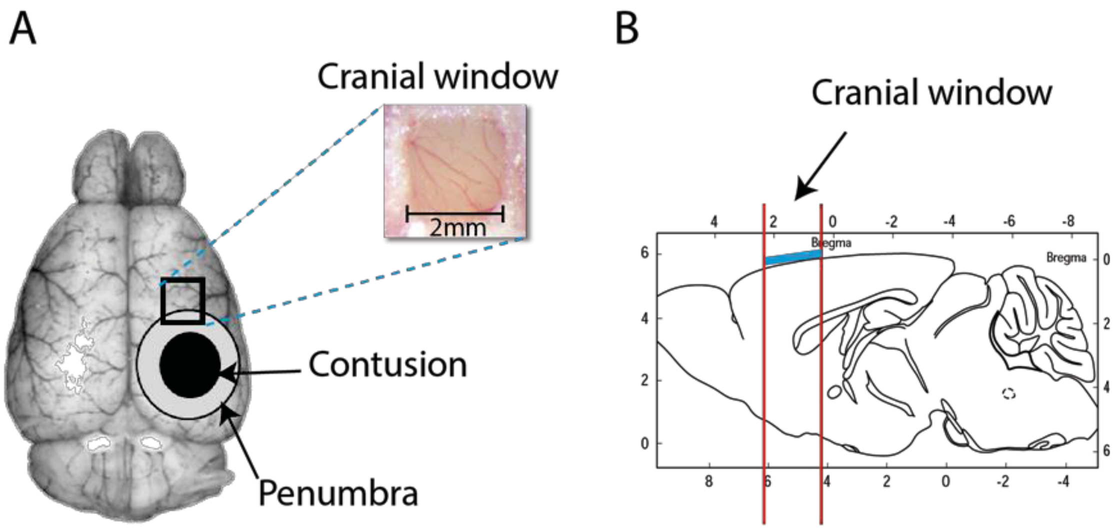

Figure 5: Location of the contusion (black), the penumbra (gray), and the cranial window on the brain.

2.2.5 2-photon Microscopy

Following CCI and preparation of the window, the anesthetized mice were placed under a 2-Photon microscope (Zeiss LSM-7MP). For imaging, the mice received an injection of 40 mg/kg Tetramethylrhodamine-dextran (TMRM; MW 40,000) through the femoral artery catheter. The molecular weight of 40,000 Dalton was chosen specifically because it mimics the size of plasma proteins which cross the BBB exclusively under pathological conditions (Guérin et al., 2001; Reyes-Aldasoro et al., 2008). The excitation wavelength for TMRM dextran was 800 nm. In order to provide an even signal intensity throughout the 3D region of interest, the laser power was increased with increasing imaging depth from 3.0% at the surface to 15.0% at 300 µm depth. Master gain and digital gain were set as 650 and 2.00, respectively. These settings were determined empirically in order to visualize the vessels and parenchyma in a three dimensional region of interest reaching 0–300 microns below the surface of the brain with equal intensity and minimized background noise.

For imaging, three regions of interest (ROI) were defined within the window as illustrated in Fig. 6. Area 1 was the ROI closest to the site of the primary injury (1.5 mm frontal to the rim of the initial contusion). Area 2 and Area 3 were located at a distance of 2 mm and 2.5 mm from the rim of the initial contusion, respectively. The side length of each area was 425 µm x 425 µm, all areas extended vertically from the surface to a depth of 300 µm into the parenchyma. Images of horizontal planes were acquired with a vertical distance of 3 µm and then digitally combined to a 3D image (z-stack). Baseline images were captured from each ROI immediately after adjustment of the microscope (within 2mins). Thereafter, z-stacks of each area were obtained every 30 min.

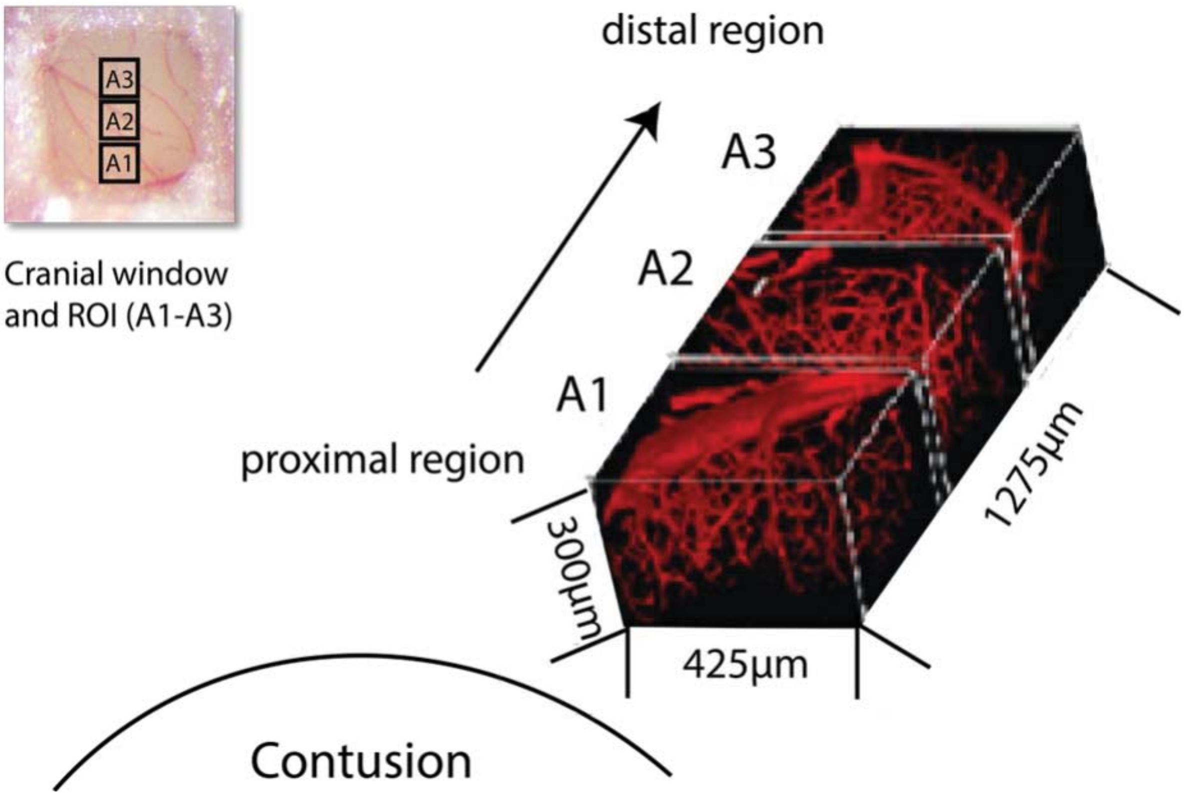

Figure 6: Scheme of the location of the ROI for imaging (A1-A3) with A1 being the most proximal region to the contusion. For each area, the side length was 425 µm x 425 µm and all areas extended vertically from the surface to a depth of 300µm into the parenchyma.

2.2.6 Blood gas Measurement

At the end of imaging, arterial blood samples were immediately collected with a glass capillary from the femoral artery catheter. The pH, pCO_2 and pO_2 were measured using a blood gas machine.

2.2.7 Brain Water Content Measurement

Before measurement, the cleaned weighing dishes were weighed with an accuracy of 0.0001 mg (empty weight (A)). After sacrificing the mouse, the brain was removed quickly and then placed and straightened in a metal matrix. The olfactory bulb and cerebellum were removed with a razor blade. The brain was divided exactly along the midline and each hemisphere was placed in a weighing dish and labeled accordingly. The dishes containing the hemispheres were measured again to assess the wet weight (B). The dishes were kept open and placed in the preheated oven at 110°C for 24h. After removal from the oven, the open dishes were transferred to the desiccator to cool for 1 hour. Thereafter the dishes were weighed again (dry weight (C)). The formula used for the calculation of brain water content was the following: (wet weight-dry weight)/ (wet weight-empty weight) X 100 = water content (%) = (B-C)/(B-A) X 100. (A) Empty weight (B) wet weight (bowl + brain) (C) dry weight (bowl +brain).

2.2.8 General Condition Monitoring

As a parameter for the general wellbeing of the animals participating in the study, the body weight was assessed before and repetitively throughout the experiment, i.e. daily for the first 3 days and at the 7th day post CCI or sham operation.

For monitoring of the general condition, the state of consciousness, behavior, general appearance, clinical condition and wound condition, were recorded daily for the first 3 days and on the7th day post CCI and evaluated according to a score scheme (Table 1). The neurologic status was measured according to the neurologic score sheet (see table 1) daily for the first 3 days and on the 7th day post CCI or sham operation in

Table 1 Neurologic score sheet

Items	Descriptions	Burden/score
1. Behavior	Unobtrusive, normal	No/0
	Reduced spontaneous movement, but normal reaction to stimulus (e.g. reaction to noise),	Low/5

	normal cooperation in neurologic testing	
	Significantly slowed down, significantly reduced spontaneous motor functions, reduced co-operation in neurologic tests, even after stimulus	Middle/10
	Apathetic, auto aggressive, making noises	High/20
2. General condition	Fur even, orifices clean, eyes clean/shiny	No/0
	Altered grooming	Low/5
	Fur dull, orifices dirty, eyes dull, piloerection	Middle/10
	Fur dirty, orifices sticky, fast, shallow breathing or gasping	High/20
3. Weight loss	< 1%	No/0
	1% - 5%	Low/5
	5% - 10%	Middle/10
	11% - 15%	High/20
4. Neurologic Deficits	No	No/0
	Only with neurologic testing for detestable deficits (e.g. muscle weakness, clumsiness)	Low/5
	Significant unilateral weakness with obvious impairment of movement	Middle/10
	Hemiplegia, locomotion and food intake/body care severely impaired	High/20
5. Wound conditions	No irritation, dry, no dehiscence	No/0
	Slight redness, dry, no dehiscence	Low/5
	Redness, swelling, fluid leakage Need for local treatment (disinfection, stitching)	Middle/10
	Not healing, infected wound	High/20
6. Vigilance	No impairment	No/0

	Epileptic seizure with subsequent vigilance reduction lasting less than 10 minutes	Low/5
	Vigilance reduction without previous epileptic seizure with subsequent reduction of vigilance between 10 and 30 minutes	Middle/10
	Comatose for more than 5 minutes without epileptic seizure, comatose for more than 30 minutes after epileptic seizure	High/20
7. Epileptic seizures	No	No/0
	Self-limiting focal seizure (duration less than 5 minutes)	Low/5
	Self-limiting generalized seizure (duration less than 5 minutes)	Middle/10
	Grand-mal status epileptics with motor dislocations/tonic seizures lasting > 15 minutes	High/20

2.2.9 Quantification of Two-photon Microscopy Images

2.2.9.1 Fluorescence Intensity Measurement

The image analysis was performed off-line by an investigator who was blind to the treatment of the animal using the software ImageJ. To avoid an analytical bias by artifacts from the operation, the superficial 50 µm of each z-stack were excluded from the analysis. The intensity threshold was adjusted to eliminate both the (very high) intravascular signal and the (very low) background signaling of the images. The adjustment for the color threshold was standardized and applied uniformly to all datasets. Subsequently, fluorescent pixels in each layer were assessed throughout the z-stack using ImageJ. Fluorescence intensity in the whole z-stack was then calculated as the mean of the values acquired from all sections. The baseline fluorescence intensity value was determined in the z-stack that was acquired immediately after TMRM injection. The data subsequently obtained in that experiment (30, 60, and 90 min) was then expressed as percentage of that specific baseline.

2.2.9.2 Extravasation Distribution Measurement

In order to better characterize the extravasation distribution after CCI, a novel method was used to analyze the original data. Firstly, the original data (z-stack) was transferred into the maximal intensity projection form. By applying a specific look-up-table (jet lut) into the image, the contrast of images was better than in monochrome images. Then, each image was gridded into 36 segments (6 X 6). In each segment, a ROI was chosen in the non-vessel area (78 pixels). The fluorescence intensity was measured within each ROI using imageJ. Based on these data, a 2D heat-map was drafted using Prism7.

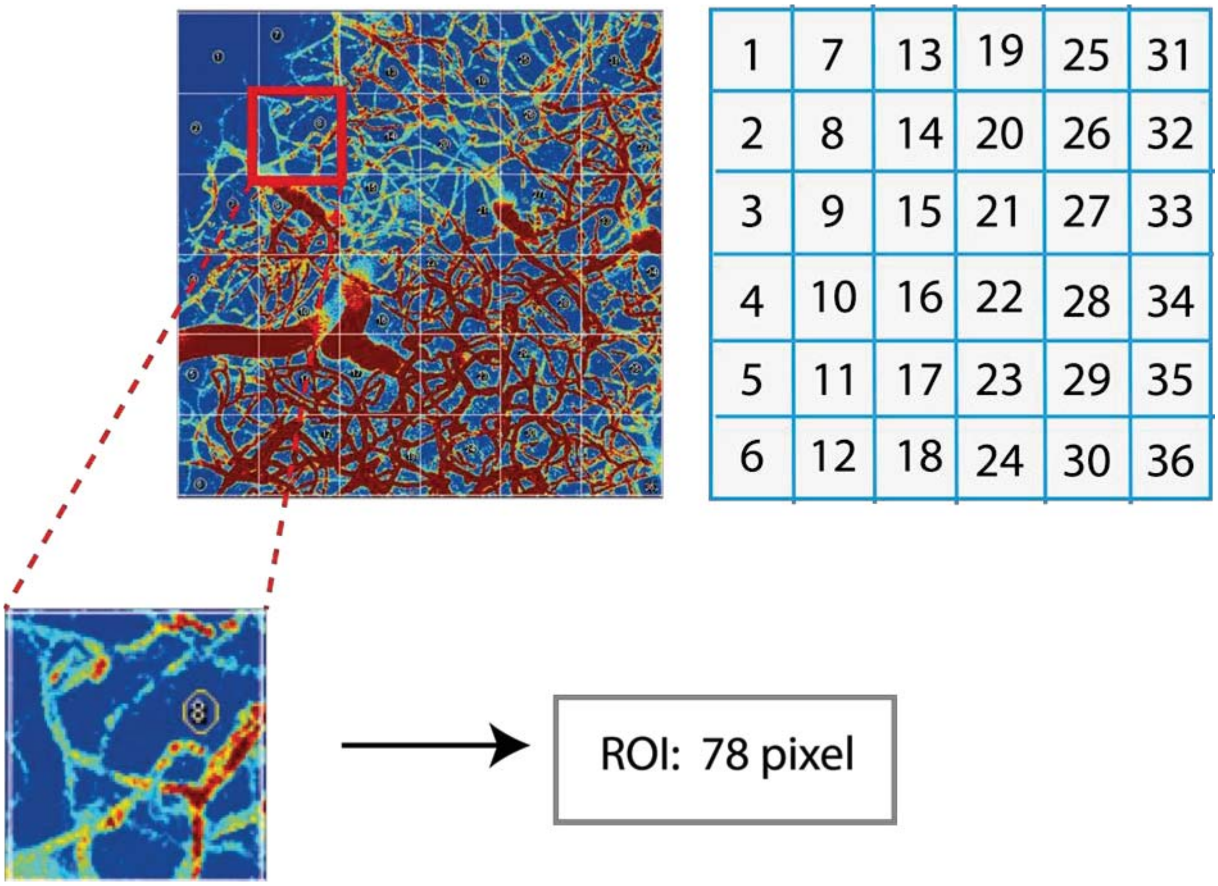

Figure 7: Distribution of TMRM extravasation measurement as well as definition of ROI.

2.2.10 Experimental Protocols

The experimental protocols used in this thesis are shown in Fig. 8.

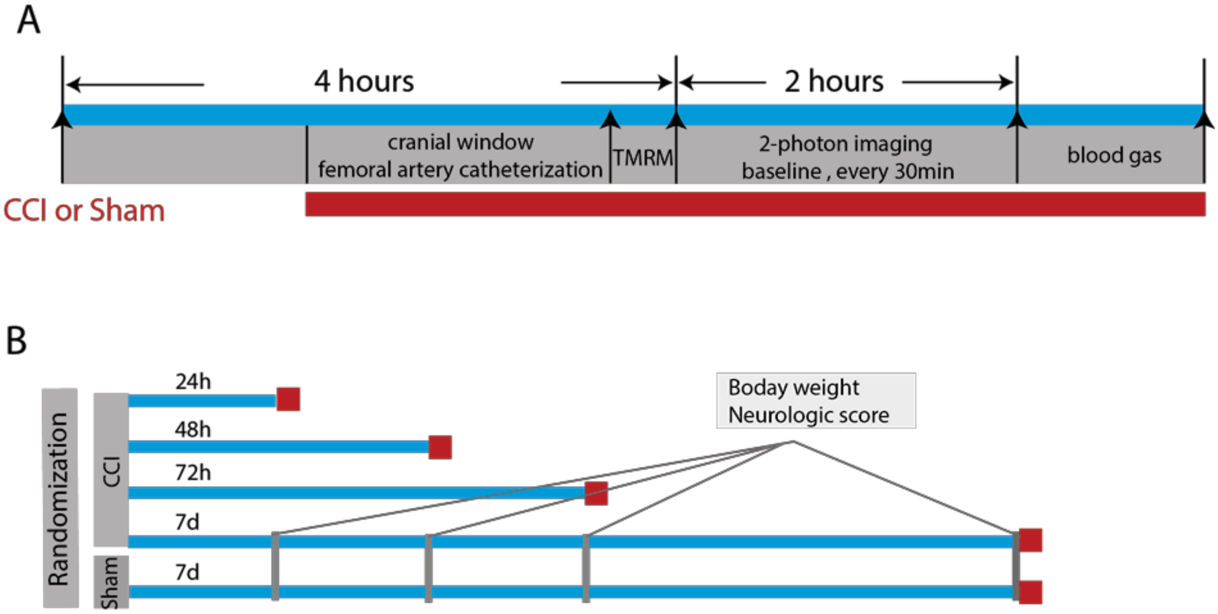

Figure 8: Timeline of the experimental setup. (A) Experimental series determining the short–term development of vasogenic brain edema formation. (B) Experimental series investigating vasogenic edema formation until 7 days post CCI. Body weight and neurologic score were assessed at day 1, 2, 3, and 7 following CCI. Animals were imaged at different time points indicated by the red cubes.

2.2.11 Statistical Analysis

Statistical analysis was performed using GraphPad Prism 6.0. All data are presented as mean ± standard deviation (SD). Sample sizes were calculated with standard deviation ranged from 25 - 30% and a biologically relevant difference of 50%. To increase the robustness of the statistical approach only non-parametrical statistical tests were used. The Mann-Whitney U test was used to analyze the differences between groups, Kruskal–Wallis analysis of variance on ranks was used to compare more than two groups. Differences with p values less than 0.05 were considered to be statistically significant.

3. Results

3.1 Brain Swelling after TBI

As a first parameter reflecting unilateral brain swelling, the midline shift was assessed. As shown in Fig. 9, the ipsilateral hemisphere started to swell as early as 4 hours after TBI. At 48 hours after injury the midline shift reached its maximum and decreased thereafter.

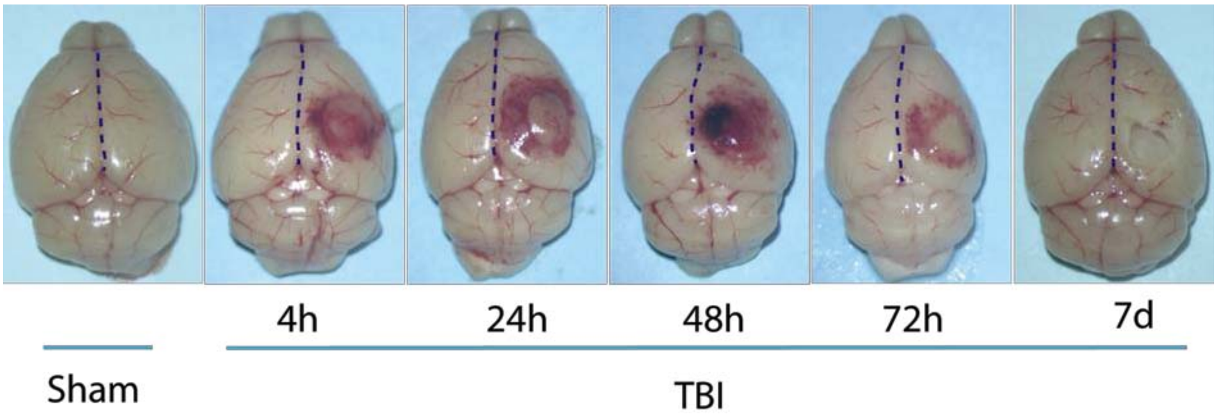

Figure 9: Gross anatomy pictures showing the contusion and midline shift at different time points following CCI.

Secondly, brain water content was determined by applying the wet-dry method. Following CCI, the water content in the ipsilateral hemisphere increased as early as 4h following CCI to 80.4±0.8% compared to 78.3±0.5% following sham operation (n=6). Thereafter, ipsilateral water content gradually increased and peaked at 24 hours following injury with 80.9±1.1% (n=6). In the ipsilateral hemisphere, brain water content remained significantly increased until 72 hours following TBI compared to brain water content after sham operation. At 7 days after injury ipsilateral brain water content decreased to 79.5±1.1%, which was only slightly more than in the contralateral hemisphere.

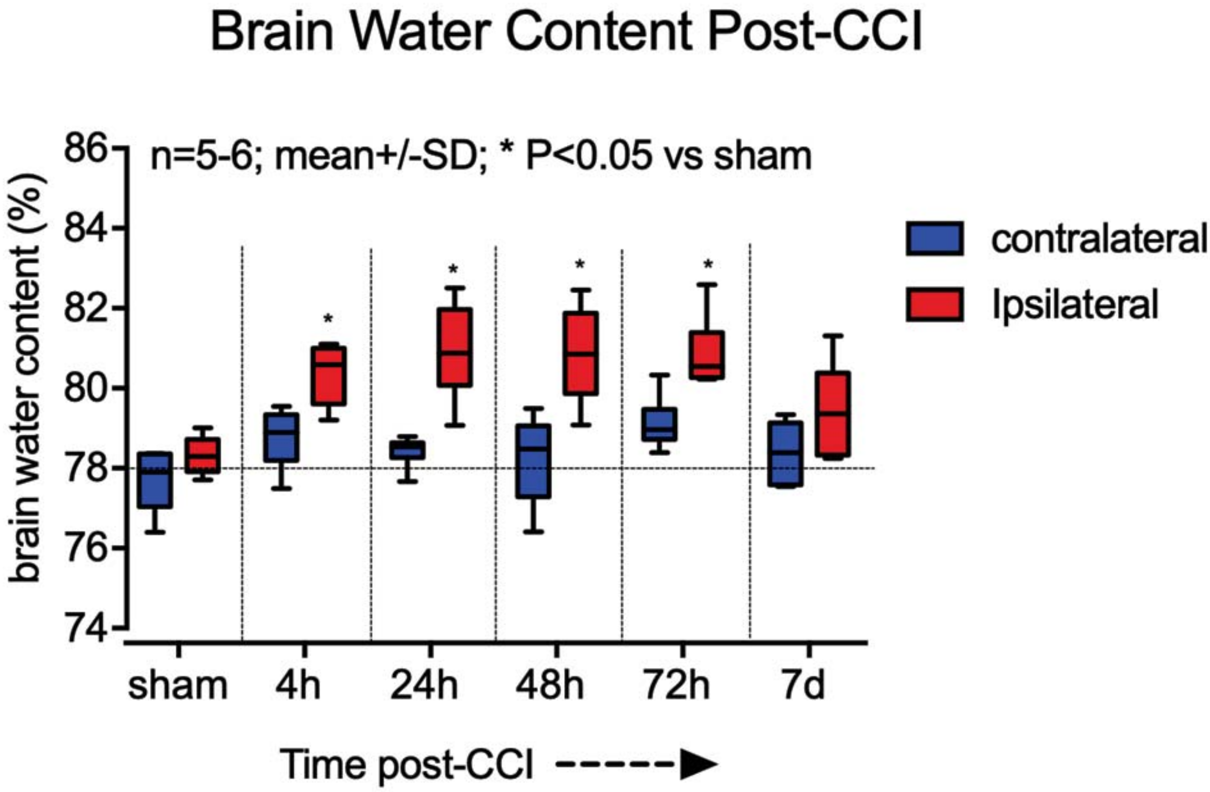

Figure 10: Water content in the injured hemisphere and control hemisphere at different time points after TBI. Ipsilateral water content gradually increased and peaked at 24 hours after TBI. *P<0.05 vs sham ipsilateral. SD = standard deviation.

3.2 Short-term Development of Vasogenic Brain Edema Formation after TBI

3.2.1 Physiological Monitoring

In the applied experimental 2-photon imaging protocol, the overall surgical and imaging time reached up to 4 hours. To ensure physiological homeostasis throughout the experiment and especially during imaging, physiological parameters including body temperature, mean arterial blood pressure and end-tidal CO_2 were continuously monitored; all values were within their respective physiological range and showed no significant difference between groups (Fig. 11). At the end of the experiment, blood gases including pH, pCO_2 and partial pressure of oxygen (pO_2) were measured. As shown in Table 2, the values did not differ significantly between groups and pCO_2 and

pO_2 were kept within the physiological range. Throughout the experiment the animal developed an acidosis with a pH of 7.2 which was similar in both groups.

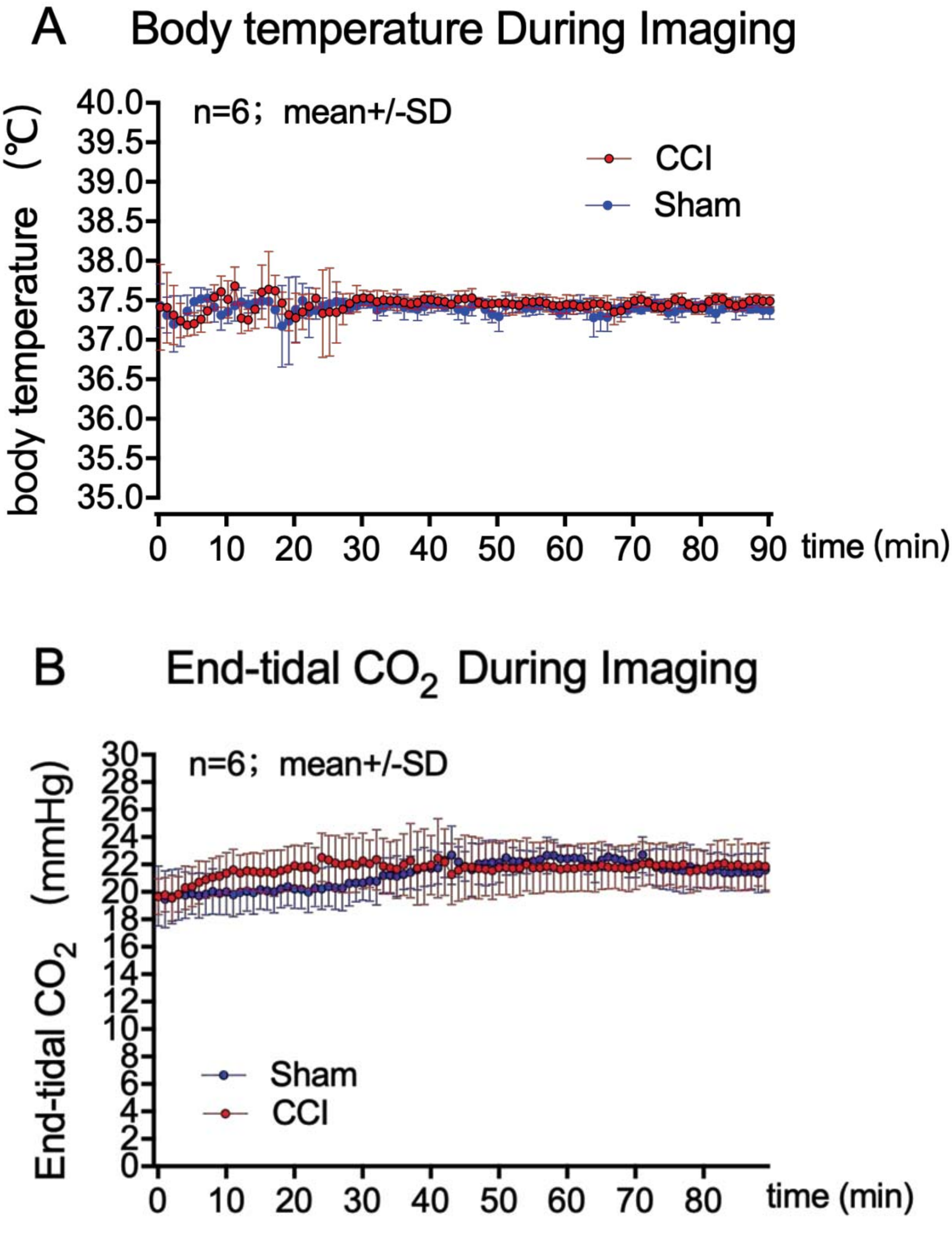

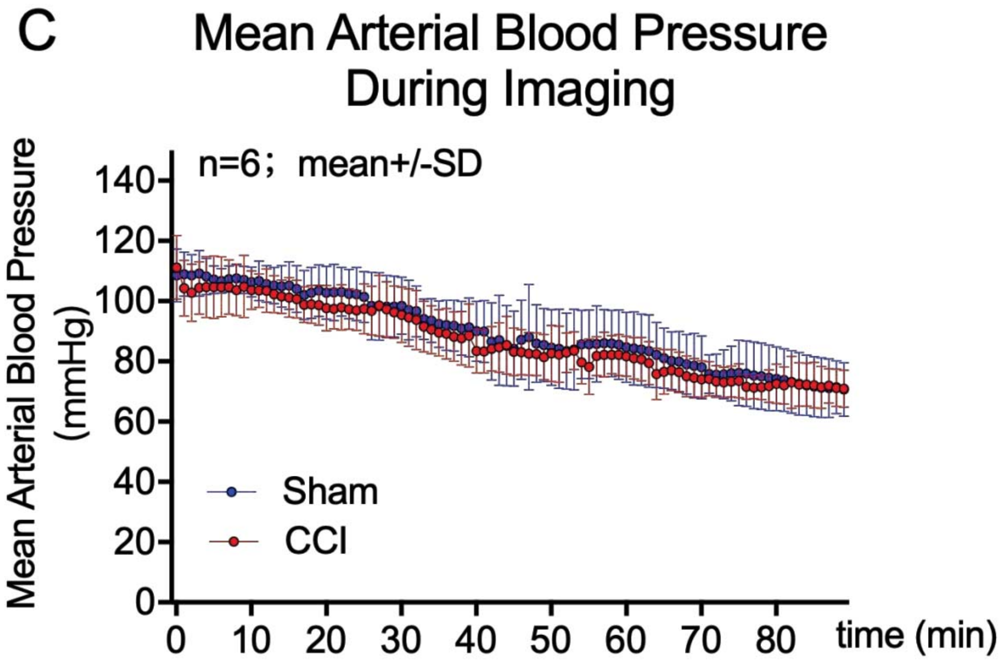

Figure 11: Physiological parameters during imaging (short-term 4h). Core body temperature (A), end-tidal CO_2 (B), and mean arterial blood pressure (C) were monitored continuously throughout the experiment.

Table 2 Arterial blood gas analysis at the end of the experiment

Group (n=6)	*pH*	*pCO_2 (mmHg)*	*pO_2 (mmHg)*
Sham	7.2±0.1	45.4±11.8	94.5±11.6
CCI	7.2±0.1	45.8±12.4	97.1±22.4

Data were shown as mean ± standard deviation

3.2.2 Temporal Profile of TMRM Extravasation

The first z-stack was acquired immediately after TMRM injection and served as baseline for the following datasets. Then, imaging was repeated every 30 minutes in the three regions of interest from proximal to distal to primary contusion (A1-A3). As demonstrated in Fig. 12, vasogenic brain edema formation after CCI could be clearly visualized by 2-photon imaging. Brain parenchyma appears black, while the vessels are labeled with TMRM and are depicted in white. The extravasation, which appears as a grey shadow across the parenchyma, could be detected in A1 as early as 4.5 hours following CCI. Subsequently, the fluorescence signal intensity increased continuously up to 90 minutes after injury. By contrast, in sham operated mice no extravasation could be detected throughout the experiment.

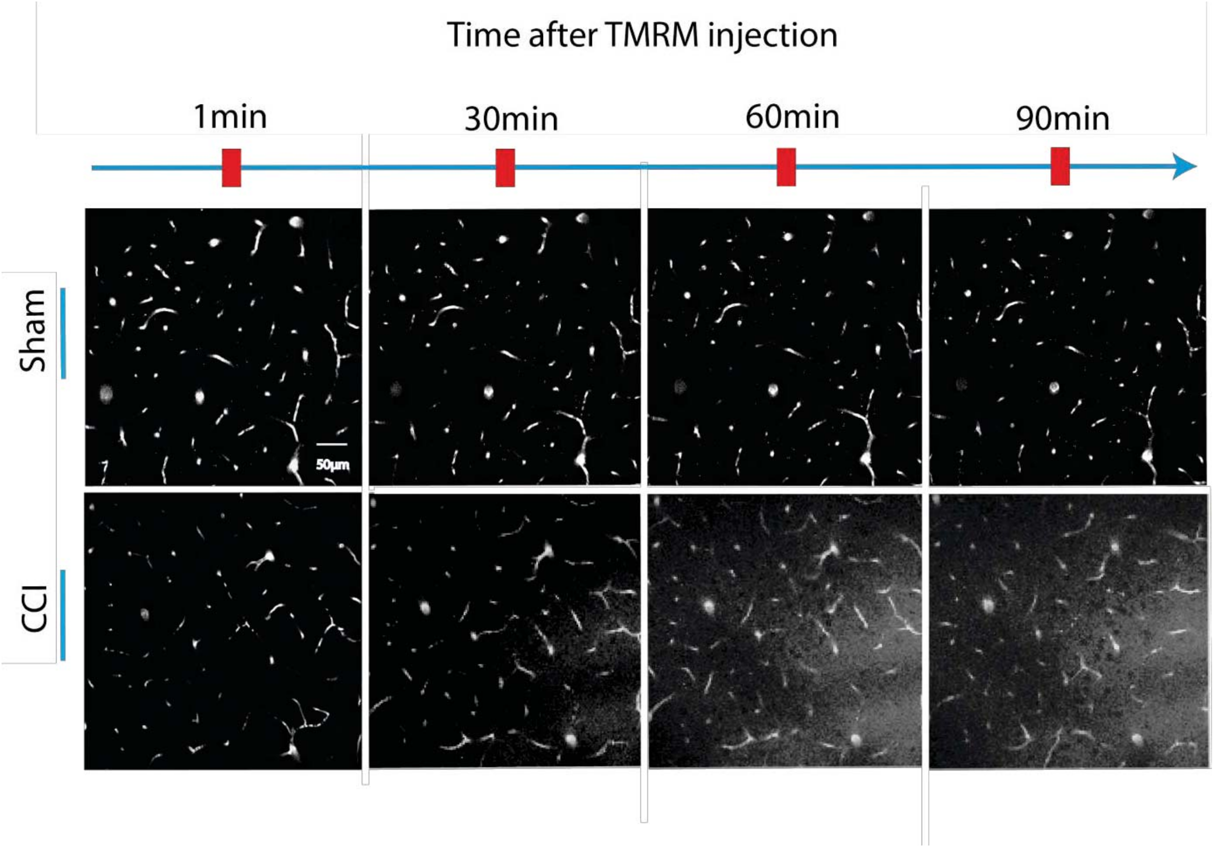

Figure 12: Short-term development of vasogenic brain edema formation after CCI (4h). Vessels were labeled with TMRM. No extravasation is visible after sham operation. In contrast, the extravasation of TMRM is clearly visible 4.5 h following CCI. Representative images from region A1, at a depth of 150 µm; scale bar: 50µm.

Fluorescence intensity was used as a parameter for TMRM extravasation and quantified in regions A1 to A3, i.e. from proximal to distal to the contusion site. In the CCI group, fluorescence intensity in A1 and A2 significantly increased compared to sham operation, reaching approximately 130% of baseline within 30 minutes ($P<0.01$, $P<0.05$ vs sham operation). Subsequently, TMRM extravasation still increased gradually until the end of the experiment. By contrast, the signal increase in A3 was much lower. In the sham group, no TMRM extravasation could be detected at any time throughout the experiment. In each figure, the baseline was assessed in the first z-stack and defined as 100%. This value is presented as a dotted reference line.

A 4h after sham or CCI (A1)

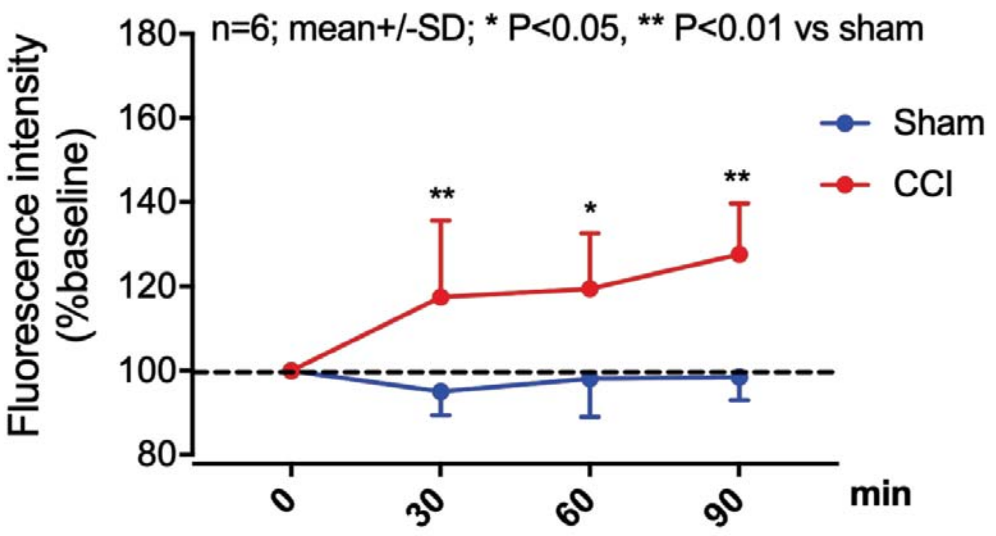

B 4h after sham or CCI (A2)

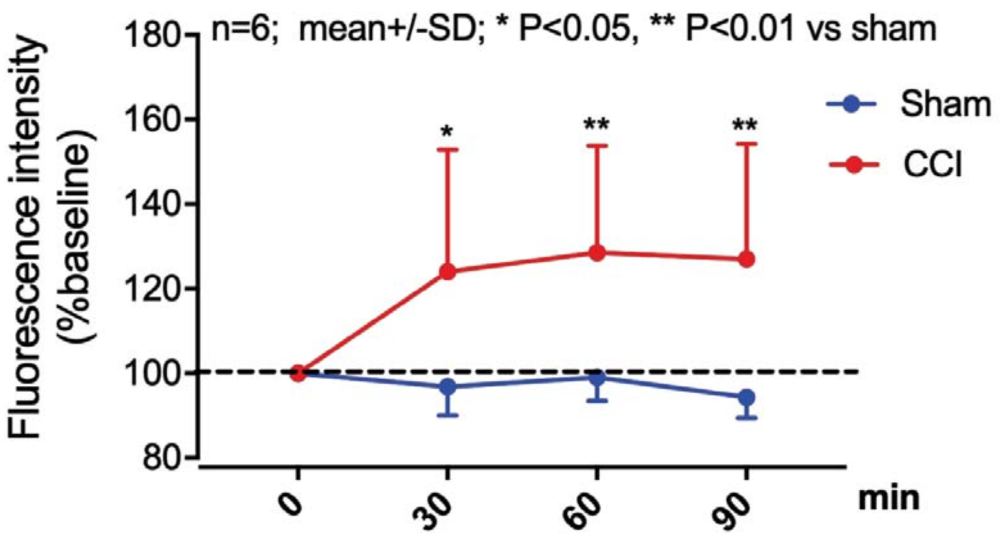

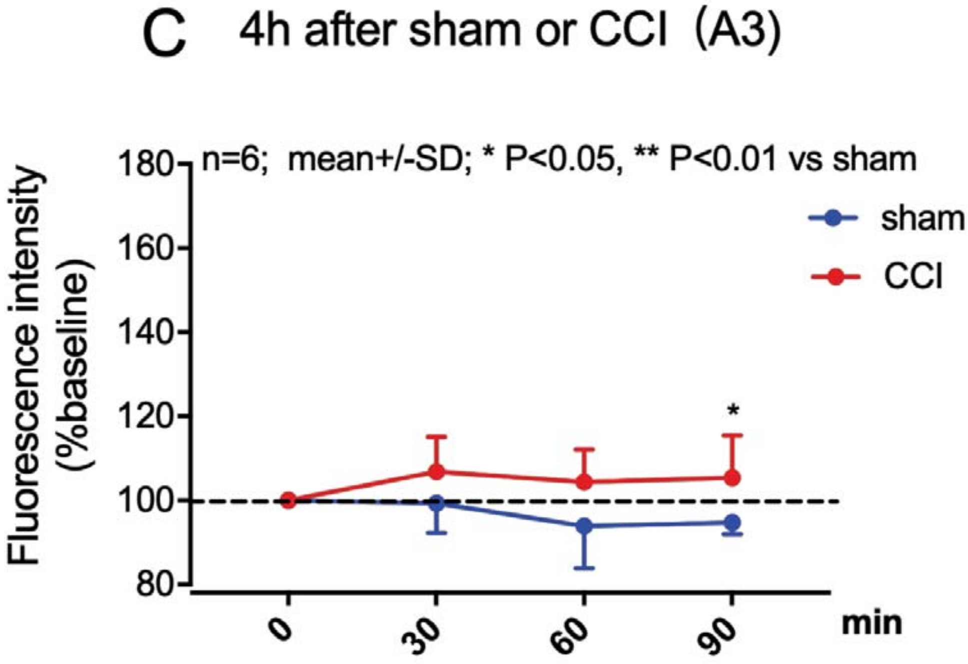

Figure 13: Extravasation of TMRM in different areas (A1-A3) over time. Fluorescence signal intensity increased significantly in A1 and A2, compared to sham operation. However, in the most distal region A3 TMRM extravasation was less strong. The dotted line represents the baseline. *P<0.05, **P<0.01 (vs sham). SD=standard deviation.

3.2.3 Spatial Distribution of Vasogenic Brain Edema Formation following Trauma

The distributions of TMRM extravasation was measured horizontally and vertically to better characterize the expansion and development of trauma-induced vasogenic edema formation. Therefore, TMRM extravasation in 5 separate layers ranging from a depth of 50 µm to 300 µm was assessed separately. The most superficial layer (0-50 µm) was excluded due to potential artefactual effects caused by cranial window preparation. As shown in Fig. 14A and 14B, TMRM extravasation was significantly higher in A1 and A2 in almost all layers compared with the sham group (P<0.01, P<0.05 vs sham). However, there was no significant difference in region A3 compared to sham group. No extravasation could be detected in sham-operated animals.

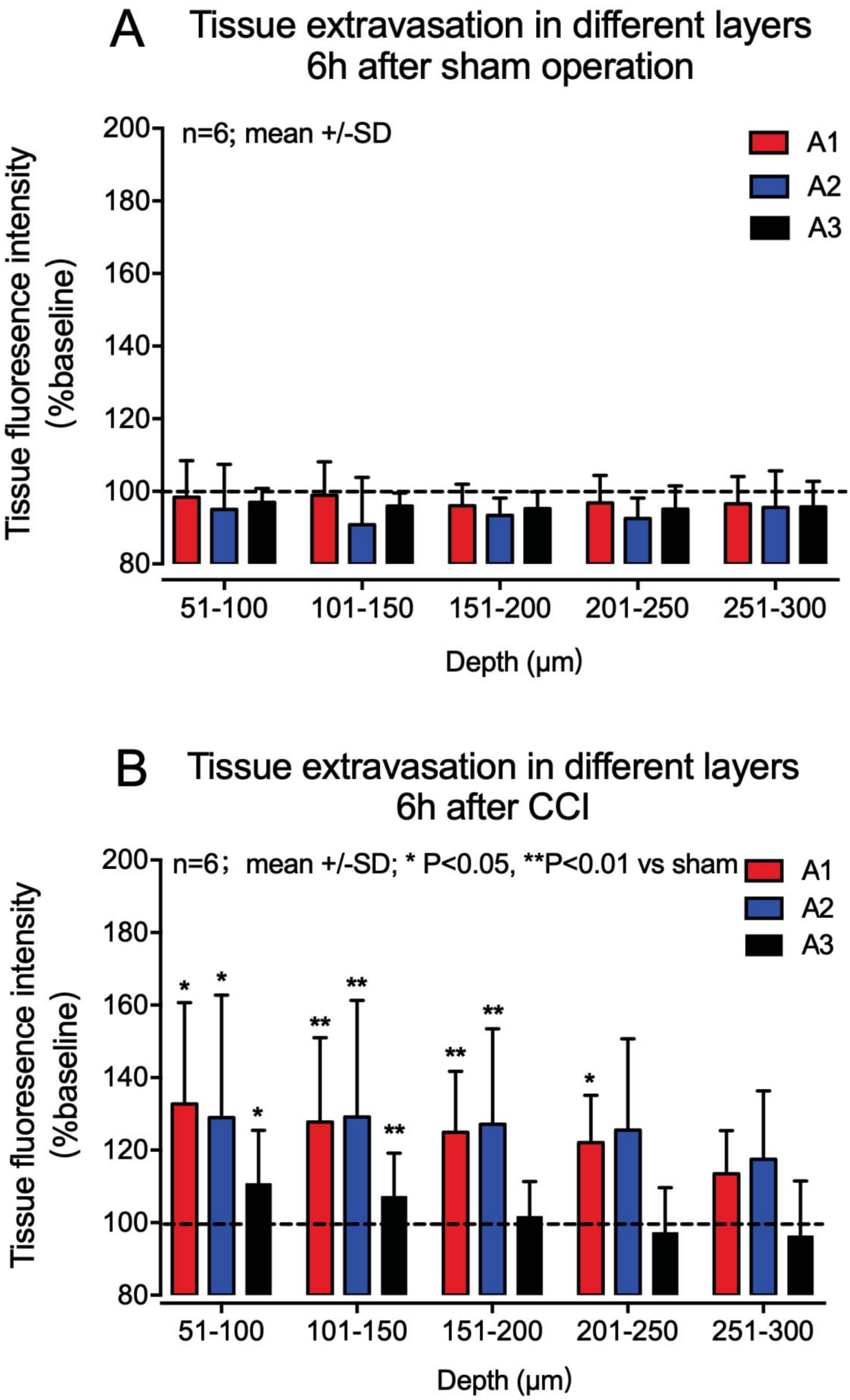
A
Tissue extravasation in different layers
6h after sham operation
n=6; mean +/-SD
A1
A2
A3
Tissue fluoresence intensity
(%baseline)
200
180
160
140
120
100
80
51-100
101-150
151-200
201-250
251-300
Depth (µm)
B
Tissue extravasation in different layers
6h after CCI
n=6; mean +/-SD; * P<0.05, **P<0.01 vs sham
A1
A2
A3
Tissue fluoresence intensity
(%baseline)
200
180
160
140
120
100
80
51-100
101-150
151-200
201-250
251-300
Depth (µm)

Figure 14: Extravasation of TMRM in the depth. Fluorescence intensity was assessed in 5 layers reaching from 50 µm to 300 µm into the brain (excluding the most superficial layer). The dotted line represents the baseline. *P<0.05, **P<0.01 (vs sham). SD=standard deviation.

3.3 Long-term Development of Vasogenic Brain Edema Formation after TBI

3.3.1 General Conditions after TBI

As one parameter for the general condition of the animals the body weight before and after surgery was measured. Before surgery, body weight did not differ significantly between groups (25.5±3.0 g in the CCI group and 25.4±2.4 in the sham group). On the first day after CCI, the animals presented a weight loss of around 1 g. Sham operated mice showed a milder weight loss; however, there was no significant difference between groups. Body weight in both groups slightly increased 2 days post-surgery and reached 25.3±2.5 and 26.1±1.8 in the CCI and sham group, respectively. There was no significantly difference between groups.

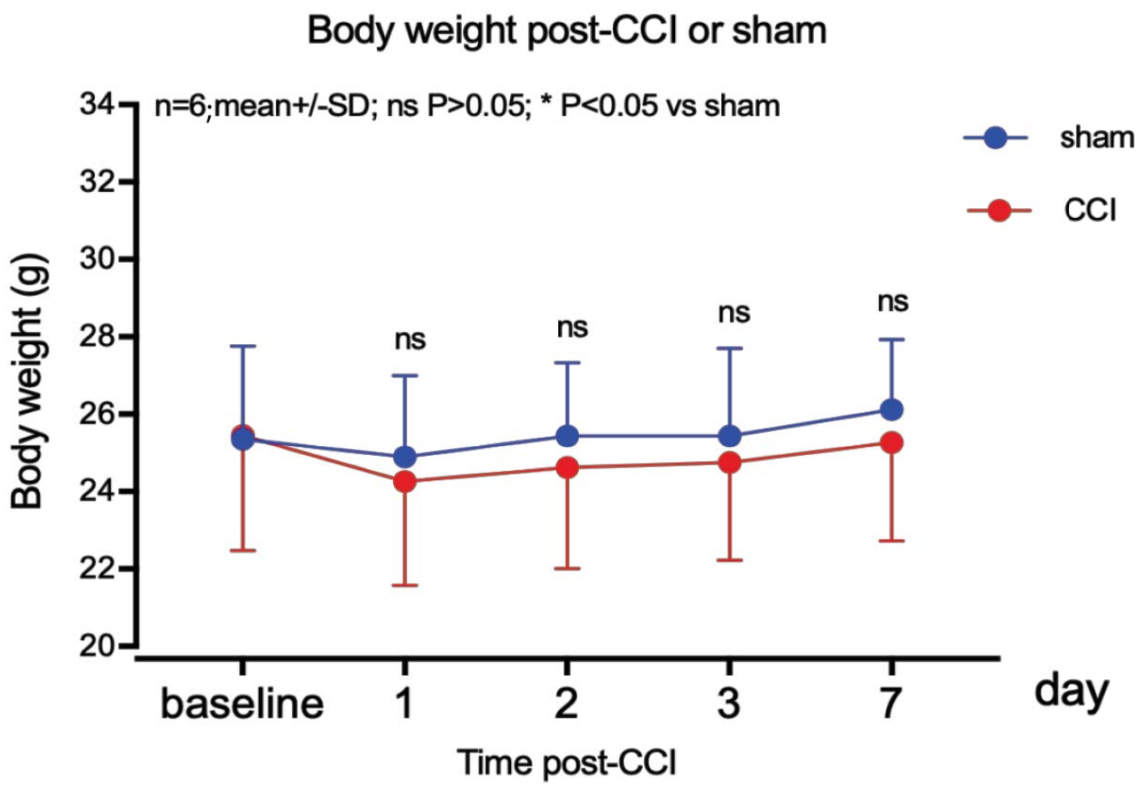

Figure 15: Body weight was measured in each group on day 1, 2, 3, and 7 following CCI or sham operation.

Additional to body weight, a neurological score was assessed to monitor the functional outcome of the animals. For this score, behavior, general condition, weight loss, neurologic deficits, wound conditions, vigilance, and epileptic seizures were recorded on day 1, 2, 3, and 7 following CCI or sham operation. A score of zero reflects no neurological deficit. On the first day following operation, there was a marked increase of the neurologic score after trauma as compared to sham surgery ($p<0.05$ vs. sham). Afterwards, the mice recovered quickly and from the 3rd day onwards there was no abnormal behavior observed in both groups.

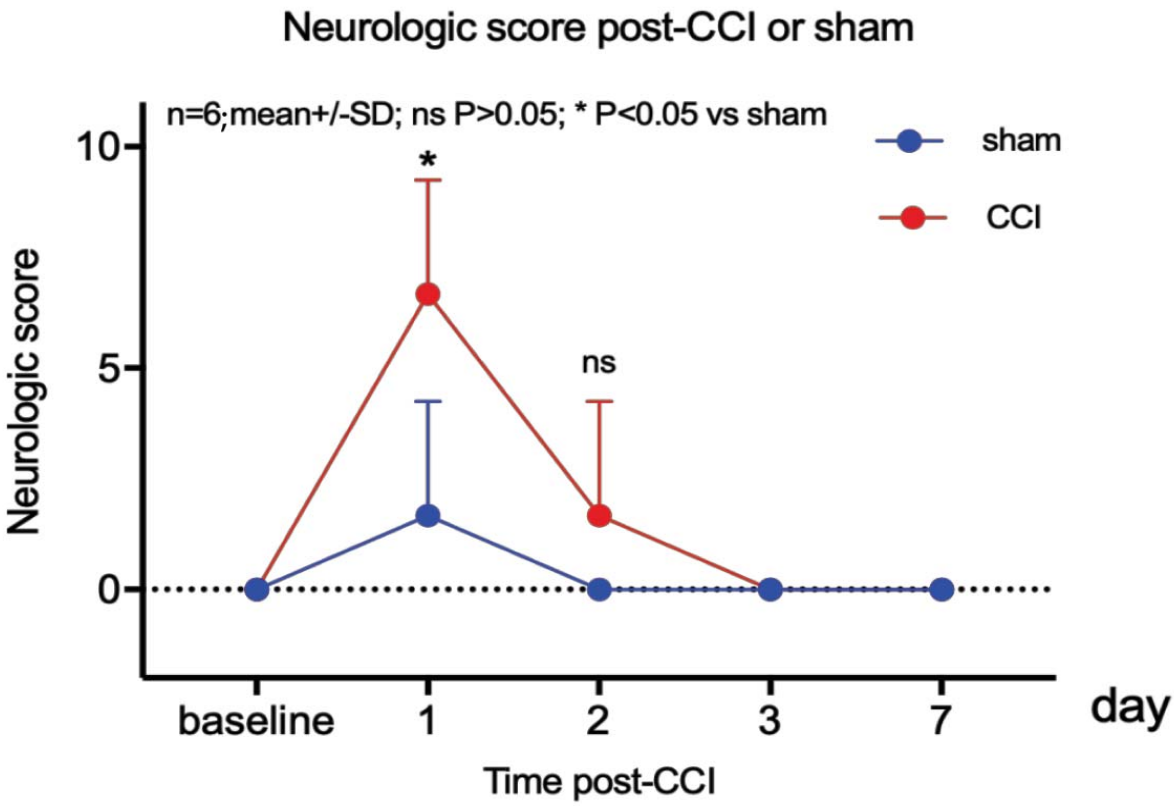

Figure 16: Neurologic score was assessed in each group at day 1, 2, 3, and 7 following CCI or sham operation.

3.3.2 Physiological Parameters during and after Imaging

In line with the experiments investigating the short term development of vasogenic brain edema, body temperature, mean arterial blood pressure and end-tidal CO_2 were also monitored throughout the experiments investigating vasogenic brain edema at later time points following CCI. All values were within their respective physiological range and showed no significant difference between groups (Fig. 17). At the end of the experiment, blood gases (pH, pCO_2 and partial pressure of oxygen (pO_2)) were determined. As shown in Table 3, all values were within their respective physiological range and did not differ significantly between groups. Also in this experimental series pH was acidotic with a range of 7.2-7.3.

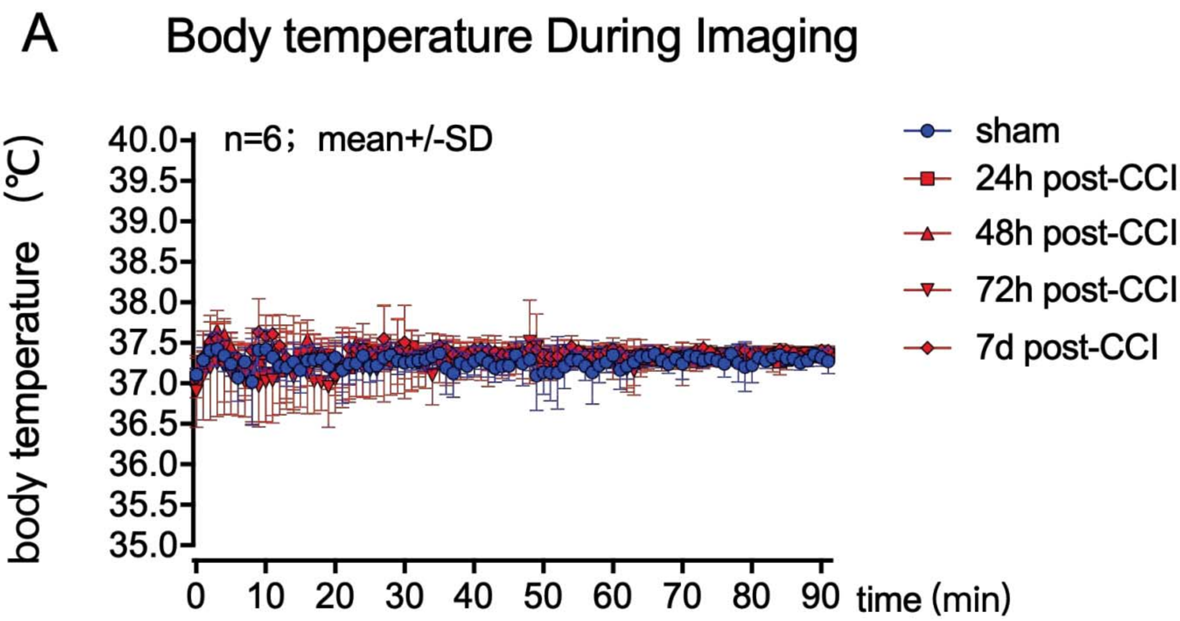

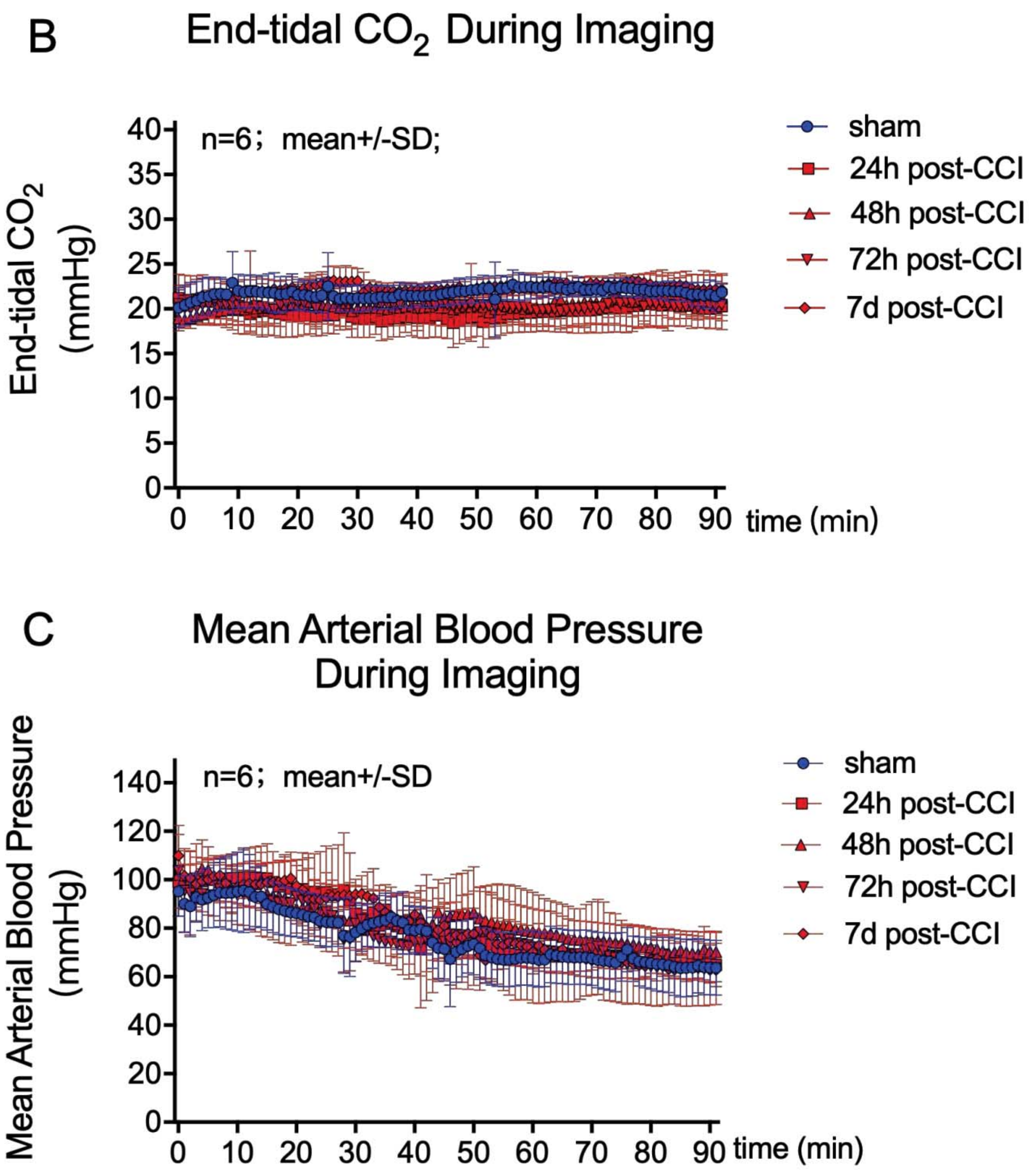

Figure 17: Physiological parameters obtained in the experiments investigating vasogenic brain edema formation 24h-7d following CCT. Core body temperature (A), End-tidal CO_2 (B), and mean arterial blood pressure (C) were monitored continuously throughout the experiments.

Table 3: Arterial blood gases and pH at the end of experiments

Group (n=6)	*pH*	*pCO_2 (mmHg)*	*pO_2 (mmHg)*
Sham	7.3±0.0	43.4±7.1	83.6±17.4
24h post-CCI	7.3±0.1	45.7±6.6	94.8±26.6
48h post-CCI	7.3±0.1	43.9±6.3	81.6±27.4
72h post-CCI	7.3±0.1	44.1±9.7	79.4±20.4
7d post-CCI	7.3±0.0	45.5±8.2	78.6±15.37

Data were shown as mean ± standard deviation

3.3.3 Temporal Profile of TMRM Extravasation

As described above, 2-photon imaging was conducted immediately after TMRM injection to determine baseline fluorescence intensity, and repeated 30, 60, and 90 minutes after TMRM injection in all regions (A1-A3). As shown in Fig. 18, no TMRM extravasation could be detected in sham operated animals at any time throughout the experiment. TMRM extravasation could be detected at all-time points following brain trauma with different intensity. The strongest signals were observed during 30 to 90 min of imaging at 48 and 72 h after CCI. At 24 h post CCI, TMRM extravasation could be detected 60 minutes after TMRM injection. At 7 days following CCI only a mild increase of fluorescence intensity was visible at 90 minutes after TMRM injection.

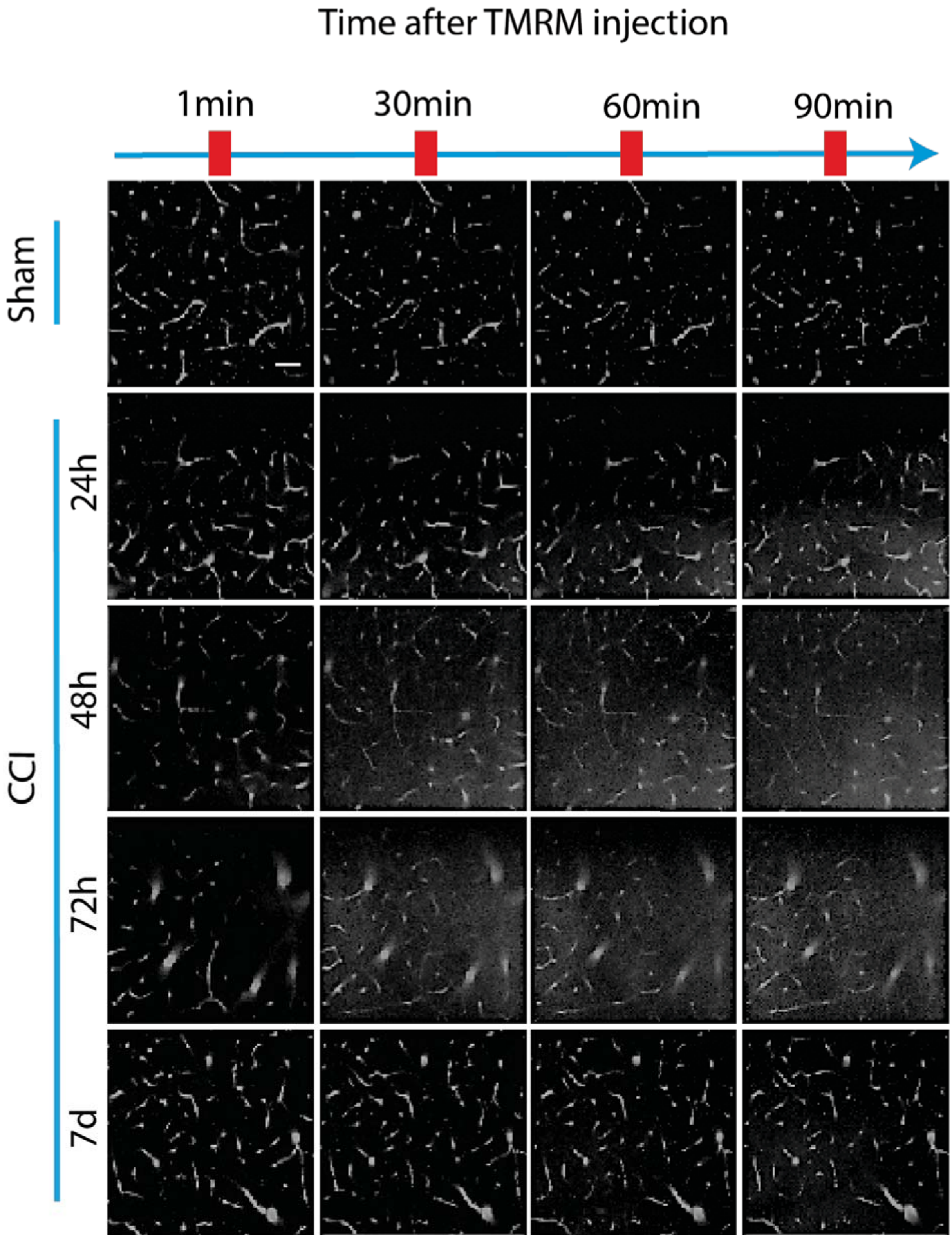

Figure 18: Long-term development of vasogenic brain edema formation 24h-7d after CCI or sham operation. Vessels were labeled with TMRM. Region A1, depth 150 µm; scale bar, 50 µm.

Again, vasogenic brain edema formation was also quantified by assessing fluorescence intensity. No change of fluorescence intensity could be detected in sham operated animals (Fig. 19A). Following trauma, fluorescence intensity in region A1 and A2 reached 120%, 140%, 140% and 110% of baseline after 24h, 48h, 72h and 7d after injury, respectively (Fig. 19B-E). However, compared with the TMRM extravasation in A1 and A2, TMRM extravasation in region A3, i.e. the region most distal to the contusion, was weaker. Furthermore, after trauma the fluorescence intensity increased continuously throughout the imaging period in all three regions (A1-A3). TMRM extravasation was most prominent 48h following CCI ($P<0.01$, vs sham, Fig. 19F). At 24h and 72h after trauma, only in region A1 and A2 a remarkably elevated fluorescence intensity could be detected ($P<0.05$, $P<0.01$, vs sham, Fig. 19F). At 7 days following injury, there was no significant difference in fluorescence intensity in all regions (A1-A3) compared to sham operation (Fig. 19F). In each figure, the baseline is presented as a dotted reference line.

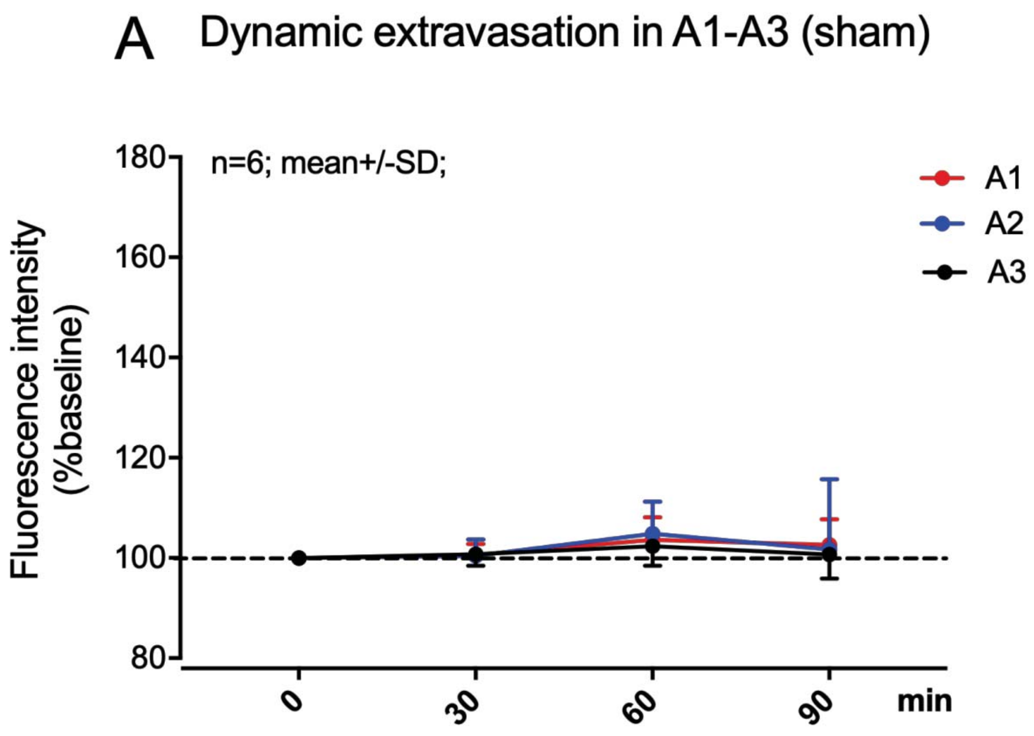

B Dynamic extravasation in A1-A3 (24h)

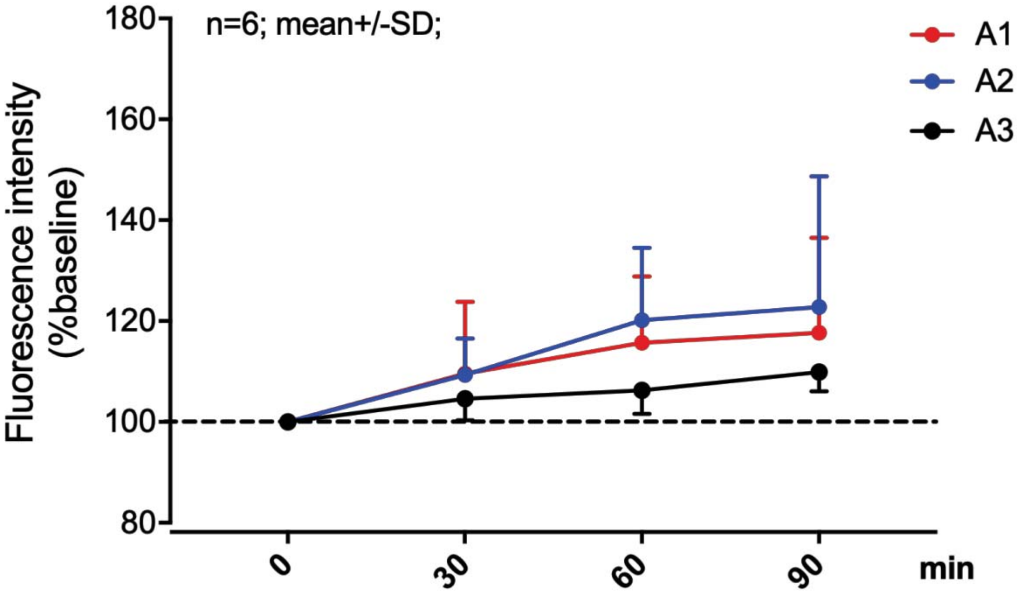

C Dynamic extravasation in A1-A3 (48h)

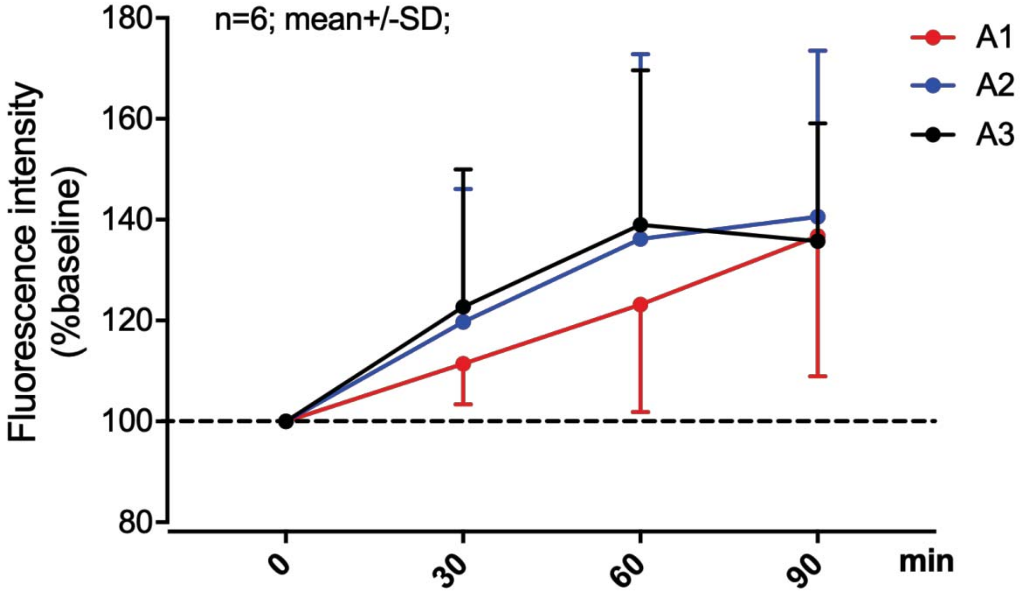

D Dynamic extravasation in A1-A3 (72h)

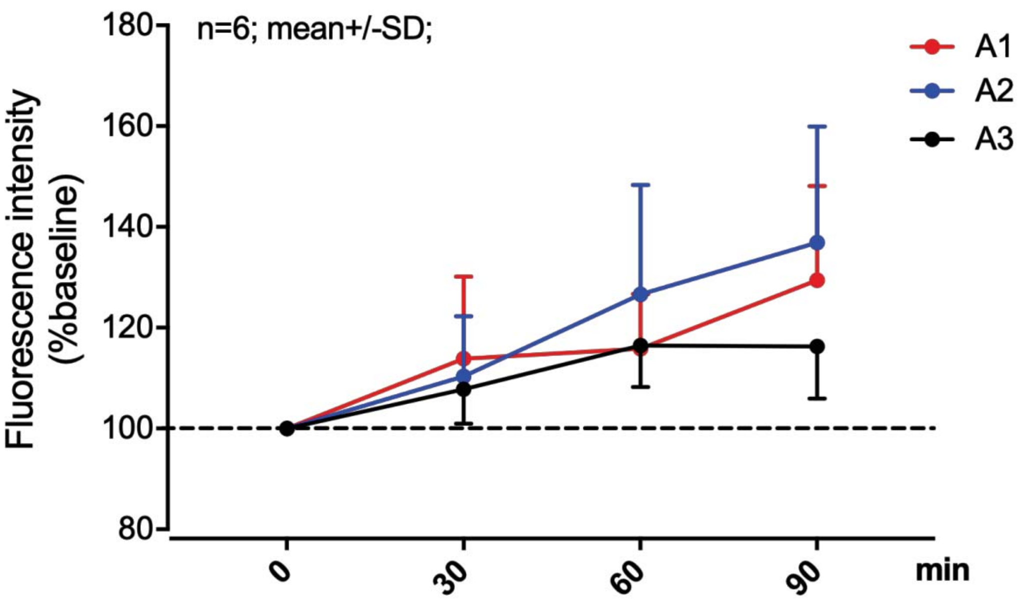

E Dynamic extravasation in A1-A3 (7d)

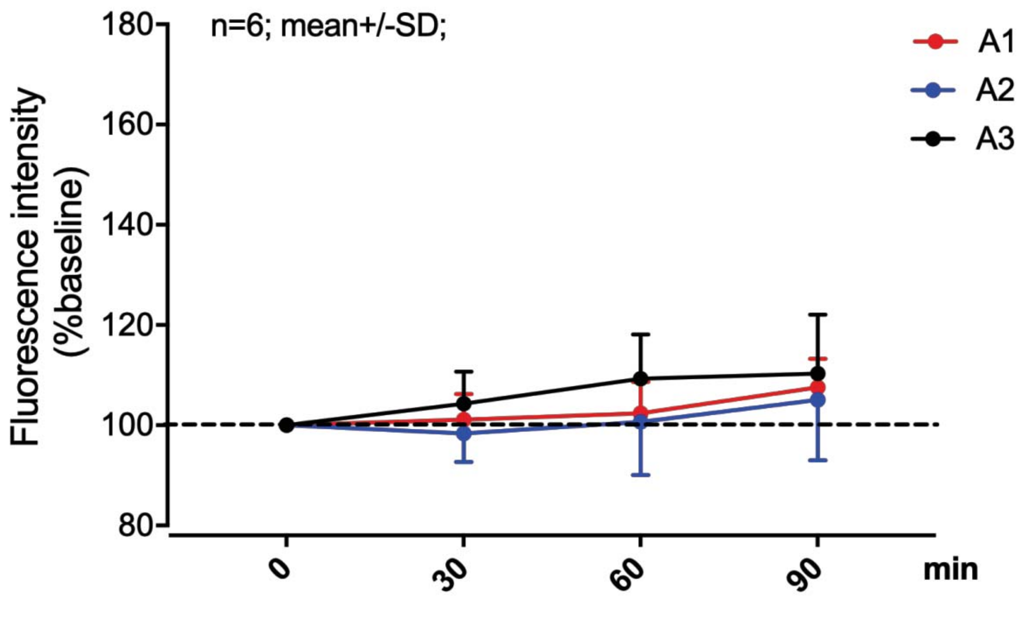

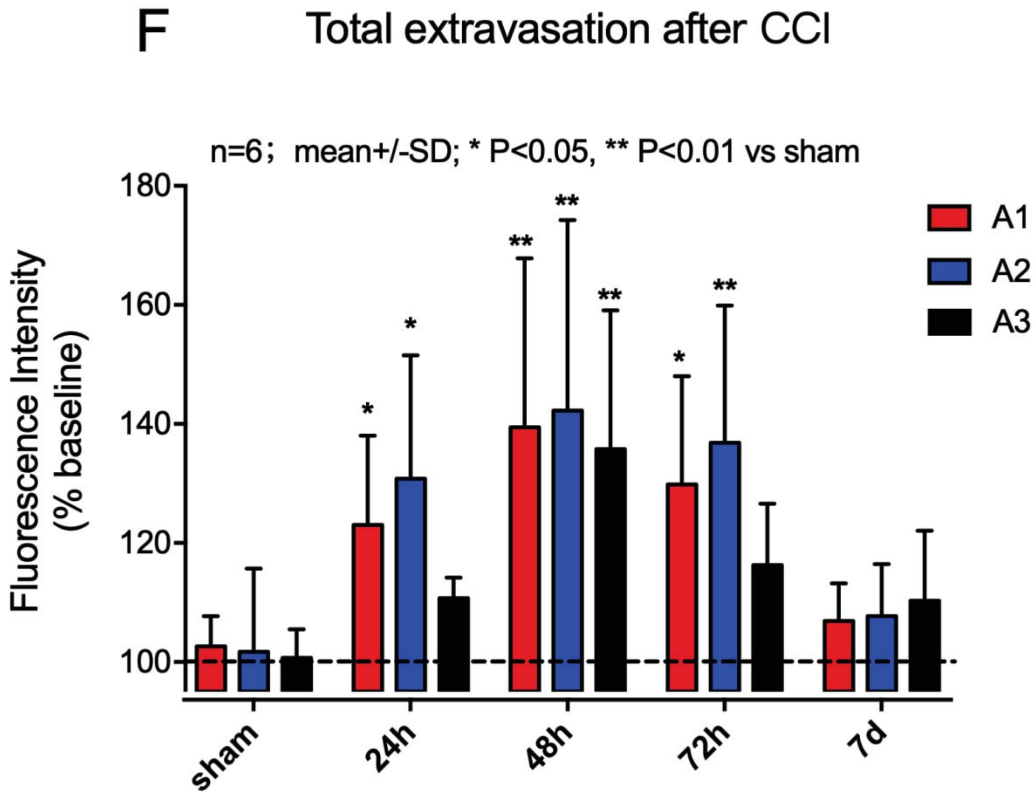

Figure 19: Long-term development of vasogenic brain edema formation after CCI or sham operation (24h-7d). TMRM extravasation is depicted as fluorescence increase in percent of the baseline fluorescence.

3.3.4 Spatial Distribution of Vasogenic Brain Edema Formation following Trauma

3.3.4.1 Spatial Distribution of TMRM Extravasation

For the vertical discrimination of vasogenic brain edema formation, TMRM extravasation was again determined in 5 separate layers of 50 µm, ranging from a depth of 50 to 300 µm. As shown in Fig. 20A, no extravasation appeared in sham-operated animals and at 7 days following trauma in all different layers. At earlier time points after injury, TMRM extravasation was most dominant in the superficial layers (P<0.05, P<0.01, vs sham (Fig. 20B). At 24, 48, and 72 h following trauma, TMRM extravasation was more pronounced in region A1 and A2, while the strongest increase in fluorescence intensity was seen in region A3 at 7 days after trauma.

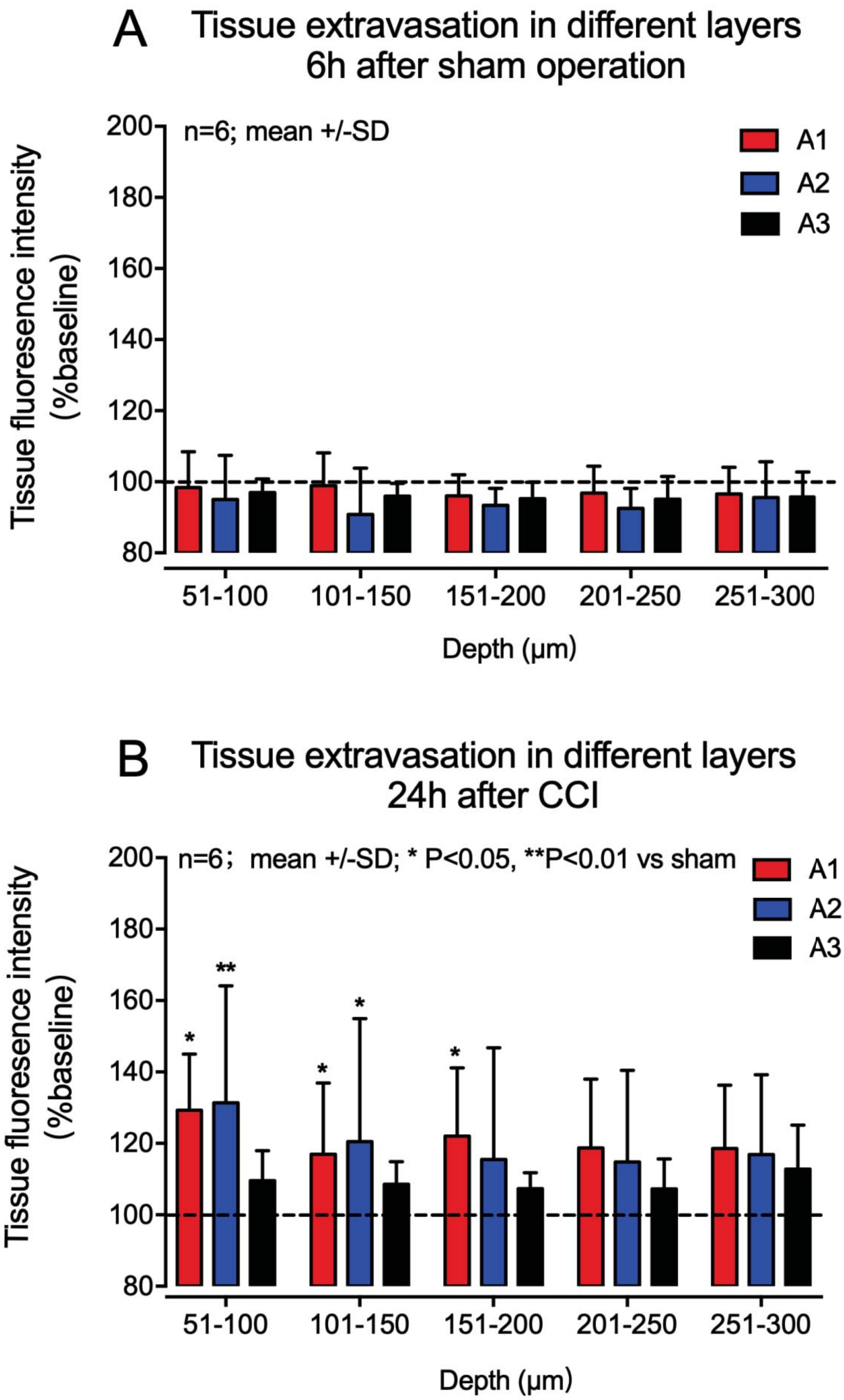
A
Tissue extravasation in different layers
6h after sham operation
n=6; mean +/-SD
A1
A2
A3
Tissue fluoresence intensity
(%baseline)
200
180
160
140
120
100
80
51-100
101-150
151-200
201-250
251-300
Depth (μm)
B
Tissue extravasation in different layers
24h after CCI
n=6; mean +/-SD; * P<0.05, **P<0.01 vs sham
A1
A2
A3
Tissue fluoresence intensity
(%baseline)
200
180
160
140
120
100
80
51-100
101-150
151-200
201-250
251-300
Depth (μm)

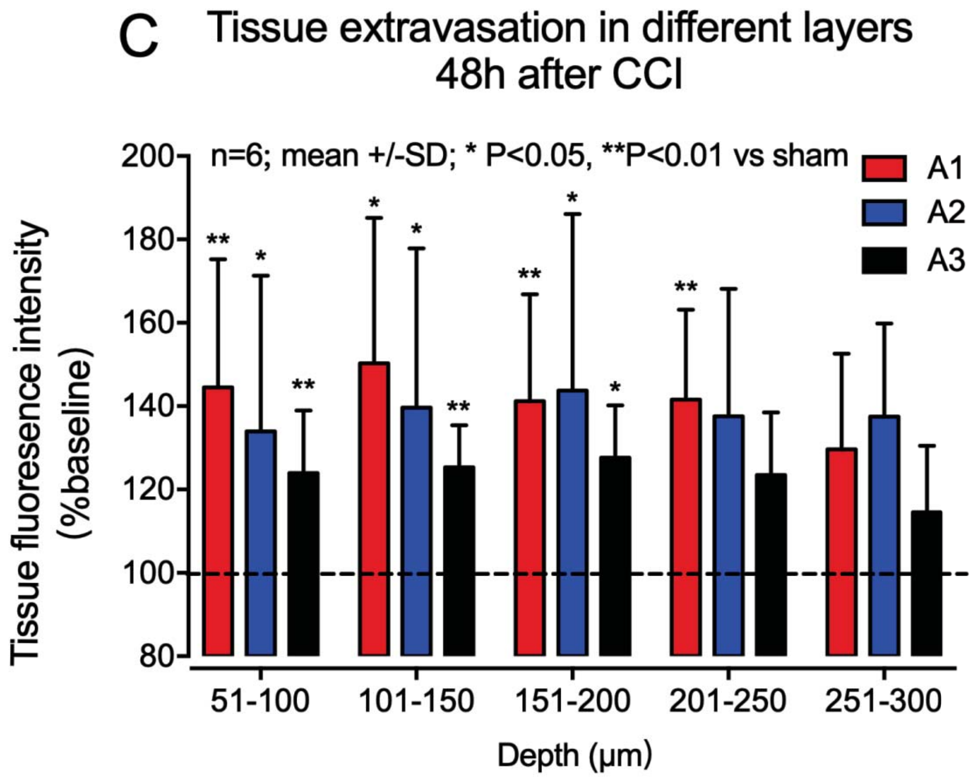
C
Tissue extravasation in different layers
48h after CCI
n=6; mean +/-SD; * P<0.05, **P<0.01 vs sham
A1
A2
A3
Tissue fluoresence intensity
(%baseline)
200
180
160
140
120
100
80
51-100
101-150
151-200
201-250
251-300
Depth (μm)

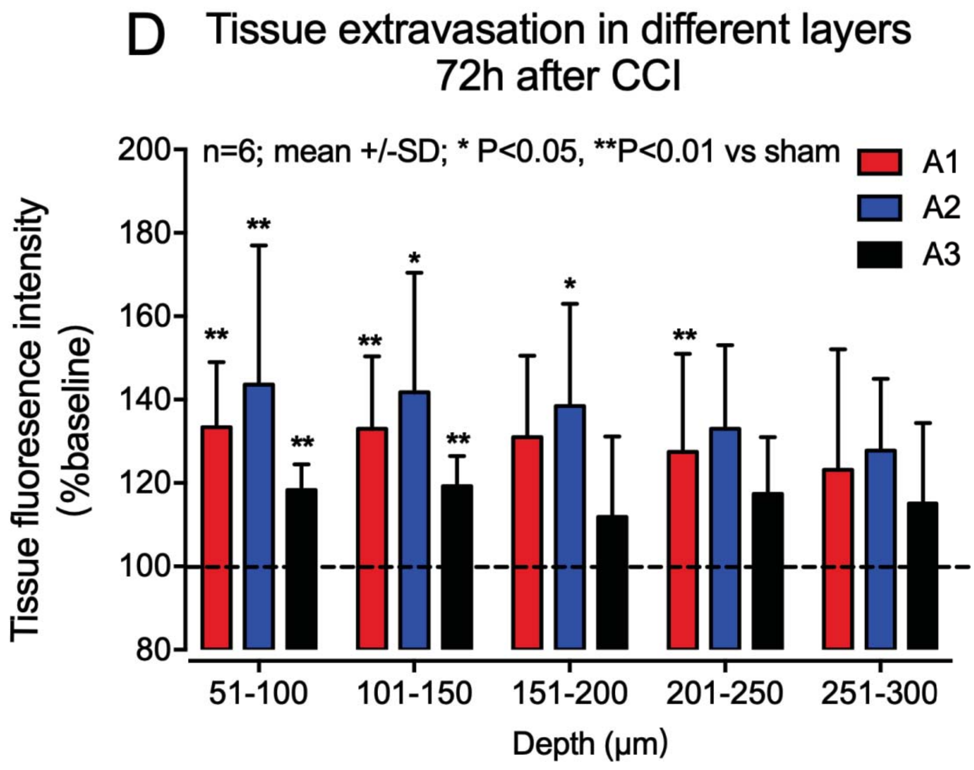
D
Tissue extravasation in different layers
72h after CCI
n=6; mean +/-SD; * P<0.05, **P<0.01 vs sham
A1
A2
A3
Tissue fluoresence intensity
(%baseline)
200
180
160
140
120
100
80
51-100
101-150
151-200
201-250
251-300
Depth (μm)

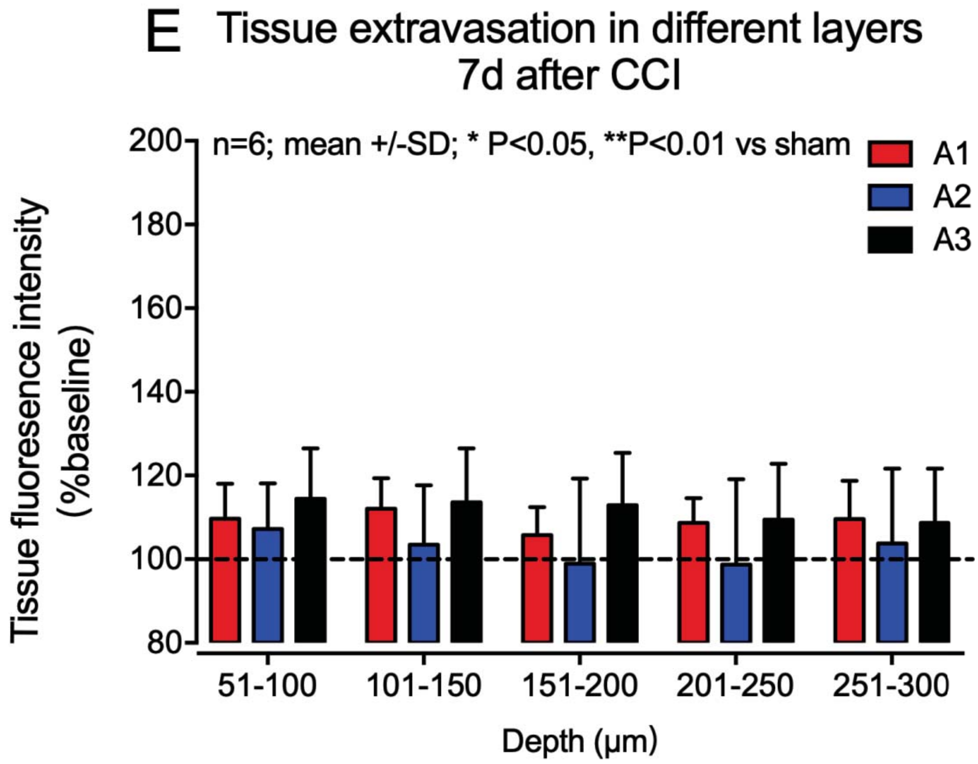

Figure 20: Vertical distribution of TMRM extravasation at different time points following CCI or sham operation. Fluorescent intensity was assessed in 5 layers reaching from 50 to 300 µm into the brain (excluding the most superficial layer reaching 0–50 µm).

3.3.4.2 Spatial Distribution of TMRM Extravasation in 2-dimensional Heat-map

To assess the spatial distribution of vasogenic edema formation the regions A1-A3 were divided into 6 x 6 sub-regions and fluorescence intensity was determined in each sub-region. The result is presented as a heat map in Fig. 21. No extravasation could be detected following sham operation. Following CCI, TMRM extravasation was most dominant in region A1 and A2, i.e. proximal to the contusion, at all time points.

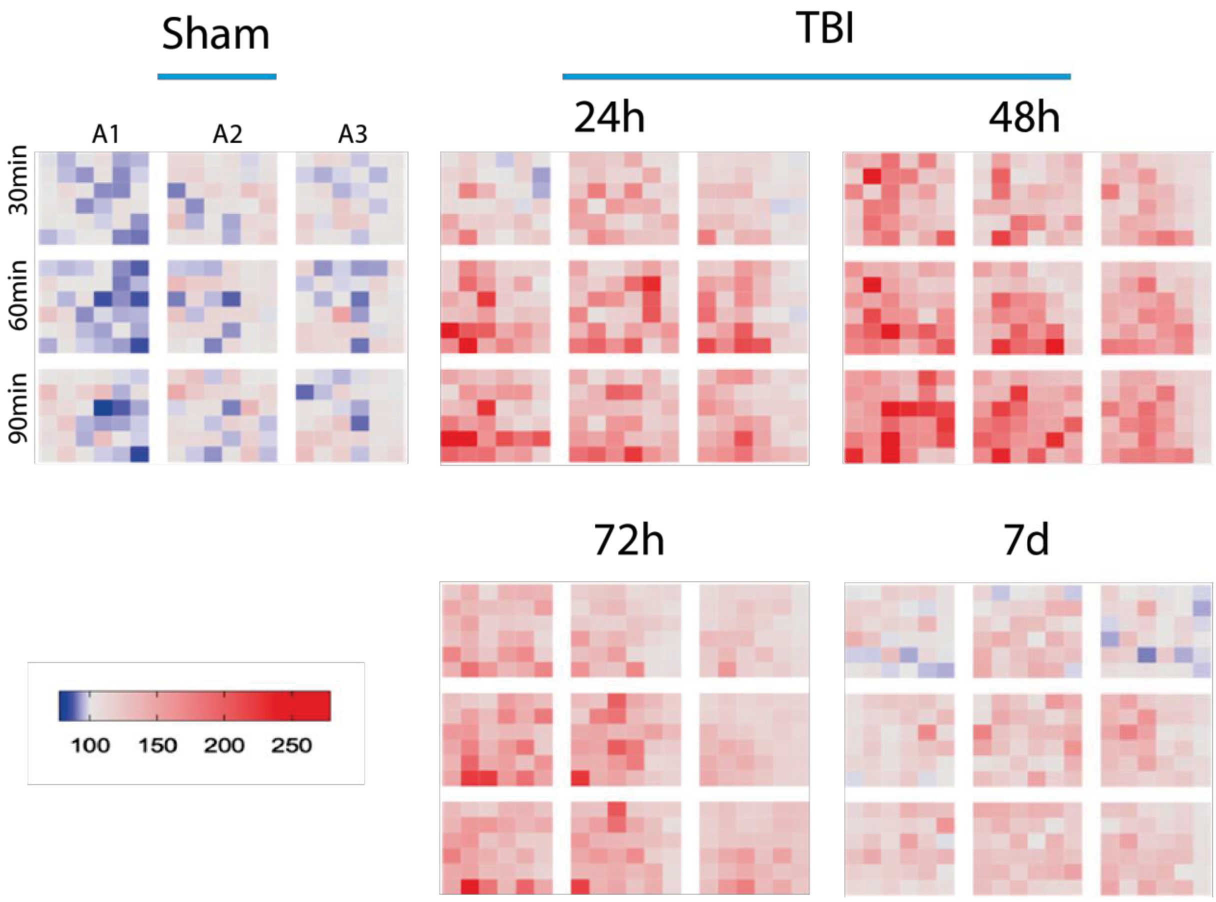

Figure 21: Spatial distribution of TMRM extravasation in 2-dimensional heat-maps.

3.4 Characterization of Extravasation Speed after TBI

In order to quantify the permeability of the BBB both short-term (4 h) and long-term (24 h-7 d) after trauma, the average speed of tissue fluorescence intensity increase was calculated using the following formula:

(Fluorescence intensity at 90 min– baseline fluorescence intensity)/90 min.

The different regions A1-A3 were analyzed separately and the results are shown in Fig. 22. Extravasation speed varied over time with two peaks at 4 h and 48 h post CCI. TMRM extravasation started as early as 4 hour following CCI, then decreased until 24 hours after injury, reached another peak at 48 hours after CCI, and slowly decreased until 7 days following trauma.

The early peak was detected in A1 at 4 h after trauma while the second and longer lasting peak from 48 to 72 hours post CCI was more dominant in A2. TMRM extravasation was slower in A3 at almost time points except at 7days post CCI.

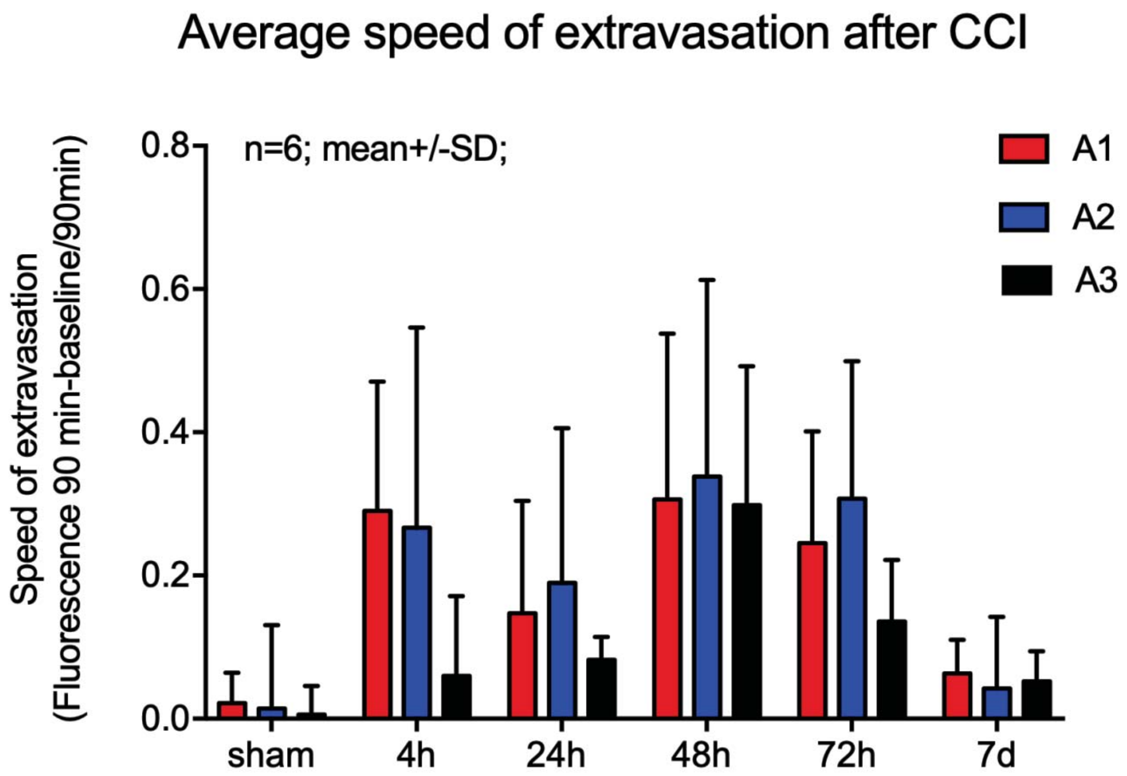

Figure 22: Average speed of extravasation after CCI or sham at different time points as a direct measure of BBB permeability

4. Discussion

4.1. Setup

BBB opening and consecutive vasogenic edema formation following TBI results in accumulation of brain water, increased ICP, and subsequent perfusion deficits and is one of the main contributors to the fate of TBI patients (Jha et al., 2019; Shlosberg et al., 2010; Unterberg et al., 2004). Consequently, brain edema formation has long been in the focus of trauma research. However, until recently, the time course and importance of vasogenic brain edema formation have been discussed controversially. A detailed spatial and temporal investigation in vivo was not possible due to technical limitations.

In the current study these limitations could be overcome by using *in vivo* 2-photon microscopy. This technique provides a high spatial resolution in 3D (Cheng et al., 2019; Denk et al., 1990). By combining a clinical relevant trauma model with *in vivo* 2-photon microscopy, a detailed and dynamic characterization of vasogenic brain edema formation with high spatial and temporal resolution was possible.

For the current study TMRM with a molecular weight of 40,000 Dalton was used as fluorescent tracer. This was specifically chosen because it is the commercially available tracer with the molecular weight closest to the one of albumin (70,000 Da). A leakage of molecules with a size of more than MW 50,000 Dalton across the BBB occurs only when its permeability is increased (Guérin et al., 2001). Such an increase in BBB permeability results not only in leakage of larger molecules but mainly in an extravasation of water (Reyes-Aldasoro et al., 2008). TMRM extravasation was visualized as increase of fluorescence intensity in the parenchyma. TMRM extravasation and fluorescence intensity in the parenchyma were then used as surrogate parameters to assess vasogenic edema formation (Cheng et al., 2019).

4.2 TBI-induced Cerebral Edema Formation

Cerebral edema is defined as an increase of brain tissue water content both in individual cells and interstitial space (Jha et al., 2019). Cerebral edema can lead to intracranial hypertension which is associated with unfavorable outcome following TBI (Maas et al., 2008; Unterberg et al., 2004; Zweckberger et al., 2003). Cerebral edema formation after TBI is a complex and highly heterogeneous process which involves various pathophysiologic pathways (Donkin and Vink, 2010; Jha et al., 2019; Lukaszewicz et al., 2011; Sahuquillo et al., 2001; Unterberg et al., 2004). The underlying mechanisms of cerebral edema formation may differ depending on the original forces (closed-head injury, penetrating injury, or blast-induced injury). However, regardless of the *in vivo* models used, TBI results in tissue deformation and inflammatory responses, and it leads to a disruption of BBB integrity (Hadass et al., 2013; Jayakumar et al., 2011; Kiening et al., 2002; Kimbler et al., 2012; Laird et al., 2014).

4.2.1 Mechanisms of Vasogenic Edema Formation – BBB Breakdown

The BBB was first described by Paul Ehrlich in the 1880 (Mayhan, 2001). Anatomically, the BBB consists of the cerebral endothelium, together with astrocytes, neurons, pericytes and the extracellular matrix, which constitutes a 'neurovascular unit' which is essential for the normal function of the central nervous system (CNS) (Ballabh et al., 2004; Daneman, 2012; Daneman et al., 2010; Obermeier et al., 2013; Zhao et al., 2015). Both animal models and clinical data proved the evidence that BBB breakdown frequently follows brain trauma and can last for a long time (Barzo et al., 1996; Csuka et al., 1999; Kirchhoff et al., 2006; Lenzlinger et al., 2002; Stahel et al., 2001). Usually, the initial injury of BBB caused by direct tissue damage, occurs in milliseconds to seconds, leading to irreversible blood vessel and cellular damage (Alluri et al., 2015). The BBB is a dynamic structure in which a closing or opening of largely depends on what proteins are expressed (Ballabh et al., 2004).

The main structures responsible for the BBB properties are the tight junctions (Brightman and Reese, 1969; Nabeshima et al., 1975; Reese and Karnovsky, 1967; van Deurs and Koehler, 1979). Tight junction proteins were identified in cerebral endothelial cell tight junctions. These proteins includes claudins (claudin-1, -5) (Liebner et al., 2000; Morita et al., 1999), occludins (Ando-Akatsuka et al., 1996; Furuse et al., 1993), zonula occludens ((ZO)-1,-2, and −3) (Balda and Anderson, 1993; Haskins et al., 1998; Jesaitis and Goodenough, 1994), and tricellulin (Haseloff et al., 2015). Tight junctions regulate major functions of endothelial cells in different ways such as modulation of gene expressions, signal transduction, and post-translational modifications (Bauer et al., 2011; Dejana et al., 2000; Matter and Balda, 2003).

Due to the importance for the tightness of the BBB, tight junctions play a key role for fluid extravasation and swelling post TBI. Abdul-Muneer *et al.* showed that the expression of tight junction proteins in brain microvessels was down-regulated following blast-induced mild TBI (Abdul-Muneer et al., 2013). The same tendency was shown in expression of claudin-5 and ZO-1 (Chen et al., 2014; Hue et al., 2014).

4.2.2 Other Molecular Candidates Responsible for Vasogenic Edema Formation

Neuroinflammation after TBI can be both can beneficial and harmful (Corrigan et al., 2016). In both focal and diffuse injury, neutrophilic infiltration and microglial response occurs in an early phase, followed by migration of monocytes, lymphocytes and astrocytes (Corrigan et al., 2016; Jassam et al., 2017; Simon et al., 2017). The activation of cells including neurons, astrocytes, endothelial cells, and leukocytes was able to induce inflammatory gene expression, further leading to release of inflammatory cytokines and chemokines (Jassam et al., 2017).

Cytokines such as TNF, IL-6, IL-8, and IL-1β, are commonly known to play important roles in the early phase of post TBI-induced inflammation (Helmy et al., 2011). Most of them have been confirmed to be associated with BBB dysfunction. For instance, in patients with TBI, TGF-β in CSF was increased and acts as an anti-inflammatory and neuro-protective mediator by regulating IL-6, thereby compromising BBB integrity (Morganti-Kossmann et al., 1999; Shen et al., 2011). In another clinical study, the level of pro-inflammatory IL-1β, IL-6, anti- inflammatory IL-10 and IL-8 were up-regulated in CSF post TBI (Buttram et al., 2007). However, another clinical study demonstrated that although the level of IL-6, IL-8 and IL-10 were found to be higher than corresponding plasma levels, there was no correlations between BBB dysfunction and cytokines (Maier et al., 2001).

Some well-studied chemokines in TBI include chemokine ligands CXCL1 and CXCL2 and CCL2 (Woodcock et al., 2017). So far, numerous studies have demonstrated that these factors were also associated with increased BBB permeability after TBI, especially in the acute phase (Chodobski et al., 2011; Kossmann et al., 1997; Stahel et al., 2001; Stamatovic et al., 2003; Yang et al., 2017).

MMPs, known as a family of zymogens, are responsible for the dynamic remodeling of the extracellular matrix (ECM). MMPs exacerbate the inflammatory cascades by activating inflammatory cytokines such as IL-1β and tumor necrosis factor α (TNF-α) and degrade ECM proteins (Rash et al., 1998). In severe human TBI, levels of MMP-8 and -9 were initially highly expressed, followed by MMP-2, MMP-3, and MMP-7 expression (Roberts et al., 2013). Wang *et al.* showed that secretion of MMP-2 and MMP-9 is significantly increased in cultured rat cortical neurons (Wang et al., 2002). During pathophysiological conditions, MMPs degrade tight junction proteins and regulate cytokines and chemokines thereby leading to BBB disruption (Tasaki et al., 2014). In TBI, several studies have suggested that MMPs can be activated by infiltrating or resident inflammatory cells, oxidative stress, and some cytokines (Price et al., 2016; Winkler et al., 2016).

Other main molecular candidates which are discussed to be involved in vasogenic edema formation include vascular endothelial growth factor A (VEGF-A), Substance P (SP) and bradykinin. VEGF-A, which is mainly expressed in neurons, astrocytes, and ependymal cells, is considered to be a critical factor for regulating microvascular permeability. There are two major VEGF-A receptors called VEGF-receptor (R)-1 and VEGFR-2 (Pan et al., 2017). Several studies have suggested that VEGF-A could bind to VEGFR1 to regulate brain endothelial cell permeability by targeting tight junction proteins (claudin-5, occludin) (Argaw et al., 2009; Murakami et al., 2009; Wang et al., 2001). VEGF is also believed to play a critical role in neuroinflammation post TBI. For instance, VEGF-C could induce alternative activation of microglia, which appears to be beneficial for recovery from TBI (Ju et al., 2019). Substance P (SP), known as a member of the tachykinin family, is associated with neurogenic inflammation and vascular permeability, which causes BBB disruption (Corrigan et al., 2016). In animal models of TBI and patients with TBI, circulating levels of SP are elevated within the first few hours after injury early, and may be associated with severity and mortality (Donkin et al., 2009; Lorente et al., 2015; Zacest et al., 2010).

4.3. Brain edema formation and brain swelling following trauma

In the first part of the current study, brain swelling and edema formation was investigated *ex vivo* in the whole brain at different time points after experimental TBI. Brain swelling was visible as early as 4 hours following CCI (Fig. 9). At the same time, brain water content in the ipsilateral hemisphere was significantly increased compared with sham operated mice. Thereafter, brain swelling continued and reached its maximum 48 hours post-trauma. Correspondingly, brain water content remained on a high level until 72 hours after TBI. At 7 days after CCI, no more swelling was visible and the brains showed a posttraumatic lesion cavity. However, brain water content was still higher than in the control group. These results demonstrate a rapid increase of brain water content already during the first few hours after CCI. Brain water content remains high in the ipsilateral hemisphere despite recovery of brain swelling. The regress in brain swelling is most likely due to a reduction in contusion size after 72 hours following injury which is caused by a physiological degradation process. Consequently, brain edema persists until at least 7 days following TBI. These results are in line with previously published data (Yang et al., 2018; Zweckberger et al., 2006; Zweckberger and Plesnila, 2009).

However, these experiments do not provide information about the underlying mechanism of brain edema formation. Traditionally, cerebral edema after TBI has been categorized as ‘vasogenic’ or ‘cytotoxic’ edema (Donkin and Vink, 2010; Jha et al., 2019; Shlosberg et al., 2010; Unterberg et al., 2004). Both forms of edema have been reported to develop within the first few minutes or hours after TBI (Jha et al., 2019). However, the exact time course of each form of edema remains controversial. While cytotoxic edema formation is believed to play an important role following brain trauma (Unterberg et al., 2004), the role of vasogenic brain edema formation has been discussed quite controversially.

4.4 Characterization of Vasogenic Brain Edema following Experimental TBI

Most published data indicate that the primary opening of BBB occurs immediately after TBI. In a study by Barzó *et al.*, a transient BBB opening was reported at the time of the trauma in a closed head injury model. However, BBB opening was reported to lasts no more than 30 minutes, and vasogenic brain edema formation was discussed to be of only minor importance (Barzo et al., 1996). In another study using *in vivo* microscopy following CCI, Whalen MJ *et al.* claimed that BBB permeability was increased immediately after TBI and was maximal 30 to 60 mins after TBI (Whalen et al., 1999). By using 2-photon microscopy and CCI, our group previously confirmed that vascular leakage started as early as 2.5 h post CCI (Schwarzmaier et al., 2015a). In the current study, an increase in BBB permeability already within the first 4h following injury was confirmed.

However, the ensuing time-course throughout the following days has been discussed controversially so far. While some stated only a minor importance of vasogenic brain edema formation in the sub-acute phase following brain trauma (Barzo et al., 1996), others reported a chronic disruption of BBB until several days to weeks following trauma. Abnormal permeability to IgG was reported to occur within the first hour after injury and to continuously increase until 24 hour thereafter (Tanno et al., 1992). In a blast injury model, Yeoh *et al.* showed that BBB disruption peaks at 1-2 days after injury (Yeoh et al., 2013). In other experimental TBI studies, the maximal BBB permeability appeared at 4 hours after injury, and lasted until 3-7 days (Baldwin et al., 1996; Baskaya et al., 1997; Habgood et al., 2007; Shapira et al., 1993), 2 weeks (Strbian et al., 2008) or even 30 days following injury (Korn et al., 2005). Moreover, some clinical studies have shown long-term BBB disruptions that can last for months to years following brain trauma (Tomkins et al., 2008).

In addition to the discrepancies reported regarding vasogenic brain edema formation during the sub-acute phase following injury, it remains unclear whether sub-acute and chronic BBB disruptions which have been reported are primary events caused by the injury or secondary events caused by ongoing pathological processes. Opening of the BBB after experimental brain injury has been reported to follow a biphasic pattern: The onset of the early phase occurs rapidly within few hours following trauma (Schwarzmaier et al., 2015a; Tanno et al., 1992). The second phase starts roughly at 3-7 days following injury (Shlosberg et al., 2010; Zlotnik et al., 2012). The exact time course of BBB disruption after TBI may be related to the different TBI models, animal species, and methods for assessing BBB integrity used in the various studies.

4.4.1 Temporal Profile of Vasogenic Brain Edema formation following TBI

To assess the temporal profile of vasogenic brain edema following TBI, two series of experiments were conducted, one short-term (4h post-CCI) and one long-term (24h-7d post-CCI). Vasogenic brain edema, reflected by extravasation of TMRM, could be detected as early as 4.5 hours following CCI. During the first week following CCI, the vascular leakage persisted and reached its peak at 48 hours post-CCI. Afterwards, it decreased gradually. At 7 days post-CCI, extravasation was still detectable, suggesting that BBB did not close completely.

In addition to the total leakage at different time points following CCI, the average speed of extravasation was determined. The results revealed a biphasic pattern: extravasation speed, a measure for the tightness of the BBB, was fastest in the early phase at 4 hours post-CCI, slowed down at 24 hours following injury and increased again for a prolonged period from 48-72 hours after trauma. These data indicate that BBB permeability changes over time, suggesting different mechanisms underlying leakage. The early peak might be caused by a direct, mechanical damage of the BBB, i.e. a disruption of tight junctions due to shear stress. This seems to recover within the first 24 hours following injury. Since maximal secondary lesion expansion occurs in the CCI model 24h following injury (Zweckberger et al., 2003), this early BBB disruption may represent a key mechanism in the pathophysiology of secondary brain damage by worsening intracranial pressure and cerebral perfusion (Shlosberg et al., 2010). This is in line with other studies describing vasogenic edema formation as an important factor which leads to increased ICP, microcirculatory disturbances and secondary brain damage (Jha et al., 2019; Maas et al., 2008; Winkler et al., 2016).

Interestingly, a second prominent and prolonged opening of the BBB occurred from 48-72 hours following trauma. Even 7 days after injury, the BBB seemed to not have fully recovered, however, TMRM extravasation showed no significant difference after trauma compared with sham operation.

Even though some previous reports argued that vasogenic brain edema occurs only very briefly following TBI (Barzo et al., 1996), others have reported a biphasic time course of increased BBB permeability (Baskaya et al., 1997; Logsdon et al., 2018; Shapira et al., 1993). However, these studies report *ex vivo* results without addressing the extravasation rate *in vivo*. In the current study a biphasic pattern concerning the extravasation speed has been confirmed *in vivo*.

So far, the underlying molecular pathophysiologic mechanisms leading to the biphasic increase of BBB permeability and vasogenic edema formation remain not fully understood. While the BBB breakdown in the acute phase following trauma is most likely directly caused by mechanical forces, a second component induced by neutrophils has been discussed already in the first hours following injury (Adelson et al., 1998; McDonald et al., 2010; Rodriguez-Baeza et al., 2003; Roth et al., 2014; Sangiorgi et al., 2013; Soares et al., 1995), however, this hypothesis remains controversial (Hartl et al., 1997; Whalen et al., 1999). The second and prolonged peak in BBB permeability (48h-72h post-CCI) is hypothesized to be a component of the brain's response to injury. Several mechanisms for the second peak of BBB opening are possible:

1) Reperfusion injury. A damage of the endothelial membranes caused by delayed reperfusion. It is known that ischemic changes in the brain occur in the first hours after brain injury (Krishnappa et al., 1999; Marion et al., 1991), and BBB breakdown may be associated with delayed reperfusion of the ischemic tissues. Correspondingly, zight junction proteins, such as claudin-5, occluding, and ZO-1, were reported to be significantly reduced within that time period, suggesting exacerbated BBB damage (Higashida et al., 2011; Logsdon et al., 2018; Wen et al., 2014; Zhiyuan et al., 2016).

2) Inflammation. Inflammatory reactions caused by leukocytes or cytokines might present another cause for delayed BBB opening. (Soares et al., 1995) since regions with leukocyte recruitment showed BBB disruption (Schwarzmaier et al., 2013). Monocyte-derived macrophages were observed within the cerebral cortex and reached peak numbers in the damaged brain 24 to 48 hours after injury (Semple et al., 2010; Soares et al., 1995). The microglia, the brain's resident inflammatory cells change morphologically and immunologically (Gehrmann et al., 1995; Raivich et al., 1999). They can either promote further damage or play a role in tissue repair. Several studies have confirmed that activation of microglia resulted in BBB disruption. For instance, da Fonseca AC *et al.* suggested that the activation of M1-like microglia is thought to increase BBB permeability by activating MMPs or tight junction proteins (Corrigan et al., 2016; da Fonseca et al., 2014).

3) Metabolic imbalances. The second peak of BBB opening could also be initiated by metabolites which are reported to be released post-trauma, such as free radicals (Hall, 1993; Wu et al., 2018), leukotrienes, prostaglandins (Baskaya et al., 1996a; Biber et al., 2009), polyamines (Baskaya et al., 1996b), and histamine (Wahl et al., 1988). Other mechanisms, such as re-absorption of edema fluid (Holmin and Mathiesen, 1995), cerebral blood flow auto regulatory failure (Rangel-Castilla et al., 2008), or vasospasm (Lee et al., 1997), might coincide with damage to the structural integrity of the BBB (Muellner et al., 2003).

4.4.2 Spatial Profile of Vasogenic Brain Edema Formation following TBI

Vasogenic brain edema formation was also investigated regarding the spatial distribution. With 2-photon microscopy, a detailed 3D scan of the parenchyma was generated and edema formation was visualized up to a depth of 300 µm.

Horizontal spreading

The results show that the degree of vascular leakage appears to be correlated to the proximity to the site of the primary contusion. In region A3, the region most distal to the site of impact, the extravasation was less pronounced than in the regions closer to the contusion. At the peak of TMRM extravasation at 48 hours after CCI, a significant increase of vascular leakage was detected in all three areas. At other time points, including 4, 24, and 72 hours following CCI, the area of BBB disruption was smaller and significant TMRM extravasation was detected only in A1 and A2. The horizontal spread of vasogenic brain edema formation reached its peak at 48 hours after CCI, which corresponds to the time of maximal total TMRM extravasation and to the second peak of increased extravasation speed.

Vertical Spreading

TMRM extravasation was determined along the vertical axis in 50 µm thick sections reaching from the surface to a depth of 300 µm. In order to avoid a bias due to the process of cranial window implantation, the superficial 50 µm were excluded from the analysis. At all time-points of significant vasogenic brain edema formation, i.e. 4, 24, 48, and 72 h post CCI, the level of TMRM extravasation was higher in the superficial layers, and the degree of vascular leakage decreased with increasing depth. However, it has to be taken into account that the outline of contusion and penumbra in the CCI model present an almost semicircular shape, while the regions of interest investigated by 2-photon microscopy followed a strictly rectangular pattern. Consequently, deeper regions are also regions more distant to the primary contusion. Accordingly, also in deeper regions TMRM extravasation in A1 and A2 were more pronounced than in A3. To avoid an artificial effect during imaging, the laser power and the detectors were adjusted dynamically according to the depth of the focus in order to achieve a fluorescence signal with stable intensity throughout the z-stack.

In summary, the *in vivo* data indicate that after CCI, vasogenic brain edema formation changes over time, suggesting that the origin of the vasogenic edema alters dynamically. Total TMRM extravasation peaks at 48 hours following injury, at the same time the vertical and horizontal distribution of vascular leakage present the widest spread. This corresponds to the maximal midline shift following TBI. Extravasation speed follows a biphasic pattern, with an early peak in the first hours following injury and a later and prolonged peak concurrent to the time of maximum TMRM extravasation.

4.3.3 Biphasic Pattern of extravasation speed

TMRM extravasation speed showed a biphasic time course, the total brain water content presented a monophasic pattern which immediately increased and remained at a high level until 72 hours following CCI. It has been described repetitively that maximum lesion expansion is reached at 24h following trauma in the CCI model (Engel et al., 2008; Zweckberger et al., 2006). Accordingly, the first peak of BBB leakage happens before and is likely to play a role in the increase of ICP following trauma (Winkler et al., 2016). However, the results of the current study indicate that the main part of vasogenic brain edema formation happens *after* maximum lesion expansion has already developed. Yet, it should be considered that in a clinical setting, the pathophysiology following TBI might follow a significantly prolonged time course. TBI patients rarely recover as quickly as experimental animals and patients often present with a combined form of injury, including contusion, diffuse axonal injury, and hematoma (Maas and Delaney, 2004). Consequently, further studies regarding vasogenic brain edema formation in other forms of TBI such as diffuse injury or closed head injury, are needed.

This second peak of vasogenic edema formation might be caused by an inflammatory reaction, reperfusion injury or pathologic metabolites as discussed above. These pathophysiological reactions happen with a delay of several hours or even days (Donkin and Vink, 2010; Jha et al., 2019; Sahuquillo et al., 2001) and are not specific for TBI, i.e. they are also observed following other forms of acute head injury such ischemic stroke or subarachnoid hemorrhage (Russin et al., 2018; Zeynalov et al., 2017). The delayed development allows time for therapeutic interventions. Further investigations regarding therapeutic interventions targeting the inflammatory reaction or the formation of pathologic metabolites are necessary to provide important information for the development of clinical therapies.

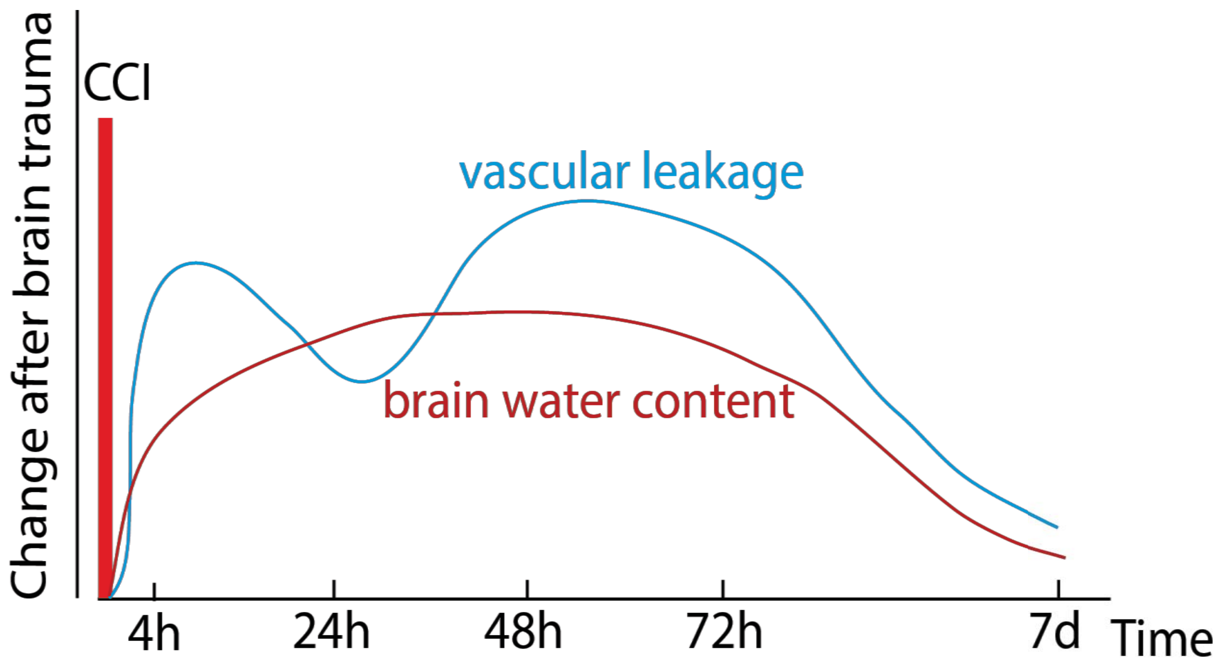

Figure 23: Schematic representation of the time course of vascular leakage and brain water content after CCI.

4.5 Clearance Routes of Vasogenic Brain Edema

Interestingly, the second peak of vascular leakage did not lead to a second peak of brain swelling. This might be explained by the following reasons:

1) Due to the defined space within the rigid skull there is an upper limit for the volume the brain might expand to (Stokum et al., 2016). Furthermore, pathologic brain water content seems also to have an upper limit.

2) Physiological clearance routes of brain edema might be induced over time resulting in a reduction of extracellular water and extravasated serum protein. Although the mechanism of these routes are incompletely understood, there are many possible mechanisms that have been considered responsible for the clearance of fluid from the extracellular space, such as pressure driven bulk flow into CSF or reverse vesicular transport from the extracellular space to the blood flow via trans-endothelial passage (Stokum et al., 2016).

In the early 1980s, studies reported that brain interstitial fluid (ISF) in the healthy brain moves by bulk flow rather than diffusion (Cserr et al., 1981; Rosenberg et al., 1980). Ohata *et al.* further described the CSF pathway via the extracellular space of the cortical neuropil as a primary route for clearance of extracellular edema proteins (Ohata and Marmarou, 1992). The widely accepted mechanism is that a sizable proportion of interstitial water is removed from the brain parenchyma along perivascular spaces and is deposited into the subarachnoid space and further removed by CSF absorption (Bradbury et al., 1981; Brinker et al., 2014; Iliff et al., 2012; Reulen et al., 1978). Another mechanism that has been controversially discussed is the clearance of ISF (Hladky and Barrand, 2014). In contrast to their role in cytotoxic edema, astrocyte end-feet and AQP-4 channels may have a clearing effect in vasogenic (non-cellular) edema. One study showed that AQP4 deletion is associated with worsened edema following injuries that precipitate vasogenic edema formation, suggesting that AQP4-mediated trans-cellular water movement is crucial for fluid clearance in vasogenic brain edema (Papadopoulos et al., 2004). However, there is still lack of evidence in TBI models regarding the clearance routes of vasogenic brain edema. *In vivo* studies are needed to improve our understanding of these edema clearance mechanisms.

4.6 Limitations and Perspectives

The combination of *in vivo* 2-photon microscopy and CCI has been newly developed (Schwarzmaier et al., 2015a). This method provides detailed 3D deep-brain images and dynamic *in vivo* quantification of vascular leakage. However, there are still several limitations that need to be considered in the current study.

1) The surgical time to prepare the cranial window and cover glass implantation is very long for each animal. The long surgical and experimental time in anesthesia increases the risk of acidosis as seen in our study, despite weight-adjusted ventilation and fluid therapy. Recent developments have made it possible to conduct prolonged experiments and to obtain repeated measurements from animals with chronic cranial windows, even in awake mice (Silasi et al., 2016).

2) Information regarding the chronic development of vasogenic brain edema formation (more than 7 days) is lacking. Several studies supported the hypothesis that BBB opening can last for weeks or even years following injury (Korn et al., 2005; Strbian et al., 2008; Tomkins et al., 2008).

Historically, vasogenic edema has long been known to be a major contributor to post-traumatic brain edema formation. However, cytotoxic edema is considered to be another major contributor to brain edema formation which is closely associated to the clinical outcomes. Moreover, it is increasingly recognized that these processes may be interrelated (Jha et al., 2019; Marmarou, 2007; Simard et al., 2007). Therefore, further studies are necessary to characterize cytotoxic edema formation following brain trauma and to understand the mechanism underlying the interaction of vasogenic edema and cytotoxic edema following TBI.

5. Summary and conclusion

In the present study, a new method to dynamically investigate the formation of vasogenic brain edema *in vivo* was used. The results show that vasogenic brain edema formation begins within 4 h following trauma and reaches its peak 48 hours following injury. There is a biphasic pattern of vascular leakage, with an early phase at 4-6 hours post-CCI and a delayed phase at 48-72 hours post-CCI. Moreover, the extravasation seems more pronounced in the areas which are closer to the primary contusion. This implies that different mechanisms might be responsible for vasogenic brain edema formation. In the initial phase, the BBB disruption is most likely associated to the acute mechanical damage to the parenchyma and vasculature. In the sub-acute phase until a week following trauma, other mechanisms like inflammation, reperfusion injury and metabolic imbalances might increase BBB permeability. These mechanisms have to be investigated further to develop therapeutic strategies for brain trauma and vasogenic brain edema formation.

The findings from the current study provide a novel insight into vasogenic brain edema formation and may help to develop more specific therapies for the treatment of brain edema following TBI.

Zusammenfassung und Schlussfolgerung

In der vorliegenden Studie wurde eine neue Methode zur dynamischen Untersuchung der Entstehung eines vasogenen Hirnödems in vivo eingesetzt. Die Ergebnisse zeigen, dass die Bildung eines vasogenen Hirnödems innerhalb von 4 Stunden nach einem Trauma beginnt und 48 Stunden nach einer Verletzung ihren Höhepunkt erreicht. Es gibt ein zweiphasiges Muster von Gefäßleckagen, mit einer frühen Phase bei 4-6 Stunden nach der CCI und einer verzögerten Phase bei 48-72 Stunden nach der CCI. Darüber hinaus scheint die Paravasation in den Bereichen, die näher an der primären Kontusion liegen, stärker ausgeprägt zu sein. Dies bedeutet, dass verschiedene Mechanismen für die Entstehung eines vasogenen Hirnödems verantwortlich sein können. In der Anfangsphase ist die BBB-Störung höchstwahrscheinlich mit der akuten mechanischen Schädigung des Parenchyms und der Gefäßversorgung verbunden. In der subakuten Phase bis eine Woche nach dem Trauma können andere Mechanismen wie Entzündungen, Reperfusionsschäden und Stoffwechselstörungen die BBB-Permeabilität erhöhen. Diese Mechanismen müssen weiter untersucht werden, um therapeutische Strategien für Hirntraumata und vasogene Hirnödembildung zu entwickeln.

Die Ergebnisse der aktuellen Studie geben einen neuen Einblick in die Entstehung eines vasogenen Hirnödems und können helfen, spezifischere Therapien für die Behandlung von Hirnödemen nach TBI zu entwickeln.

6. References

Abdul-Muneer, P.M., Schuetz, H., Wang, F., Skotak, M., Jones, J., Gorantla, S., Zimmerman, M.C., Chandra, N., and Haorah, J. (2013). Induction of oxidative and nitrosative damage leads to cerebrovascular inflammation in an animal model of mild traumatic brain injury induced by primary blast. Free radical biology & medicine *60*, 282-291.

Acosta, S.A., Tajiri, N., Shinozuka, K., Ishikawa, H., Grimmig, B., Diamond, D.M., Sanberg, P.R., Bickford, P.C., Kaneko, Y., and Borlongan, C.V. (2013). Long-term upregulation of inflammation and suppression of cell proliferation in the brain of adult rats exposed to traumatic brain injury using the controlled cortical impact model. PLoS One *8*, e53376.

Adelson, P.D., Whalen, M.J., Kochanek, P.M., Robichaud, P., and Carlos, T.M. (1998). Blood brain barrier permeability and acute inflammation in two models of traumatic brain injury in the immature rat: a preliminary report. Acta Neurochir Suppl *71*, 104-106.

Allen, T.H., and Orahovats, P.D. (1948). Spectrophotometric measurement of traces of the dye T-1824 by extraction with cellophane from both blood serum and urine of normal dogs. The American journal of physiology *154*, 27-37.

Alluri, H., Wiggins-Dohlvik, K., Davis, M.L., Huang, J.H., and Tharakan, B. (2015). Blood-brain barrier dysfunction following traumatic brain injury. Metab Brain Dis *30*, 1093-1104.

Alves, J.L. (2014). Blood-brain barrier and traumatic brain injury. J Neurosci Res *92*, 141-147.

Ando-Akatsuka, Y., Saitou, M., Hirase, T., Kishi, M., Sakakibara, A., Itoh, M., Yonemura, S., Furuse, M., and Tsukita, S. (1996). Interspecies diversity of the occludin sequence: cDNA cloning of human, mouse, dog, and rat-kangaroo homologues. The Journal of cell biology *133*, 43-47.

Argaw, A.T., Gurfein, B.T., Zhang, Y., Zameer, A., and John, G.R. (2009). VEGF-mediated disruption of endothelial CLN-5 promotes blood-brain barrier breakdown. Proc Natl Acad Sci U S A *106*, 1977-1982.

Baethmann, A., Eriskat, J., Stoffel, M., Chapuis, D., Wirth, A., and Plesnila, N. (1998). Special aspects of severe head injury: recent developments. Curr Opin Anaesthesiol *11*, 193-200.

Balda, M.S., and Anderson, J.M. (1993). Two classes of tight junctions are revealed by ZO-1 isoforms. The American journal of physiology *264*, C918-924.

Baldwin, S.A., Fugaccia, I., Brown, D.R., Brown, L.V., and Scheff, S.W. (1996). Blood-brain barrier breach following cortical contusion in the rat. Journal of neurosurgery *85*, 476-481.

Ballabh, P., Braun, A., and Nedergaard, M. (2004). The blood-brain barrier: an overview: structure, regulation, and clinical implications. Neurobiol Dis *16*, 1-13.

Barzo, P., Marmarou, A., Fatouros, P., Corwin, F., and Dunbar, J. (1996). Magnetic resonance imaging-monitored acute blood-brain barrier changes in experimental traumatic brain injury. Journal of neurosurgery *85*, 1113-1121.

Baskaya, M.K., Hu, Y., Donaldson, D., Maley, M., Rao, A.M., Prasad, M.R., and Dempsey, R.J. (1996a). Protective effect of the 5-lipoxygenase inhibitor AA-861 on cerebral edema after transient ischemia. Journal of neurosurgery *85*, 112-116.

Baskaya, M.K., Rao, A.M., Dogan, A., Donaldson, D., and Dempsey, R.J. (1997). The biphasic opening of the blood-brain barrier in the cortex and hippocampus after traumatic brain injury in rats. Neurosci Lett *226*, 33-36.

Baskaya, M.K., Rao, A.M., Prasad, M.R., and Dempsey, R.J. (1996b). Regional activity of ornithine decarboxylase and edema formation after traumatic brain injury. Neurosurgery *38*, 140-145.

Bauer, H.C., Traweger, A., Zweimueller-Mayer, J., Lehner, C., Tempfer, H., Krizbai, I., Wilhelm, I., and Bauer, H. (2011). New aspects of the molecular constituents of tissue barriers. J Neural Transm (Vienna) *118*, 7-21.

Biber, N., Toklu, H.Z., Solakoglu, S., Gultomruk, M., Hakan, T., Berkman, Z., and Dulger, F.G. (2009). Cysteinyl-leukotriene receptor antagonist montelukast decreases blood-brain barrier permeability but does not prevent oedema formation in traumatic brain injury. Brain Inj *23*, 577-584.

Blixt, J., Svensson, M., Gunnarson, E., and Wanecek, M. (2015a). Aquaporins and blood-brain barrier permeability in early edema development after traumatic brain injury. Brain Res *1611*, 18-28.

Blixt, J., Svensson, M., Gunnarson, E., and Wanecek, M. (2015b). Aquaporins and blood-brain barrier permeability in early edema development after traumatic brain injury. Brain Res *1611*, 18-28.

Bouma, G.J., and Muizelaar, J.P. (1992). Cerebral blood flow, cerebral blood volume, and cerebrovascular reactivity after severe head injury. Journal of neurotrauma *9 Suppl 1*, S333-348.

Bouma, G.J., Muizelaar, J.P., Choi, S.C., Newlon, P.G., and Young, H.F. (1991). Cerebral circulation and metabolism after severe traumatic brain injury: the elusive role of ischemia. Journal of neurosurgery *75*, 685-693.

Bouma, G.J., Muizelaar, J.P., Stringer, W.A., Choi, S.C., Fatouros, P., and Young, H.F. (1992). Ultra-early evaluation of regional cerebral blood flow in severely head-injured patients using xenon-enhanced computerized tomography. Journal of neurosurgery *77*, 360-368.

Bradbury, M.W., Cserr, H.F., and Westrop, R.J. (1981). Drainage of cerebral interstitial fluid into deep cervical lymph of the rabbit. The American journal of physiology *240*, F329-336.

Brazinova, A., Rehorcikova, V., Taylor, M.S., Buckova, V., Majdan, M., Psota, M., Peeters, W., Feigin, V., Theadom, A., Holkovic, L*., et al.* (2016). Epidemiology of Traumatic Brain Injury in Europe: A Living Systematic Review. Journal of neurotrauma.

Brightman, M.W., and Reese, T.S. (1969). Junctions between intimately apposed cell membranes in the vertebrate brain. The Journal of cell biology *40*, 648-677.

Brinker, T., Stopa, E., Morrison, J., and Klinge, P. (2014). A new look at cerebrospinal fluid circulation. Fluids and barriers of the CNS *11*, 10.

Broadwell, R.D., and Salcman, M. (1981). Expanding the definition of the blood-brain barrier to protein. Proc Natl Acad Sci U S A *78*, 7820-7824.

Broux, B., Gowing, E., and Prat, A. (2015). Glial regulation of the blood-brain barrier in health and disease. Semin Immunopathol *37*, 577-590.

Bruns, J., Jr., and Hauser, W.A. (2003). The epidemiology of traumatic brain injury: a review. Epilepsia *44*, 2-10.

Bullock, R., Sakas, D., Patterson, J., Wyper, D., Hadley, D., Maxwell, W., and Teasdale, G.M. (1992). Early post-traumatic cerebral blood flow mapping: correlation with structural damage after focal injury. Acta neurochirurgica Supplementum *55*, 14-17.

Buttram, S.D., Wisniewski, S.R., Jackson, E.K., Adelson, P.D., Feldman, K., Bayir, H., Berger, R.P., Clark, R.S., and Kochanek, P.M. (2007). Multiplex assessment of cytokine and chemokine levels in cerebrospinal fluid following severe pediatric traumatic brain injury: effects of moderate hypothermia. Journal of neurotrauma *24*, 1707-1717.

Chen, X., Zhao, Z., Chai, Y., Luo, L., Jiang, R., and Zhang, J. (2014). The incidence of critical-illness-related-corticosteroid-insufficiency is associated with severity of traumatic brain injury in adult rats. Journal of the neurological sciences *342*, 93-100.

Cheng, H., Tong, S., Deng, X., Liu, H., Du, Y., He, C., Qiu, P., and Wang, K. (2019). Deep-brain 2-photon fluorescence microscopy in vivo excited at the 1700 nm window. Optics letters *44*, 4432-4435.

Chodobski, A., Zink, B.J., and Szmydynger-Chodobska, J. (2011). Blood-brain barrier pathophysiology in traumatic brain injury. Translational stroke research *2*, 492-516.

Coronado, V.G., McGuire, L.C., Sarmiento, K., Bell, J., Lionbarger, M.R., Jones, C.D., Geller, A.I., Khoury, N., and Xu, L. (2012). Trends in Traumatic Brain Injury in the U.S. and the public health response: 1995-2009. J Safety Res *43*, 299-307.

Corrigan, F., Mander, K.A., Leonard, A.V., and Vink, R. (2016). Neurogenic inflammation after traumatic brain injury and its potentiation of classical inflammation. J Neuroinflammation *13*, 264.

Cserr, H.F., Cooper, D.N., Suri, P.K., and Patlak, C.S. (1981). Efflux of radiolabeled polyethylene glycols and albumin from rat brain. The American journal of physiology *240*, F319-328.

Csuka, E., Morganti-Kossmann, M.C., Lenzlinger, P.M., Joller, H., Trentz, O., and Kossmann, T. (1999). IL-10 levels in cerebrospinal fluid and serum of patients with severe traumatic brain injury: relationship to IL-6, TNF-alpha, TGF-beta1 and blood-brain barrier function. Journal of neuroimmunology *101*, 211-221.

da Fonseca, A.C., Matias, D., Garcia, C., Amaral, R., Geraldo, L.H., Freitas, C., and Lima, F.R. (2014). The impact of microglial activation on blood-brain barrier in brain diseases. Frontiers in cellular neuroscience *8*, 362.

da Silva Meirelles, L., Simon, D., and Regner, A. (2017). Neurotrauma: The Crosstalk between Neurotrophins and Inflammation in the Acutely Injured Brain. Int J Mol Sci *18*.

Daneman, R. (2012). The blood-brain barrier in health and disease. Annals of neurology *72*, 648-672.

Daneman, R., Zhou, L., Kebede, A.A., and Barres, B.A. (2010). Pericytes are required for blood-brain barrier integrity during embryogenesis. Nature *468*, 562-566.

Daneshvar, D.H., Goldstein, L.E., Kiernan, P.T., Stein, T.D., and McKee, A.C. (2015). Post-traumatic neurodegeneration and chronic traumatic encephalopathy. Mol Cell Neurosci *66*, 81-90.

Dash, P.K., Zhao, J., Kobori, N., Redell, J.B., Hylin, M.J., Hood, K.N., and Moore, A.N. (2016). Activation of Alpha 7 Cholinergic Nicotinic Receptors Reduce Blood-Brain Barrier Permeability following Experimental Traumatic Brain Injury. The Journal of neuroscience : the official journal of the Society for Neuroscience *36*, 2809-2818.

Dejana, E., Lampugnani, M.G., Martinez-Estrada, O., and Bazzoni, G. (2000). The molecular organization of endothelial junctions and their functional role in vascular morphogenesis and permeability. The International journal of developmental biology *44*, 743-748.

Denk, W., Strickler, J.H., and Webb, W.W. (1990). Two-photon laser scanning fluorescence microscopy. Science *248*, 73-76.

Dixon, K.J. (2017). Pathophysiology of Traumatic Brain Injury. Phys Med Rehabil Clin N Am *28*, 215-225.

Donkin, J.J., Nimmo, A.J., Cernak, I., Blumbergs, P.C., and Vink, R. (2009). Substance P is associated with the development of brain edema and functional deficits after traumatic brain injury. Journal of cerebral blood flow and metabolism : official journal of the International Society of Cerebral Blood Flow and Metabolism *29*, 1388-1398.

Donkin, J.J., and Vink, R. (2010). Mechanisms of cerebral edema in traumatic brain injury: therapeutic developments. Curr Opin Neurol *23*, 293-299.

Engel, D.C., Mies, G., Terpolilli, N.A., Trabold, R., Loch, A., De Zeeuw, C.I., Weber, J.T., Maas, A.I., and Plesnila, N. (2008). Changes of cerebral blood flow during the secondary expansion of a cortical contusion assessed by 14C-iodoantipyrine autoradiography in mice using a non-invasive protocol. J Neurotrauma *25*, 739-753.

Faden, A.I., Demediuk, P., Panter, S.S., and Vink, R. (1989). The role of excitatory amino acids and NMDA receptors in traumatic brain injury. Science *244*, 798-800.

Fleminger, S., Oliver, D.L., Lovestone, S., Rabe-Hesketh, S., and Giora, A. (2003). Head injury as a risk factor for Alzheimer's disease: the evidence 10 years on; a partial replication. J Neurol Neurosurg Psychiatry *74*, 857-862.

Frederix, K., Chauhan, A.K., Kisucka, J., Zhao, B.Q., Hoff, E.I., Spronk, H.M., Ten Cate, H., and Wagner, D.D. (2007). Platelet adhesion receptors do not modulate infarct volume after a photochemically induced stroke in mice. Brain Res *1185*, 239-245.

Furuse, M., Hirase, T., Itoh, M., Nagafuchi, A., Yonemura, S., Tsukita, S., and Tsukita, S. (1993). Occludin: a novel integral membrane protein localizing at tight junctions. The Journal of cell biology *123*, 1777-1788.

Gehrmann, J., Matsumoto, Y., and Kreutzberg, G.W. (1995). Microglia: intrinsic immuneffector cell of the brain. Brain research Brain research reviews *20*, 269-287.

Guérin, C.J., Nolan, C.C., Mavroudis, G., Lister, T., Davidson, G.M., Holton, J.L., and Ray, D.E. (2001). The dynamics of blood–brain barrier breakdown in an experimental model of glial cell degeneration. Neuroscience *103*, 873-883.

Habgood, M.D., Bye, N., Dziegielewska, K.M., Ek, C.J., Lane, M.A., Potter, A., Morganti-Kossmann, C., and Saunders, N.R. (2007). Changes in blood-brain barrier permeability to large and small molecules following traumatic brain injury in mice. The European journal of neuroscience *25*, 231-238.

Hadass, O., Tomlinson, B.N., Gooyit, M., Chen, S., Purdy, J.J., Walker, J.M., Zhang, C., Giritharan, A.B., Purnell, W., Robinson, C.R., 2nd*, et al.* (2013). Selective inhibition of matrix metalloproteinase-9 attenuates secondary damage resulting from severe traumatic brain injury. PLoS One *8*, e76904.

Hall, E.D. (1993). The role of oxygen radicals in traumatic injury: clinical implications. The Journal of emergency medicine *11 Suppl 1*, 31-36.

Hartl, R., Medary, M., Ruge, M., Arfors, K.E., and Ghajar, J. (1997). Blood-brain barrier breakdown occurs early after traumatic brain injury and is not related to white blood cell adherence. Acta Neurochir Suppl *70*, 240-242.

Haseloff, R.F., Dithmer, S., Winkler, L., Wolburg, H., and Blasig, I.E. (2015). Transmembrane proteins of the tight junctions at the blood-brain barrier: structural and functional aspects. Semin Cell Dev Biol *38*, 16-25.

Haskins, J., Gu, L., Wittchen, E.S., Hibbard, J., and Stevenson, B.R. (1998). ZO-3, a novel member of the MAGUK protein family found at the tight junction, interacts with ZO-1 and occludin. The Journal of cell biology *141*, 199-208.

Helmchen, F. (2009). Frontiers in Neuroscience,Two-Photon Functional Imaging of Neuronal Activity. In In Vivo Optical Imaging of Brain Function, nd, and R.D. Frostig, eds. (Boca Raton (FL): CRC Press/Taylor & Francis, Taylor & Francis Group, LLC.).

Helmy, A., Carpenter, K.L., Menon, D.K., Pickard, J.D., and Hutchinson, P.J. (2011). The cytokine response to human traumatic brain injury: temporal profiles and evidence for cerebral parenchymal production. Journal of cerebral blood flow and metabolism : official journal of the International Society of Cerebral Blood Flow and Metabolism *31*, 658-670.

Hiebert, J.B., Shen, Q., Thimmesch, A.R., and Pierce, J.D. (2015). Traumatic brain injury and mitochondrial dysfunction. The American journal of the medical sciences *350*, 132-138.

Higashida, T., Kreipke, C.W., Rafols, J.A., Peng, C., Schafer, S., Schafer, P., Ding, J.Y., Dornbos, D., 3rd, Li, X., Guthikonda, M.*, et al.* (2011). The role of hypoxia-inducible factor-1alpha, aquaporin-4, and matrix metalloproteinase-9 in blood-brain barrier disruption and brain edema after traumatic brain injury. Journal of neurosurgery *114*, 92-101.

Hill, R.L., Singh, I.N., Wang, J.A., and Hall, E.D. (2017). Time courses of post-injury mitochondrial oxidative damage and respiratory dysfunction and neuronal cytoskeletal degradation in a rat model of focal traumatic brain injury. Neurochemistry international *111*, 45-56.

Hladky, S.B., and Barrand, M.A. (2014). Mechanisms of fluid movement into, through and out of the brain: evaluation of the evidence. Fluids and barriers of the CNS *11*, 26.

Holmin, S., and Mathiesen, T. (1995). Biphasic edema development after experimental brain contusion in rat. Neurosci Lett *194*, 97-100.

Holmin, S., and Mathiesen, T. (2000). Intracerebral administration of interleukin-1beta and induction of inflammation, apoptosis, and vasogenic edema. Journal of neurosurgery *92*, 108-120.

Hudak, A.M., Peng, L., Marquez de la Plata, C., Thottakara, J., Moore, C., Harper, C., McColl, R., Babcock, E., and Diaz-Arrastia, R. (2014). Cytotoxic and vasogenic cerebral oedema in traumatic brain injury: assessment with FLAIR and DWI imaging. Brain Inj *28*, 1602-1609.

Hue, C.D., Cao, S., Dale Bass, C.R., Meaney, D.F., and Morrison, B., 3rd (2014). Repeated primary blast injury causes delayed recovery, but not additive disruption, in an in vitro blood-brain barrier model. Journal of neurotrauma *31*, 951-960.

Iliff, J.J., Wang, M., Liao, Y., Plogg, B.A., Peng, W., Gundersen, G.A., Benveniste, H., Vates, G.E., Deane, R., Goldman, S.A.*, et al.* (2012). A paravascular pathway facilitates CSF flow through the brain parenchyma and the clearance of interstitial solutes, including amyloid beta. Science translational medicine *4*, 147ra111.

Jafari, S., Etminan, M., Aminzadeh, F., and Samii, A. (2013). Head injury and risk of Parkinson disease: a systematic review and meta-analysis. Movement disorders : official journal of the Movement Disorder Society *28*, 1222-1229.

Jassam, Y.N., Izzy, S., Whalen, M., McGavern, D.B., and El Khoury, J. (2017). Neuroimmunology of Traumatic Brain Injury: Time for a Paradigm Shift. Neuron *95*, 1246-1265.

Jayakumar, A.R., Panickar, K.S., Curtis, K.M., Tong, X.Y., Moriyama, M., and Norenberg, M.D. (2011). Na-K-Cl cotransporter-1 in the mechanism of cell swelling in cultured astrocytes after fluid percussion injury. Journal of neurochemistry *117*, 437-448.

Jesaitis, L.A., and Goodenough, D.A. (1994). Molecular characterization and tissue distribution of ZO-2, a tight junction protein homologous to ZO-1 and the Drosophila discs-large tumor suppressor protein. The Journal of cell biology *124*, 949-961.

Jha, R.M., and Kochanek, P.M. (2018). A Precision Medicine Approach to Cerebral Edema and Intracranial Hypertension after Severe Traumatic Brain Injury: Quo Vadis? Curr Neurol Neurosci Rep *18*, 105.

Jha, R.M., Kochanek, P.M., and Simard, J.M. (2019). Pathophysiology and treatment of cerebral edema in traumatic brain injury. Neuropharmacology *145*, 230-246.

Johnson, W.D., and Griswold, D.P. (2017). Traumatic brain injury: a global challenge. The Lancet Neurology *16*, 949-950.

Ju, S., Xu, C., Wang, G., and Zhang, L. (2019). VEGF-C Induces Alternative Activation of Microglia to Promote Recovery from Traumatic Brain Injury. Journal of Alzheimer's disease : JAD *68*, 1687-1697.

Kannurpatti, S.S. (2017). Mitochondrial calcium homeostasis: Implications for neurovascular and neurometabolic coupling. Journal of cerebral blood flow and metabolism : official journal of the International Society of Cerebral Blood Flow and Metabolism *37*, 381-395.

Kassner, A., Roberts, T.P., Moran, B., Silver, F.L., and Mikulis, D.J. (2009). Recombinant tissue plasminogen activator increases blood-brain barrier disruption in acute ischemic stroke: an MR imaging permeability study. AJNR American journal of neuroradiology *30*, 1864-1869.

Katayama, Y., and Kawamata, T. (2003). Edema fluid accumulation within necrotic brain tissue as a cause of the mass effect of cerebral contusion in head trauma patients. Acta Neurochir Suppl *86*, 323-327.

Kiening, K.L., van Landeghem, F.K., Schreiber, S., Thomale, U.W., von Deimling, A., Unterberg, A.W., and Stover, J.F. (2002). Decreased hemispheric Aquaporin-4 is linked to evolving brain edema following controlled cortical impact injury in rats. Neurosci Lett *324*, 105-108.

Kimbler, D.E., Shields, J., Yanasak, N., Vender, J.R., and Dhandapani, K.M. (2012). Activation of P2X7 promotes cerebral edema and neurological injury after traumatic brain injury in mice. PLoS One *7*, e41229.

Kirchhoff, C., Stegmaier, J., Bogner, V., Buhmann, S., Mussack, T., Kreimeier, U., Mutschler, W., and Biberthaler, P. (2006). Intrathecal and systemic concentration of NT-proBNP in patients with severe traumatic brain injury. Journal of neurotrauma *23*, 943-949.

Klatzo, I. (1994). Evolution of brain edema concepts. Acta neurochirurgica Supplementum *60*, 3-6.

Klohs, J., Steinbrink, J., Bourayou, R., Mueller, S., Cordell, R., Licha, K., Schirner, M., Dirnagl, U., Lindauer, U., and Wunder, A. (2009). Near-infrared fluorescence imaging with fluorescently labeled albumin: a novel method for non-invasive optical imaging of blood-brain barrier impairment after focal cerebral ischemia in mice. Journal of neuroscience methods *180*, 126-132.

Korn, A., Golan, H., Melamed, I., Pascual-Marqui, R., and Friedman, A. (2005). Focal cortical dysfunction and blood-brain barrier disruption in patients with Postconcussion syndrome. Journal of clinical neurophysiology : official publication of the American Electroencephalographic Society *22*, 1-9.

Kossmann, T., Stahel, P.F., Morganti-Kossmann, M.C., Jones, J.L., and Barnum, S.R. (1997). Elevated levels of the complement components C3 and factor B in ventricular cerebrospinal fluid of patients with traumatic brain injury. Journal of neuroimmunology *73*, 63-69.

Krieg, S.M., Trabold, R., and Plesnila, N. (2017). Time-Dependent Effects of Arginine-Vasopressin V1 Receptor Inhibition on Secondary Brain Damage after Traumatic Brain Injury. Journal of neurotrauma *34*, 1329-1336.

Krishnappa, I.K., Contant, C.F., and Robertson, C.S. (1999). Regional changes in cerebral extracellular glucose and lactate concentrations following severe cortical impact injury and secondary ischemia in rats. Journal of neurotrauma *16*, 213-224.

Laird, M.D., Shields, J.S., Sukumari-Ramesh, S., Kimbler, D.E., Fessler, R.D., Shakir, B., Youssef, P., Yanasak, N., Vender, J.R., and Dhandapani, K.M. (2014). High mobility group box protein-1 promotes cerebral edema after traumatic brain injury via activation of toll-like receptor 4. Glia *62*, 26-38.

Lee, J.H., Martin, N.A., Alsina, G., McArthur, D.L., Zaucha, K., Hovda, D.A., and Becker, D.P. (1997). Hemodynamically significant cerebral vasospasm and outcome after head injury: a prospective study. Journal of neurosurgery *87*, 221-233.

Lenzlinger, P.M., Marx, A., Trentz, O., Kossmann, T., and Morganti-Kossmann, M.C. (2002). Prolonged intrathecal release of soluble Fas following severe traumatic brain injury in humans. Journal of neuroimmunology *122*, 167-174.

Liebner, S., Fischmann, A., Rascher, G., Duffner, F., Grote, E.H., Kalbacher, H., and Wolburg, H. (2000). Claudin-1 and claudin-5 expression and tight junction morphology are altered in blood vessels of human glioblastoma multiforme. Acta Neuropathol *100*, 323-331.

Logsdon, A.F., Meabon, J.S., Cline, M.M., Bullock, K.M., Raskind, M.A., Peskind, E.R., Banks, W.A., and Cook, D.G. (2018). Blast exposure elicits blood-brain barrier disruption and repair mediated by tight junction integrity and nitric oxide dependent processes. Scientific reports *8*, 11344.

Lorente, L., Martin, M.M., Almeida, T., Hernandez, M., Ramos, L., Argueso, M., Caceres, J.J., Sole-Violan, J., and Jimenez, A. (2015). Serum substance P levels are associated with severity and mortality in patients with severe traumatic brain injury. Critical care (London, England) *19*, 192.

Lozano, D., Gonzales-Portillo, G.S., Acosta, S., de la Pena, I., Tajiri, N., Kaneko, Y., and Borlongan, C.V. (2015). Neuroinflammatory responses to traumatic brain injury: etiology, clinical consequences, and therapeutic opportunities. Neuropsychiatr Dis Treat *11*, 97-106.

Lukaszewicz, A.C., Soyer, B., and Payen, D. (2011). Water, water, everywhere: sodium and water balance and the injured brain. Curr Opin Anaesthesiol *24*, 138-143.

Maas, A.I., Stocchetti, N., and Bullock, R. (2008). Moderate and severe traumatic brain injury in adults. The Lancet Neurology *7*, 728-741.

Maas, A.I.R., Menon, D.K., Adelson, P.D., Andelic, N., Bell, M.J., Belli, A., Bragge, P., Brazinova, A., Buki, A., Chesnut, R.M.*, et al.* (2017). Traumatic brain injury: integrated approaches to improve prevention, clinical care, and research. The Lancet Neurology *16*, 987-1048.

Maas, M.L., and Delaney, C. (2004). Nursing process outcome linkage research: issues, current status, and health policy implications. Medical care *42*, Ii40-48.

Maier, B., Schwerdtfeger, K., Mautes, A., Holanda, M., Muller, M., Steudel, W.I., and Marzi, I. (2001). Differential release of interleukines 6, 8, and 10 in cerebrospinal fluid and plasma after traumatic brain injury. Shock (Augusta, Ga) *15*, 421-426.

Marion, D.W., Darby, J., and Yonas, H. (1991). Acute regional cerebral blood flow changes caused by severe head injuries. Journal of neurosurgery *74*, 407-414.

Marmarou, A. (2007). A review of progress in understanding the pathophysiology and treatment of brain edema. Neurosurgical focus *22*, E1.

Matter, K., and Balda, M.S. (2003). Functional analysis of tight junctions. Methods (San Diego, Calif) *30*, 228-234.

Mayhan, W.G. (2001). Regulation of blood-brain barrier permeability. Microcirculation *8*, 89-104.

Mayhan, W.G., and Heistad, D.D. (1985). Permeability of blood-brain barrier to various sized molecules. The American journal of physiology *248*, H712-718.

McDonald, B., Pittman, K., Menezes, G.B., Hirota, S.A., Slaba, I., Waterhouse, C.C., Beck, P.L., Muruve, D.A., and Kubes, P. (2010). Intravascular danger signals guide neutrophils to sites of sterile inflammation. Science *330*, 362-366.

Menon, D.K., Schwab, K., Wright, D.W., Maas, A.I., Demographics, Clinical Assessment Working Group of the, I., Interagency Initiative toward Common Data Elements for Research on Traumatic Brain, I., and Psychological, H. (2010). Position statement: definition of traumatic brain injury. Arch Phys Med Rehabil *91*, 1637-1640.

Mokri, B. (2001). The Monro-Kellie hypothesis: applications in CSF volume depletion. Neurology *56*, 1746-1748.

Moretti, R., Pansiot, J., Bettati, D., Strazielle, N., Ghersi-Egea, J.F., Damante, G., Fleiss, B., Titomanlio, L., and Gressens, P. (2015). Blood-brain barrier dysfunction in disorders of the developing brain. Front Neurosci *9*, 40.

Morganti-Kossmann, M.C., Hans, V.H., Lenzlinger, P.M., Dubs, R., Ludwig, E., Trentz, O., and Kossmann, T. (1999). TGF-beta is elevated in the CSF of patients with severe traumatic brain injuries and parallels blood-brain barrier function. Journal of neurotrauma *16*, 617-628.

Morganti-Kossmann, M.C., Satgunaseelan, L., Bye, N., and Kossmann, T. (2007). Modulation of immune response by head injury. Injury *38*, 1392-1400.

Morita, K., Sasaki, H., Furuse, M., and Tsukita, S. (1999). Endothelial claudin: claudin-5/TMVCF constitutes tight junction strands in endothelial cells. The Journal of cell biology *147*, 185-194.

Muellner, A., Benz, M., Kloss, C.U., Mautes, A., Burggraf, D., and Hamann, G.F. (2003). Microvascular basal lamina antigen loss after traumatic brain injury in the rat. Journal of neurotrauma *20*, 745-754.

Murakami, K., Kondo, T., Yang, G., Chen, S.F., Morita-Fujimura, Y., and Chan, P.H. (1999). Cold injury in mice: a model to study mechanisms of brain edema and neuronal apoptosis. Progress in Neurobiology *57*, 289-299.

Murakami, T., Felinski, E.A., and Antonetti, D.A. (2009). Occludin phosphorylation and ubiquitination regulate tight junction trafficking and vascular endothelial growth factor-induced permeability. The Journal of biological chemistry *284*, 21036-21046.

Nabeshima, S., Reese, T.S., Landis, D.M., and Brightman, M.W. (1975). Junctions in the meninges and marginal glia. The Journal of comparative neurology *164*, 127-169.

Nag, S., Kapadia, A., and Stewart, D.J. (2011). Review: molecular pathogenesis of blood-brain barrier breakdown in acute brain injury. Neuropathology and applied neurobiology *37*, 3-23.

Nagata, K., Suto, Y., Cognetti, J., Browne, K.D., Kumasaka, K., Johnson, V.E., Kaplan, L., Marks, J., Smith, D.H., and Pascual, J.L. (2018). Early low-anticoagulant desulfated heparin after traumatic brain injury: Reduced brain edema and leukocyte mobilization is associated with improved watermaze learning ability weeks after injury. J Trauma Acute Care Surg *84*, 727-735.

Nortje, J., and Menon, D.K. (2004). Traumatic brain injury: physiology, mechanisms, and outcome. Curr Opin Neurol *17*, 711-718.

Obermeier, B., Daneman, R., and Ransohoff, R.M. (2013). Development, maintenance and disruption of the blood-brain barrier. Nat Med *19*, 1584-1596.

Ohata, K., and Marmarou, A. (1992). Clearance of brain edema and macromolecules through the cortical extracellular space. Journal of neurosurgery *77*, 387-396.

Pan, Z.G., Mao, Y., and Sun, F.Y. (2017). [VEGF enhances reconstruction of neurovascular units in the brain after injury]. Sheng li xue bao : [Acta physiologica Sinica] *69*, 96-108.

Papadopoulos, M.C., Manley, G.T., Krishna, S., and Verkman, A.S. (2004). Aquaporin-4 facilitates reabsorption of excess fluid in vasogenic brain edema. FASEB journal : official publication of the Federation of American Societies for Experimental Biology *18*, 1291-1293.

Peeters, W., van den Brande, R., Polinder, S., Brazinova, A., Steyerberg, E.W., Lingsma, H.F., and Maas, A.I. (2015). Epidemiology of traumatic brain injury in Europe. Acta Neurochir (Wien) *157*, 1683-1696.

Pierce, J.D., Gupte, R., Thimmesch, A., Shen, Q., Hiebert, J.B., Brooks, W.M., Clancy, R.L., Diaz, F.J., and Harris, J.L. (2018). Ubiquinol treatment for TBI in male rats: Effects on mitochondrial integrity, injury severity, and neurometabolism. J Neurosci Res *96*, 1080-1092.

Prager, O., Chassidim, Y., Klein, C., Levi, H., Shelef, I., and Friedman, A. (2010). Dynamic in vivo imaging of cerebral blood flow and blood-brain barrier permeability. Neuroimage *49*, 337-344.

Price, L., Wilson, C., and Grant, G. (2016). Frontiers in Neuroscience; Blood-Brain Barrier Pathophysiology following Traumatic Brain Injury. In Translational Research in Traumatic Brain Injury, D. Laskowitz, and G. Grant, eds. (Boca Raton (FL): CRC Press/Taylor and Francis Group (c) 2016 by Taylor & Francis Group, LLC.).

Pun, P.B., Lu, J., and Moochhala, S. (2009). Involvement of ROS in BBB dysfunction. Free Radic Res *43*, 348-364.

Raivich, G., Bohatschek, M., Kloss, C.U., Werner, A., Jones, L.L., and Kreutzberg, G.W. (1999). Neuroglial activation repertoire in the injured brain: graded response, molecular mechanisms and cues to physiological function. Brain research Brain research reviews *30*, 77-105.

Rangel-Castilla, L., Gasco, J., Nauta, H.J., Okonkwo, D.O., and Robertson, C.S. (2008). Cerebral pressure autoregulation in traumatic brain injury. Neurosurgical focus *25*, E7.

Rash, J.E., Yasumura, T., Hudson, C.S., Agre, P., and Nielsen, S. (1998). Direct immunogold labeling of aquaporin-4 in square arrays of astrocyte and ependymocyte plasma membranes in rat brain and spinal cord. Proc Natl Acad Sci U S A *95*, 11981-11986.

Raymond, S.B., Skoch, J., Hynynen, K., and Bacskai, B.J. (2007). Multiphoton imaging of ultrasound/Optison mediated cerebrovascular effects in vivo. Journal of cerebral blood flow and metabolism : official journal of the International Society of Cerebral Blood Flow and Metabolism *27*, 393-403.

Reese, T.S., and Karnovsky, M.J. (1967). Fine structural localization of a blood-brain barrier to exogenous peroxidase. The Journal of cell biology *34*, 207-217.

Ren, Z., Shi, L., Wei, D., and Qiu, J. (2019). Brain Functional Basis of Subjective Well-being During Negative Facial Emotion Processing Task-Based fMRI. Neuroscience.

Reulen, H.J., Tsuyumu, M., Tack, A., Fenske, A.R., and Prioleau, G.R. (1978). Clearance of edema fluid into cerebrospinal fluid. A mechanism for resolution of vasogenic brain edema. Journal of neurosurgery *48*, 754-764.

Reyes-Aldasoro, C.C., Wilson, I., Prise, V.E., Barber, P.R., Ameer-Beg, M., Vojnovic, B., Cunningham, V.J., and Tozer, G.M. (2008). Estimation of apparent tumor vascular permeability from multiphoton fluorescence microscopic images of P22 rat sarcomas in vivo. Microcirculation *15*, 65-79.

Roberts, D.J., Jenne, C.N., Leger, C., Kramer, A.H., Gallagher, C.N., Todd, S., Parney, I.F., Doig, C.J., Yong, V.W., Kubes, P.*, et al.* (2013). A prospective evaluation of the temporal matrix metalloproteinase response after severe traumatic brain injury in humans. Journal of neurotrauma *30*, 1717-1726.

Rodriguez-Baeza, A., Reina-de la Torre, F., Poca, A., Marti, M., and Garnacho, A. (2003). Morphological features in human cortical brain microvessels after head injury: a three-dimensional and immunocytochemical study. Anat Rec A Discov Mol Cell Evol Biol *273*, 583-593.

Rosas-Hernandez, H., Cuevas, E., Escudero-Lourdes, C., Lantz, S.M., Gomez-Crisostomo, N.P., Sturdivant, N.M., Balachandran, K., Imam, S.Z., Slikker, W., Paule, M.G.*, et al.* (2018). Characterization of Biaxial Stretch as an In Vitro Model of Traumatic Brain Injury to the Blood-Brain Barrier. Molecular Neurobiology *55*, 258-266.

Rosenberg, G.A., Kyner, W.T., and Estrada, E. (1980). Bulk flow of brain interstitial fluid under normal and hyperosmolar conditions. The American journal of physiology *238*, F42-49.

Roth, T.L., Nayak, D., Atanasijevic, T., Koretsky, A.P., Latour, L.L., and McGavern, D.B. (2014). Transcranial amelioration of inflammation and cell death after brain injury. Nature *505*, 223-228.

Russin, J.J., Montagne, A., D'Amore, F., He, S., Shiroishi, M.S., Rennert, R.C., Depetris, J., Zlokovic, B.V., and Mack, W.J. (2018). Permeability imaging as a predictor of delayed cerebral ischemia after aneurysmal subarachnoid hemorrhage. Journal of cerebral blood flow and metabolism : official journal of the International Society of Cerebral Blood Flow and Metabolism *38*, 973-979.

Sahuquillo, J., Poca, M.A., and Amoros, S. (2001). Current aspects of pathophysiology and cell dysfunction after severe head injury. Curr Pharm Des *7*, 1475-1503.

Salehi, A., Zhang, J.H., and Obenaus, A. (2017). Response of the cerebral vasculature following traumatic brain injury. Journal of cerebral blood flow and metabolism : official journal of the International Society of Cerebral Blood Flow and Metabolism *37*, 2320-2339.

Sangiorgi, S., De Benedictis, A., Protasoni, M., Manelli, A., Reguzzoni, M., Cividini, A., Dell'orbo, C., Tomei, G., and Balbi, S. (2013). Early-stage microvascular alterations of a new model of controlled cortical traumatic brain injury: 3D morphological analysis using scanning electron microscopy and corrosion casting. Journal of neurosurgery *118*, 763-774.

Saria, A., and Lundberg, J.M. (1983). Evans blue fluorescence: quantitative and morphological evaluation of vascular permeability in animal tissues. Journal of neuroscience methods *8*, 41-49.

Schwarzmaier, S.M., de Chaumont, C., Balbi, M., Terpolilli, N.A., Kleinschnitz, C., Gruber, A., and Plesnila, N. (2016). The Formation of Microthrombi in Parenchymal Microvessels after Traumatic Brain Injury Is Independent of Coagulation Factor XI. Journal of neurotrauma *33*, 1634-1644.

Schwarzmaier, S.M., Gallozzi, M., and Plesnila, N. (2015a). Identification of the Vascular Source of Vasogenic Brain Edema following Traumatic Brain Injury Using In Vivo 2-Photon Microscopy in Mice. Journal of neurotrauma *32*, 990-1000.

Schwarzmaier, S.M., and Plesnila, N. (2014). Contributions of the immune system to the pathophysiology of traumatic brain injury - evidence by intravital microscopy. Frontiers in cellular neuroscience *8*, 358.

Schwarzmaier, S.M., Terpolilli, N.A., Dienel, A., Gallozzi, M., Schinzel, R., Tegtmeier, F., and Plesnila, N. (2015b). Endothelial nitric oxide synthase mediates arteriolar vasodilatation after traumatic brain injury in mice. Journal of neurotrauma *32*, 731-738.

Schwarzmaier, S.M., Zimmermann, R., McGarry, N.B., Trabold, R., Kim, S.-W., and Plesnila, N. (2013). In vivo temporal and spatial profile of leukocyte adhesion and migration after experimental traumatic brain injury in mice. Journal of Neuroinflammation *10*, 1-17.

Semple, B.D., Bye, N., Rancan, M., Ziebell, J.M., and Morganti-Kossmann, M.C. (2010). Role of CCL2 (MCP-1) in traumatic brain injury (TBI): evidence from severe TBI patients and CCL2-/- mice. Journal of cerebral blood flow and metabolism : official journal of the International Society of Cerebral Blood Flow and Metabolism *30*, 769-782.

Shapira, Y., Setton, D., Artru, A.A., and Shohami, E. (1993). Blood-brain barrier permeability, cerebral edema, and neurologic function after closed head injury in rats. Anesthesia and analgesia *77*, 141-148.

Shen, Q., Watts, L.T., Li, W., and Duong, T.Q. (2016). Magnetic Resonance Imaging in Experimental Traumatic Brain Injury. In Injury Models of the Central Nervous System: Methods and Protocols, F.H. Kobeissy, C.E. Dixon, R.L. Hayes, and S. Mondello, eds. (New York, NY: Springer New York), pp. 645-658.

Shen, W., Li, S., Chung, S.H., Zhu, L., Stayt, J., Su, T., Couraud, P.O., Romero, I.A., Weksler, B., and Gillies, M.C. (2011). Tyrosine phosphorylation of VE-cadherin and claudin-5 is associated with TGF-beta1-induced permeability of centrally derived vascular endothelium. European journal of cell biology *90*, 323-332.

Shlosberg, D., Benifla, M., Kaufer, D., and Friedman, A. (2010). Blood-brain barrier breakdown as a therapeutic target in traumatic brain injury. Nat Rev Neurol *6*, 393-403.

Silasi, G., Xiao, D., Vanni, M.P., Chen, A.C., and Murphy, T.H. (2016). Intact skull chronic windows for mesoscopic wide-field imaging in awake mice. Journal of neuroscience methods *267*, 141-149.

Simard, J.M., Kent, T.A., Chen, M., Tarasov, K.V., and Gerzanich, V. (2007). Brain oedema in focal ischaemia: molecular pathophysiology and theoretical implications. The Lancet Neurology *6*, 258-268.

Simon, D.W., McGeachy, M.J., Bayir, H., Clark, R.S., Loane, D.J., and Kochanek, P.M. (2017). The far-reaching scope of neuroinflammation after traumatic brain injury. Nat Rev Neurol *13*, 171-191.

Singh, A., Haris, M., Rathore, D., Purwar, A., Sarma, M., Bayu, G., Husain, N., Rathore, R.K., and Gupta, R.K. (2007). Quantification of physiological and hemodynamic indices using T(1) dynamic contrast-enhanced MRI in intracranial mass lesions. Journal of magnetic resonance imaging : JMRI *26*, 871-880.

Soares, H.D., Hicks, R.R., Smith, D., and McIntosh, T.K. (1995). Inflammatory leukocytic recruitment and diffuse neuronal degeneration are separate pathological processes resulting from traumatic brain injury. The Journal of neuroscience : the official journal of the Society for Neuroscience *15*, 8223-8233.

Sourbron, S.P., and Buckley, D.L. (2013). Classic models for dynamic contrast-enhanced MRI. NMR in biomedicine *26*, 1004-1027.

Stahel, P.F., Morganti-Kossmann, M.C., Perez, D., Redaelli, C., Gloor, B., Trentz, O., and Kossmann, T. (2001). Intrathecal levels of complement-derived soluble membrane attack complex (sC5b-9) correlate with blood-brain barrier dysfunction in patients with traumatic brain injury. Journal of neurotrauma *18*, 773-781.

Stamatovic, S.M., Keep, R.F., Kunkel, S.L., and Andjelkovic, A.V. (2003). Potential role of MCP-1 in endothelial cell tight junction 'opening': signaling via Rho and Rho kinase. J Cell Sci *116*, 4615-4628.

Starr, J.M., Farrall, A.J., Armitage, P., McGurn, B., and Wardlaw, J. (2009). Blood-brain barrier permeability in Alzheimer's disease: a case-control MRI study. Psychiatry research *171*, 232-241.

Starr, J.M., Wardlaw, J., Ferguson, K., MacLullich, A., Deary, I.J., and Marshall, I. (2003). Increased blood-brain barrier permeability in type II diabetes demonstrated by gadolinium magnetic resonance imaging. J Neurol Neurosurg Psychiatry *74*, 70-76.

Stocchetti, N., and Maas, A.I. (2014). Traumatic intracranial hypertension. The New England journal of medicine *370*, 2121-2130.

Stokum, J.A., Gerzanich, V., and Simard, J.M. (2016). Molecular pathophysiology of cerebral edema. Journal of cerebral blood flow and metabolism : official journal of the International Society of Cerebral Blood Flow and Metabolism *36*, 513-538.

Strbian, D., Durukan, A., Pitkonen, M., Marinkovic, I., Tatlisumak, E., Pedrono, E., Abo-Ramadan, U., and Tatlisumak, T. (2008). The blood-brain barrier is continuously open for several weeks following transient focal cerebral ischemia. Neuroscience *153*, 175-181.

Tagliaferri, F., Compagnone, C., Korsic, M., Servadei, F., and Kraus, J. (2006). A systematic review of brain injury epidemiology in Europe. Acta Neurochirurgica *148*, 255-268.

Tanno, H., Nockels, R.P., Pitts, L.H., and Noble, L.J. (1992). Breakdown of the blood-brain barrier after fluid percussive brain injury in the rat. Part 1: Distribution and time course of protein extravasation. Journal of neurotrauma *9*, 21-32.

Tasaki, A., Shimizu, F., Sano, Y., Fujisawa, M., Takahashi, T., Haruki, H., Abe, M., Koga, M., and Kanda, T. (2014). Autocrine MMP-2/9 secretion increases the BBB permeability in neuromyelitis optica. J Neurol Neurosurg Psychiatry *85*, 419-430.

Teasdale, G., and Jennett, B. (1974). Assessment of coma and impaired consciousness. A practical scale. Lancet (London, England) *2*, 81-84.

Teichberg, V.I., Cohen-Kashi-Malina, K., Cooper, I., and Zlotnik, A. (2009). Homeostasis of glutamate in brain fluids: an accelerated brain-to-blood efflux of excess glutamate is produced by blood glutamate scavenging and offers protection from neuropathologies. Neuroscience *158*, 301-308.

Thal, S.C., and Plesnila, N. (2007). Non-invasive intraoperative monitoring of blood pressure and arterial pCO2 during surgical anesthesia in mice. J Neurosci Methods *159*, 261-267.

Tian, R., Hou, Z., Hao, S., Wu, W., Mao, X., Tao, X., Lu, T., and Liu, B. (2016). Hydrogen-rich water attenuates brain damage and inflammation after traumatic brain injury in rats. Brain Res *1637*, 1-13.

Tomkins, O., Shelef, I., Kaizerman, I., Eliushin, A., Afawi, Z., Misk, A., Gidon, M., Cohen, A., Zumsteg, D., and Friedman, A. (2008). Blood-brain barrier disruption in post-traumatic epilepsy. J Neurol Neurosurg Psychiatry *79*, 774-777.

Trabold, R., Eros, C., Zweckberger, K., Relton, J., Beck, H., Nussberger, J., Muller-Esterl, W., Bader, M., Whalley, E., and Plesnila, N. (2010). The role of bradykinin B(1) and B(2) receptors for secondary brain damage after traumatic brain injury in mice. Journal of cerebral blood flow and metabolism : official journal of the International Society of Cerebral Blood Flow and Metabolism *30*, 130-139.

Unterberg, A.W., Stover, J., Kress, B., and Kiening, K.L. (2004). Edema and brain trauma. Neuroscience *129*, 1021-1029.

van der Bliek, A.M., Sedensky, M.M., and Morgan, P.G. (2017). Cell Biology of the Mitochondrion. Genetics *207*, 843-871.

van Deurs, B., and Koehler, J.K. (1979). Tight junctions in the choroid plexus epithelium. A freeze-fracture study including complementary replicas. The Journal of cell biology *80*, 662-673.

Verant, P., Serduc, R., van der Sanden, B., Chantal, R., Ricard, C., Coles, J.A., and Vial, J.C. (2008). Subtraction method for intravital two-photon microscopy: intraparenchymal imaging and quantification of extravasation in mouse brain cortex. Journal of biomedical optics *13*, 011002.

Wahl, M., Unterberg, A., and Baethmann, A. (1985). Intravital fluorescence microscopy for the study of blood-brain-barrier function. International journal of microcirculation, clinical and experimental *4*, 3-18.

Wahl, M., Unterberg, A., Baethmann, A., and Schilling, L. (1988). Mediators of blood-brain barrier dysfunction and formation of vasogenic brain edema. Journal of cerebral blood flow and metabolism : official journal of the International Society of Cerebral Blood Flow and Metabolism *8*, 621-634.

Wang, C.C., Schoenberg, B.S., Li, S.C., Yang, Y.C., Cheng, X.M., and Bolis, C.L. (1986). Brain injury due to head trauma. Epidemiology in urban areas of the People's Republic of China. Archives of neurology *43*, 570-572.

Wang, W., Dentler, W.L., and Borchardt, R.T. (2001). VEGF increases BMEC monolayer permeability by affecting occludin expression and tight junction assembly. Am J Physiol Heart Circ Physiol *280*, H434-440.

Wang, X., Mori, T., Jung, J.C., Fini, M.E., and Lo, E.H. (2002). Secretion of matrix metalloproteinase-2 and -9 after mechanical trauma injury in rat cortical cultures and involvement of MAP kinase. Journal of neurotrauma *19*, 615-625.

Wardlaw, J.M., Doubal, F., Armitage, P., Chappell, F., Carpenter, T., Munoz Maniega, S., Farrall, A., Sudlow, C., Dennis, M., and Dhillon, B. (2009). Lacunar stroke is associated with diffuse blood-brain barrier dysfunction. Annals of neurology *65*, 194-202.

Wardlaw, J.M., Farrall, A., Armitage, P.A., Carpenter, T., Chappell, F., Doubal, F., Chowdhury, D., Cvoro, V., and Dennis, M.S. (2008). Changes in background blood-brain barrier integrity between lacunar and cortical ischemic stroke subtypes. Stroke *39*, 1327-1332.

Wei, X.E., Zhang, Y.Z., Li, Y.H., Li, M.H., and Li, W.B. (2012). Dynamics of rabbit brain edema in focal lesion and perilesion area after traumatic brain injury: a MRI study. Journal of neurotrauma *29*, 2413-2420.

Wen, J., Qian, S., Yang, Q., Deng, L., Mo, Y., and Yu, Y. (2014). Overexpression of netrin-1 increases the expression of tight junction-associated proteins, claudin-5, occludin, and ZO-1, following traumatic brain injury in rats. Experimental and therapeutic medicine *8*, 881-886.

Whalen, M.J., Carlos, T.M., Kochanek, P.M., Clark, R.S., Heineman, S., Schiding, J.K., Franicola, D., Memarzadeh, F., Lo, W., Marion, D.W., *et al.* (1999). Neutrophils do not mediate blood-brain barrier permeability early after controlled cortical impact in rats. Journal of neurotrauma *16*, 583-594.

Wick, M.J., Harral, J.W., Loomis, Z.L., and Dempsey, E.C. (2018). An Optimized Evans Blue Protocol to Assess Vascular Leak in the Mouse. Journal of visualized experiments : JoVE.

Willis, C.L., Nolan, C.C., Reith, S.N., Lister, T., Prior, M.J., Guerin, C.J., Mavroudis, G., and Ray, D.E. (2004). Focal astrocyte loss is followed by microvascular damage, with subsequent repair of the blood-brain barrier in the apparent absence of direct astrocytic contact. Glia *45*, 325-337.

Wilson, L., Stewart, W., Dams-O'Connor, K., Diaz-Arrastia, R., Horton, L., Menon, D.K., and Polinder, S. (2017). The chronic and evolving neurological consequences of traumatic brain injury. The Lancet Neurology *16*, 813-825.

Winkler, E.A., Minter, D., Yue, J.K., and Manley, G.T. (2016). Cerebral Edema in Traumatic Brain Injury: Pathophysiology and Prospective Therapeutic Targets. Neurosurgery clinics of North America *27*, 473-488.

Woodcock, T.M., Frugier, T., Nguyen, T.T., Semple, B.D., Bye, N., Massara, M., Savino, B., Besio, R., Sobacchi, C., Locati, M.*, et al.* (2017). The scavenging chemokine receptor ACKR2 has a significant impact on acute mortality rate and early lesion development after traumatic brain injury. PLoS One *12*, e0188305.

Wu, Q., Gao, C., Wang, H., Zhang, X., Li, Q., Gu, Z., Shi, X., Cui, Y., Wang, T., Chen, X.*, et al.* (2018). Mdivi-1 alleviates blood-brain barrier disruption and cell death in experimental traumatic brain injury by mitigating autophagy dysfunction and mitophagy activation. The international journal of biochemistry & cell biology *94*, 44-55.

Yang, L., Wang, F., Yang, L., Yuan, Y., Chen, Y., Zhang, G., and Fan, Z. (2018). HMGB1 a-Box Reverses Brain Edema and Deterioration of Neurological Function in a Traumatic Brain Injury Mouse Model. Cellular physiology and biochemistry : international journal of experimental cellular physiology, biochemistry, and pharmacology *46*, 2532-2542.

Yang, M., Wang, X., Fan, Y., Chen, Y., Sun, D., Xu, X., Wang, J., Gu, G., Peng, R., Shen, T.*, et al.* (2019). Semaphorin 3A Contributes to Secondary Blood–Brain Barrier Damage After Traumatic Brain Injury. Frontiers in cellular neuroscience *13*.

Yang, T., Liu, Y.W., Zhao, L., Wang, H., Yang, N., Dai, S.S., and He, F. (2017). Metabotropic glutamate receptor 5 deficiency inhibits neutrophil infiltration after traumatic brain injury in mice. Scientific reports *7*, 9998.

Yeoh, S., Bell, E.D., and Monson, K.L. (2013). Distribution of blood-brain barrier disruption in primary blast injury. Annals of biomedical engineering *41*, 2206-2214.

Yu, M., Wang, M., Yang, D., Wei, X., and Li, W. (2019). Dynamics of blood brain barrier permeability and tissue microstructure following controlled cortical impact injury in rat: A dynamic contrast-enhanced magnetic resonance imaging and diffusion kurtosis imaging study. Magnetic resonance imaging *62*, 1-9.

Zacest, A.C., Vink, R., Manavis, J., Sarvestani, G.T., and Blumbergs, P.C. (2010). Substance P immunoreactivity increases following human traumatic brain injury. Acta Neurochir Suppl *106*, 211-216.

Zeynalov, E., Jones, S.M., and Elliott, J.P. (2017). Therapeutic time window for conivaptan treatment against stroke-evoked brain edema and blood-brain barrier disruption in mice. PLoS One *12*, e0183985.

Zhao, Z., Nelson, A.R., Betsholtz, C., and Zlokovic, B.V. (2015). Establishment and Dysfunction of the Blood-Brain Barrier. Cell *163*, 1064-1078.

Zhiyuan, Q., Qingyong, L., Shengming, H., and Hui, M. (2016). Protective effect of rhEPO on tight junctions of cerebral microvascular endothelial cells early following traumatic brain injury in rats. Brain Inj *30*, 462-467.

Ziebell, J.M., and Morganti-Kossmann, M.C. (2010). Involvement of pro- and anti-inflammatory cytokines and chemokines in the pathophysiology of traumatic brain injury. Neurotherapeutics : the journal of the American Society for Experimental NeuroTherapeutics *7*, 22-30.

Zlotnik, A., Klin, Y., Gruenbaum, B.F., Gruenbaum, S.E., Ohayon, S., Leibowitz, A., Kotz, R., Dubilet, M., Boyko, M., Shapira, Y.*, et al.* (2012). b2 Adrenergic-mediated Reduction of Blood Glutamate Levels and Improved Neurological Outcome After Traumatic Brain Injury in Rats. Journal of neurosurgical anesthesiology *24*, 30–38.

Zweckberger, K., Erös, C., Zimmermann, R., Kim, S.-W., Engel, D., and Plesnila, N. (2006). Effect of Early and Delayed Decompressive Craniectomy on Secondary Brain Damage after Controlled Cortical Impact in Mice. Journal of neurotrauma *23*, 1083–1093.

Zweckberger, K., and Plesnila, N. (2009). Anatibant, a selective non-peptide bradykinin B2 receptor antagonist, reduces intracranial hypertension and histopathological damage after experimental traumatic brain injury. Neurosci Lett *454*, 115-117.

Zweckberger, K., Stoffel, M., Baethmann, A., and Plesnila, N. (2003). Effect of Decompression Craniotomy on Increase of Contusion Volume and Functional Outcome after Controlled Cortical Impact in Mice. Journal of neurotrauma *20*, 1307-1315.

7. List of Abbreviations

AQP	Aquaporin
ATP	Adenosine triphosphate
AVP	Arginine vasopressin
BBB	Blood–brain barrier
CBF	Cerebral blood flow
CCI	Controlled cortical impact
CCL2	Chemokine (C-C motif) ligand 2
CNS	Central nervous system
CPP	Cerebral perfusion pressure
CSF	Cerebrospinal fluid
CXCL	Chemokine (C-X-C motif) ligand
DAI	Diffuse axonal injury
DAMPs	Danger associated molecular patterns
DCE-MRI	Dynamic contrast-enhanced MRI
ECM	Extracellular matrix
FPI	Fluid percussion injury
GCS	Glasgow Coma Scale
ICP	Intracranial pressure
IL	Interleukin
ISF	Brain interstitial fluid

IVM	Intravital fluorescence microscopy
LTP	Long-term potentiation
MMP	Matrix metalloproteinases
MRI	Magnetic resonance imaging
NIRS	Near-infrared fluorescence
NOS	Nitric oxide synthase
pCO_2	Partial pressure of carbon dioxide
PRRs	Pattern recognition receptors
RCT	Randomized controlled trial
ROI	Regions of interest
ROS	Reactive oxygen species
SD	Standard deviation
SDF	Side-stream dark-field
SP	Substance P
TBI	Traumatic brain injury
TMRM	Tetramethylrhodamine dextran
TNF-α	Tumor necrosis factor-α
VEGF	Vascular endothelial growth factor

8. Acknowledgements

My deepest gratitude goes first and foremost to Prof. Dr. med. Nikolaus Plesnila for giving me the opportunity to perform my doctoral study in his group and leading me into the interesting research filed. Thanks for his supervision, support and encouragement throughout the past three years. I also would like to particularly thank my co-supervisor Dr. Susanne Schwarzmaier, thanks for her excellent guidance, endless help and constant care. It is the two of you who inspired me to overcome the difficulties I faced, trained me to thinking academically, gave me a chance to have a glimpse of the vastness of the scientific ocean.

I am also greatly indebted to all lab fellows from the AG Plesnila group, thanks for the friendly, enjoyable, inspiring and open working atmosphere you created. Whenever I need, a helping hand was always there. Special thanks to Severin and Josh, who generously helped me in solving some technical problems in my project and giving me useful advices. Thanks to Uta, Hedwig, Farida, Xiang, Susana, Burcu, Rebecca, Igor, Shiqi, Ziyu, Xiangjiang, Antonia, Bernhard for their selfless help. I felt so lucky to share the last 3 years in lab with all of you.

I would like to thank the First Teaching Hospital of Tianjin University of Traditional Chinese Medicine and my Chinese supervisor Junping Zhang. Thanks for the support to make it possible for me to study abroad.

I am also thankful to all the lovely friends I got in Munich, Yan, Sijia, Kaihui, thanks for all the happy time we spent together, thanks for the comforting and cheering you provided when I was down.

Last but not least my thanks would go to my beloved family for their loving considerations and great confidence in me all through these years.

Affidavit

Hu, Yue

Surname, first name

Address

I hereby declare, that the submitted thesis entitled

Characterization of Vasogenic Brain Edema Formation by after Experimental Traumatic Brain Injury by in vivo 2-Photon Microscopy

is my own work. I have only used the sources indicated and have not made unauthorised use of services of a third party. Where the work of others has been quoted or reproduced, the source is always given.

I further declare that the submitted thesis or parts thereof have not been presented as part of an examination degree to any other university.

Munich,15.05.2020

Place, Date

Yue Hu

Signature doctoral candidate

Confirmation of congruency between printed and electronic version of the doctoral thesis

Doctoral candidate: Ms. Yue Hu

Address:

I hereby declare that the electronic version of the submitted thesis, entitled

Characterization of Vasogenic Brain Edema Formation by after Experimental Traumatic Brain Injury by in vivo 2-Photon Microscopy

is congruent with the printed version both in content and format.

Munich,15.05.2020

Place, Date

Yue Hu

Signature doctoral candidate